631.51:631.434

MEDEDELINGEN LANDBOUWHOGESCHOOL
WAGENINGEN • NEDERLAND • 77-17 (1977)

SOIL LOOSENING PROCESSES IN TILLAGE ANALYSIS, SYSTEMATICS AND PREDICTABILITY

A. J. KOOLEN

Tillage Laboratory, Agricultural University, Wageningen, The Netherlands

(with a summary in Dutch)
(received 8-VI-1977)

H. VEENMAN & ZONEN B.V. – WAGENINGEN – 1977

Mededelingen Landbouwhogeschool
Wageningen 77-17 (1977)
(Communications Agricultural University)
is also published as a thesis

CONTENTS

1. INTRODUCTION

Tillage processes for loosening soil have been performed all over the world for many centuries now; the aim being to produce the most desirable tillage results with the minimum amount of effort. This goal is often achieved due to the much tried application of the 'cut and try' method of improving tillage implements and methods. This development based on experience will fail however where:

- farms are flexible rather than traditional, in order to be able to respond to economical changes adequately,
- new farms are planned in still unknown environments,
- knowledge is no longer transferred from father to son, but through schooling,
- new implements must be developed for new markets.

In these situations there is a need for a knowledge of tillage processes so as to allow the costs and results of a tillage treatment to be predicted in a clear and efficient way. Such knowledge is not simply available, but must largely be obtained (*analysis*). This is a tremendous task because of the complexity of the problem. The variables are tool shape, working depth, forward speed, soil type, soil moisture content, soil porosity and structure, which can all vary widely. In addition, when one of these factors is gradually changed, a non-gradual change in the process may occur, that is, the process may totally change its shape. This latter fact especially necessitates the putting together of knowledge (*systematics*). As the various process shapes are identified more completely, it will be more possible to develop methods for predicting whether a process shape will occur or not, or even to predict quantitative information for a process shape (*predictability*).

Since the turn of the century many articles representing the results of research on tillage tool action have been published. Generally an article on tillage tools only deals with one or a few implements, operating in a very limited number of soil conditions. In most cases it represents a description of the observed phenomena. Sometimes an attempt to arrange these phenomena is also given, which may be accompanied by efforts to predict them. In the following publication the literature is presented in a recast form, comprising a more or less general systematics (sections 2–5) and a treatise of predictability (sections 6–9). The latter sections also include some aids to prediction adopted from engineering mechanics. After reading the general systematics it will be clear that this, as yet, is insufficient, and needs to be extended. It is therefore followed by a perspective towards such an extension, indicating that a two-dimensional curved blade with a small cutting angle provides a reasonable basis for a complete systematics (section 10.1). In the remaining sections this kind of blade is discussed more fully:

- section 10.2 presents means of investigating the processes that this blade can induce,

– sections 10.3, 10.5 (partly) and 10.6 are devoted to a detailed systematics,
– contributions to the predictability of these processes can be found in sections 10.4, 10.5 and 10.7.

Some mathematical results, which are not directly essential for understanding 'the main line' are included as an appendix.

2. INTRODUCTORY REMARKS ON SYSTEMATICS

2.1. From machine to operating tool

Soil tillage implements and wheel assemblies of tractors, harvesters, trailers etc. can exhibit a multitude of forms and dimensions. This report is only concerned with those machine parts which touch the soil directly, such as plough-bottoms, chisels, drums of land-rollers, and tyres. Such parts will be called operating tools. This report mainly deals with operating tools that move at a constant velocity along a straight horizontal path, their action not being affected by near-by operating tools. Studying them may help us to understand processes that involve more complicated tool paths, non-constant velocities or interactions, such as:

- cycloid paths of rotary tines,
- reciprocating movements of oscillating tools,
- non-steady forward velocities of flexible tines,
- interactions between the soil break-up actions of tines that work side by side,
- sinkage of wheels travelling in ruts of foregoing wheels.

2.2. Loosening and load-bearing processes

The soil tillage process of a given tool, tool handling, soil combination exists during the time the tool is subjected to this handling in this soil, and, at any moment of its existence, the process comprises the movements and the forces in the soil that is influenced by the tool *at that moment*.

Soil tillage processes can be divided into loosening and load-bearing processes. Loosening processes are considered to change cohering soil (soil exhibiting cohesion) into a mass of soil aggregates having little or no mutual coherence (ploughing, discing etc.). Load-bearing processes are considered to be characterized by soil strength increases in the process (processes under tyres, land-rollers etc.). This report deals with loosening processes.

2.3. Introduction to soil loosening processes

A further explanation of soil loosening

Fig. 1b gives an instantaneous picture of a tillage process performed in a soil. Fig. 1a gives a vertical section of this soil. The soil may be considered to consist of imaginary volume-elements (cube-like soil masses) corresponding with the meshes drawn in the figure. The size of these volume-elements should be so small that the stress on any side of an element is rather evenly distributed,

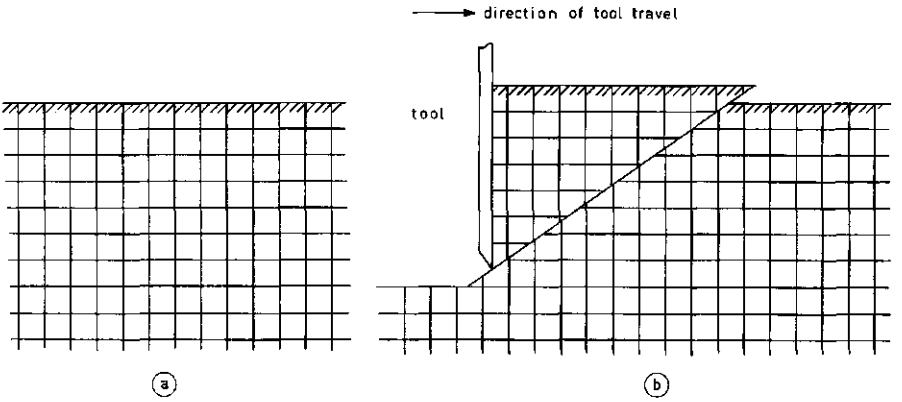

FIG. 1. Breaking of soil volume elements in a soil loosening process.

but not so small that the soil in the element may no longer be considered continuous. In loosening processes many of these elements will be broken.

Breaking involves the following mechanical-physical phenomenon: in an element, on a micro-scale, loading will cause strains that are not homogeneously distributed, but that are concentrated at some locations in the element, inducing the breaking of bonds between soil particles at a number of these locations. Such places are referred to as failure planes. Concentrations of large strains occur at concentrations of high stresses and when deformation is unstable.

Concentrations of high stresses. Generally a concentration of high stresses is accompanied by a concentration of large strains, thus enabling failure to occur. Examples of this type of failure are the splitting action of an acute wedge penetrating into a soil block, and the crushing of clods by a vertical load (Fig. 2).

Unstable deformations. For a better understanding of unstable deformations it is also useful to recognize stable deformations, see Fig. 3a. In this figure, the volume-element is loaded by a hydrostatic stress p. In most cases strength distribution within the element is heterogeneous on a micro-scale. When p is

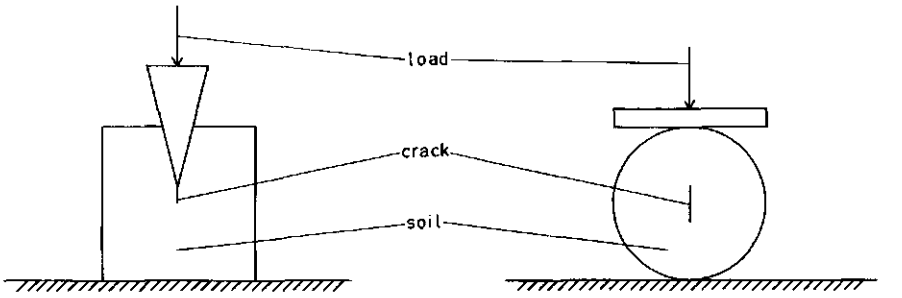

FIG. 2. Concentration of deformation caused by stress concentration.

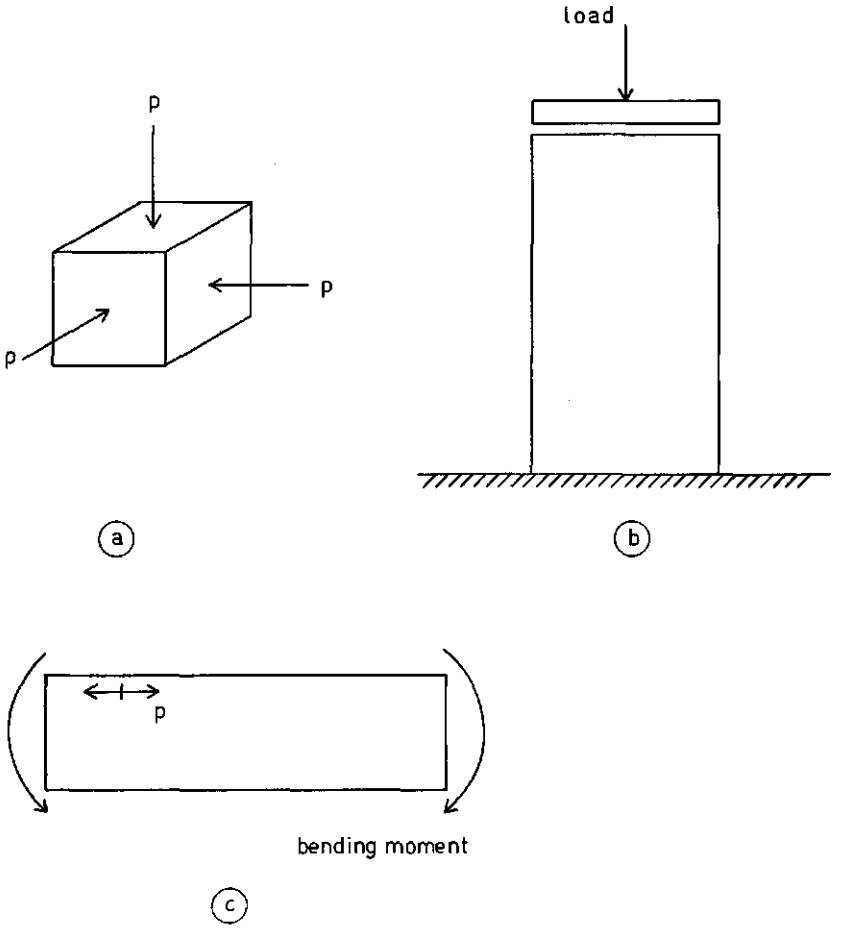

FIG. 3. Stable (a) and unstable (b and c) deformation.

increased, deformation (compaction) will result, especially where the soil is weakest. However, compaction makes such a weak spot stronger, causing other spots to be ranked as weakest and to be compacted in their turn when p increases further. In this way, compaction takes place throughout the element. Figs. 3b and 3c show unstable deformations. The volume-element in Fig. 3b, which has a vertical load and no lateral support, is assumed to consist of compact soil. When increasing the load, the element will shorten, which induces relative movements between soil particles. Because, initially, the soil was already compact, such a relative movement involves a slight loosening of the packing state. This loosening especially occurs at the weakest spots in the element, making them even weaker. At further increases of the load, deformation and loosening will be more and more concentrated in those spots, and local failures will finally result. In Fig. 3c tensile stresses are present in the

upper part of a soil beam. The tensile stresses near the top surface will be denoted by p. When the bending moment is increased, p increases and can attain values close to soil tensile strength. Because of the soil's natural heterogeneity, tensile strength varies a little along the upper boundary. If the tensile strength of the weakest spot is reached, a small crack will develop. This crack deminishes the area of the vertical beam section under that spot, which causes the local tensile stresses to increase, making the initial crack grow further.

Whether deformation is stable or not will depend on the state of stress and the character of the soil. Unstability is accompanied by stress states that are not compacting but volume increasing (dilating), and by soils tending to exhibit very much dilation when being deformed. The question of whether there is a sharp boundary, has not yet been solved. Starting points are presented by theories such as critical state soil mechanics (KURTEY and REECE, 1970). The character of the soil has a double meaning in stability, because the state of stress in a tillage process is also affected by soil character: in very plastic soils excessive deformation sometimes inhibits the existence of stress states that favour unstable phenomena.

Historical notes on the studies of loosening processes

From an examination of literature it was apparent that research on soil loosening processes has been concentrated on the following tillage tool groups:
- tines,
- plough-bodies,
- two-dimensional blades.

For each group, research developed along a distinct line, which is easily understood considering the characteristics of the processes. Tine research started with recognizing the soil break-up action of tines and the periodicity of that action. This lead to classical soil mechanics theories, which appeared to be useful as far as draft prediction was concerned. Though the research workers realized that the tine problem has a dynamic character, they concentrated on static soil mechanics for a long time, and it was not until 1967 that a synthesis was made between static and dynamic characteristics (VORNKAHL, 1967).

On the other hand, the flow-like character of the movement of soil induced by a plough-body can be noticed very easily. The dynamic part of the process was therefore recognized very early (Gorjatchkin 1898, according to VORNKAHL, 1967), and sometimes went as far as considering only the acceleration forces as being significant (O'CALLAGHAN and MCCOY, 1965; CARLSON, 1961). The ploughing process appeared to be too complicated for research workers to be able to understand the significance of their theories, and it can be seen that most of them developed correct or incorrect models to demonstrate only parts of the process (NICHOLS and KUMMER, 1932; DONER and NICHOLS, 1934; GUPTA and PANDYA, 1967).

The two-dimensional blades are the least difficult group and it is mainly here that soil dynamics (mechanics for soil tillage) is developing its own identity: the two-dimensional blade problem is easily accessible to experimental and

analytical methods. Founders are Söhne and Weber, whereas Reece gave classical soil mechanics its rightful position in the blade theories.

The following sections do not use the above scheme, but a scheme based on considerations concerning practical application.

Tines and plough-bodies as main groups

When soil has to be loosened, a body (operating tool) can be moved through the soil. Such a body will be labelled tine if the loosening effect reaches considerably further than the width of the body, and plough-body if the loosening effect is mainly confined to the soil within the width of the operating tool (this deviates somewhat from common idiom. For instance, the given definitions classify a shank with sweep as a plough-body, and not as a tine). The definitions given imply that there is no distinct dividing line between either type, for each tool influences the soil within its width and also strips of soil outside its width. The phenomena occurring in front of a tine look like the ones induced by plough-bodies. Similarly, phenomena at the sides of a plough-body resemble tine phenomena.

Some important differences are:

- for the same amount of soil loosened per unit of travelling length a tine will be simpler and cheaper than a plough-body,
- plough-bodies are often streamlined to maintain a continuous soil flow over the body,
- plough-bodies involve better possibilities for process control (plough-bodies
- and tines are sometimes associated with the terms 'controlled' and 'random' soil transport, respectively).

3. SYSTEMATICS OF TINE PROCESSES

A multitude of tine forms and positions are possible. In order to make the description of all tine phenomena more simple, a few tines can be treated exhaustively, while processes of other tines may be described with reference to those few tines. For a tine to be exhaustively treated it should have the capacity of inducing processes that are rather general and be no more complicated in its shape than is necessary for these general processes to exist. Fig. 4 gives the tines treated here:

- the straight, vertical tine without profile (A),
- the straight, slightly forward raked tine without profile (B),
- the straight, slightly backward raked tine without profile (C),
- the straight, very backward raked tine without profile (D), tine (E),
- the straight, vertical, wedge-shaped tine (F),
- the curved tine without profile (G).

3.1. THE STRAIGHT VERTICAL TINE WITHOUT PROFILE

In the literature several process shapes are described for this tine. A few types can be distinguished. Soil type, soil condition, tine size and tine speed determine which type of process shape will occur. The following process types have been deduced from literature. Because systematic tine studies to distinguish all possible process types have never been carried out, the following is not expected to be complete, and other process types may exist. For the same reason it is uncertain whether the chosen divisions are optimal.

3.1.1. *Process type A (fracture type)*

The most general process type has the form presented in Figs. 5a and 5b. Fig. 5a shows an instantaneous picture of a tine moving through a soil block,

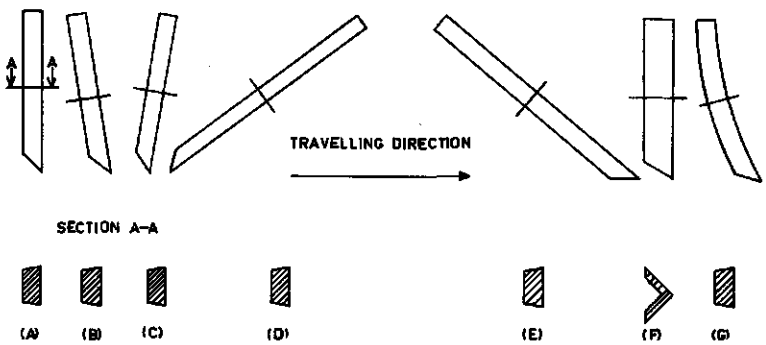

FIG. 4. Some tine shapes.

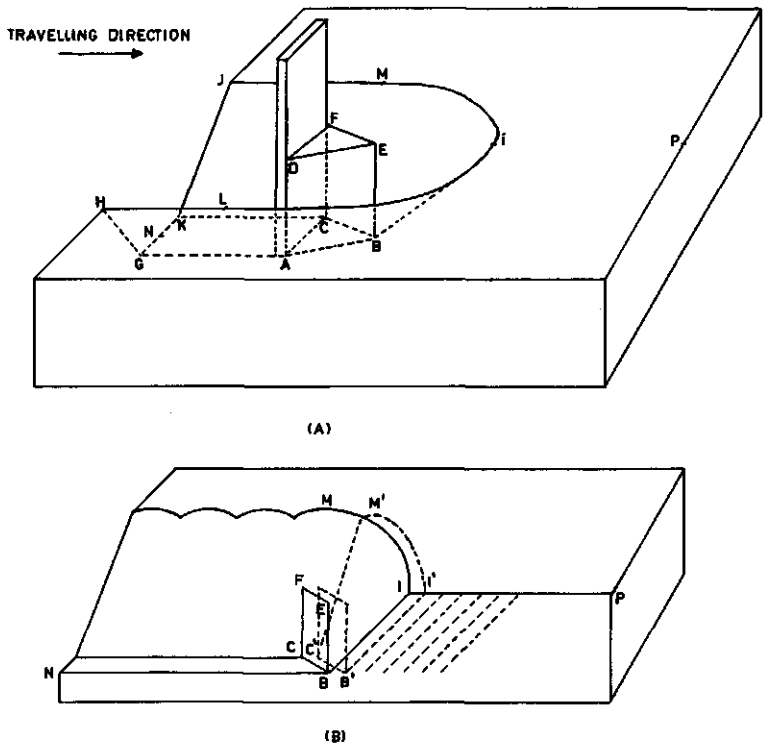

FIG. 5. Tine process-type A.

and also the accompanying process. In front of the tine there is a compact soil mass, which can clearly be distinguished from the surrounding soil. This soil mass, usually called soil-wedge, is indicated by A, B, C, D, E, F. Surface G, H, I, J, K, C, B, A, G is a boundary between the loosened soil and the still firm soil. The loose soil in front of and beside the wedge has just been loosened, and will be called crescent soil. In the soil block the tine made a furrow, which has been partly filled again with loose soil. A small trench, however, behind the tine is always left. Another part of the loose soil has moved outside the lines H, L and J, M and rests on top of the firm soil surface.

Where Fig. 5a is an instantaneous picture, Fig. 5b presents the progress in time of the soil breaking process. The plane passing N, B, I, P is a vertical plane of symmetry through the tine in the direction of travel. At a given moment C, B, E, F is one side of the soil wedge and C, B, I, M is half the boundary between firm and loose soil in front of the tine. As the tine moves further to the right, surface C, B, I, M will be loaded by the underside of the wedge and by the loose soil present in front of the tine (which loose soil actually transmits the loading exerted by the vertical sides of the wedge). At a given moment the load on C, B, I, M has become so large as to cause failure along a new failure surface C′, B′, I′, M′ and the soil from C, B, I, M, C′, B′, I′, M′ will partly join the

compact wedge, and partly the loose soil. When the tine moves further, the process is repeated. During the forward movement of the tine the wedge moves slowly upwards, the upper part being broken off and left aside at regular intervals. There is loose soil in front of and to the sides of the tine being transported in forward, upward and sideways directions, as well as loose soil falling back into the furrow behind the tine.

The soil wedge. The soil wedge that moves upwards will be refilled from beneath with soil from the lower part of the tilled layer (PAYNE, 1956: WILLATT and WILLIS, 1965). It consists of compacted soil, the density being higher at the tine side than at the tip (WILLATT and WILLIS, 1965). The wedge shape almost follows the outline of Fig. 5a, with the edges rounded (PAYNE, 1956). The upward wedge speed fluctuates. Sometimes the wedge, or part of it, tends to adhere to the tine. In literature the soil adhering to the tine is sometimes called 'cone'. Distinct cone formation may occur at low speeds and/or when the soil – metal friction angle is large (TANNER, 1960; WILLATT and WILLIS, 1965; PAYNE, 1956).

The crescent soil. The degree of crescent soil pulverization can vary strongly. An extreme case happens when, after shearing, there is little or no further pulverization of the soil in C, B, I, M, C′, B′, I′, M′. Then the freshly formed soil lump will keep its crescent-like shape (PAYNE, 1956). However, in most cases some further pulverization occurs, which is more pronounced at higher speeds and at greater natural soil heterogeneity (PAYNE, 1956).

The furrow. Furrow geometry is indicated in Fig. 6. From the data for furrow width y, presented in literature (PAYNE, 1956; O'CALLAGHAN and FARRELLY, 1964; WILLATT and WILLIS, 1965), those of O'CALLAGHAN and FARRELLY (1964) are the most exploratory. Fig. 7 refers to this article. It shows that as the working depth is increased, furrow width becomes less dependent on working depth. Furrow width slightly increases with higher speeds (WILLATT and WILLIS, 1965). Values for the distance between the tine and the furrow tip are given for different soils in Fig. 8 (PAYNE, 1956). Furrow walls and the furrow bottom can exhibit fissures. The longer axes of these fissures are perpendicular to the tine travelling direction (O'CALLAGHAN and FARRELLY, 1964).

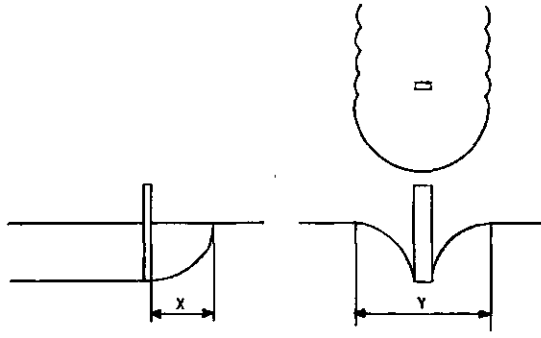

FIG. 6. Furrow shape in the case of process-type A.

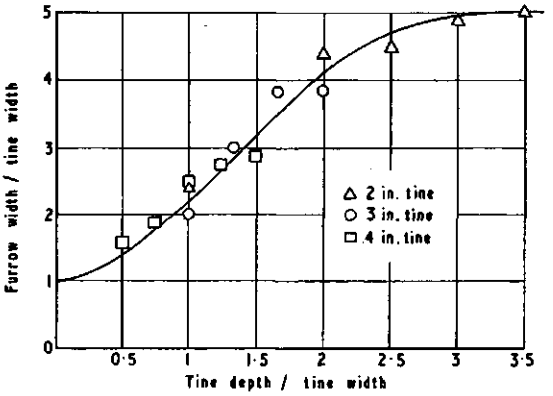

FIG. 7. Furrow width y as a function of tine depth (O'CALLAGHAN and FARRELLY, 1964).

The loose soil left behind by the tine. The loose soil pushed away by the tine partly falls back into the furrow, and partly comes to rest outside the furrow on top of the still firm soil surface. Usually, a small trench is left in the middle of the furrow, with a small ridge on either side. If there is not much crescent soil pulverization, the soil clods that have come to rest can have equal shapes and positions and exhibit a very regular pattern. It is shown in the work done by PAYNE (1956).

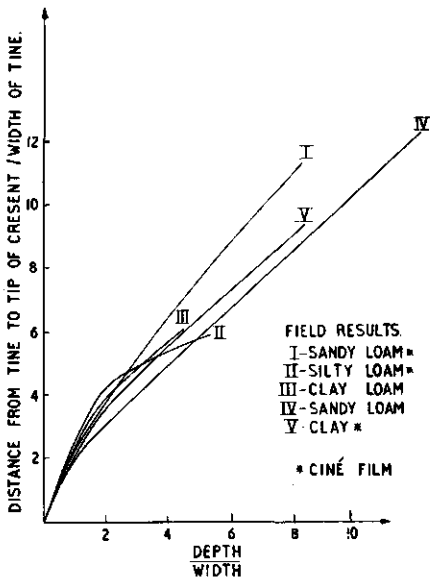

FIG. 8. Distance x as a function of tine depth (PAYNE, 1956).

3.1.2. *Process type B (flow type)*

For certain tine dimensions, soil properties and forward speeds the moving tine mainly deforms the soil, inducing only very few or no failure surfaces (PAYNE, 1956; PAYNE and TANNER, 1959). The soil bulges out at the sides and in front of the tine. The furrow is a small slot, bounded on either side by a permanent bulge. The process type accompanies tines that are too narrow for pushing away the soil far enough to induce failure surfaces, and/or soils that need large deformations before failures start to develop. Sand, being relatively rigid, needs a narrower tine for this process type to occur than most other soils. The order of magnitude of the tine width, below which the process type may occur, is about 1 cm.

3.2. FURTHER TINES

3.2.1. *Some tines derived from the straight, vertical tine without profile*

Confining attention to process type A (described in 3.1.1.) it may be stated that this type can also be induced by:

- the straight, slightly forward raked tine without profile (B),
- the straight, slightly backward raked tine without profile (C),
- the straight, very backward raked tine without profile (D),
- the straight, vertical wedge-shaped tine (F),

observing the following pertinent extensions to the presented description of A.

With the increasing forward rake of the slightly forward raked tine (B):

- the soil wedge becomes less compacted (WILLATT and WILLIS, 1965),
- wedge shape is more irregular (PAYNE and TANNER, 1959),
- there is more upward movement of the wedge and less adhering to the tine (TANNER, 1960),
- furrow width increases and length of the horizontal projection of the distance between the tine tip and the furrow tip decreases (PAYNE and TANNER, 1959).

With increasing backward rake of the slightly backward raked tine (C):

- there is less upward movement of the wedge and more adhering to the tine (TANNER, 1960),
- furrow width decreases and length of the horizontal projection of the distance between tine tip and furrow tip increases (PAYNE and TANNER, 1959).

In the case of the very backward raked tine (D) there is no relative movement between the tine and the soil wedge, so the wedge becomes part of the tine. The wedge neither crumbles off nor is refilled (PAYNE and TANNER, 1959; TANNER, 1960). For the wedge-shaped tine (F) it should be noted that, provided the tip angle of the wedge shape of the tine is small enough, there is no soil wedge, its function being taken over by the wedge-shaped tine (O'CALLAGHAN and MCCULLEN' 1965).

3.2.2. *The straight, very forward raked tine without profile*

The literature does not give any process shapes for this tine. Presumably, the tine has the capacity of inducing specific process shapes, similar to those found in research on plough-bodies with small cutting angles.

3.2.3. *The curved tine without profile*

No process shapes have been described for this tine either, but we do know that plough-body curvature can give rise to specific process shapes. The existence of some similarity between curved tines and curved plough-bodies appears from (WILLATT and WILLIS, 1965), where it is stated that... 'a deeper rut is created by a curved tine than by a plane vertical tine', a phenomenon well known for plough-bodies.

4. SYSTEMATICS OF PLOUGH-BODY PROCESSES

A multitude of plough-body forms and positions are possible. As in the case of tines, the definition of phenomena can be greatly simplified by treating a few plough-bodies exhaustively and others with reference to those few plough-bodies.

4.1. Process parts

The process induced by a plough-body can be assumed to be composed of process parts. For these tools it is useful to define the following process parts: intake, main flow and output process. The intake process separates a soil-strip from the untouched soil. The main flow is the process during which the soil-strip flows along the plough-body. The output process includes the changes after the soil strip has left the plough-body.

Fig. 9 represents some plough-bodies: The plough-bodies a through h can be called 2-dimensional blades. They are characterized by:

- an infinite width,
- a horizontal cutting edge that is always perpendicular to the direction of travel.

In this way the process does not vary along a horizontal direction perpendicular to the travel direction, when soil heterogeneity effects are not being considered. For 2-dimensional blades important characteristics are the shape of the surface, the cutting angle and working depth in relation to the size, i.e. the height of the tool. If, for each of these three characteristics, two categories are chosen, a set of 8 standard blades arises, according to Table I.

The other plough-bodies in Fig. 9 are more widely known in agricultural practice: a mouldboard plough, a rotatiller blade, a sweep, and a potato harvester lifting blade. Within each plough-body process in the figure the intake is indicated by A, the main flow by B, and the output by C. As can be seen from the figure, the process parts may not be all clearly present for each plough-body.

Table I. Two-dimensional blades.

Cutting angle	Small				Large			
Shape	curved		plane		curved		plane	
Working depth-blade height ratio	small	large	small	large	small	large	small	large
Type in Fig. 9	a	b	c	d	g	h	e	f

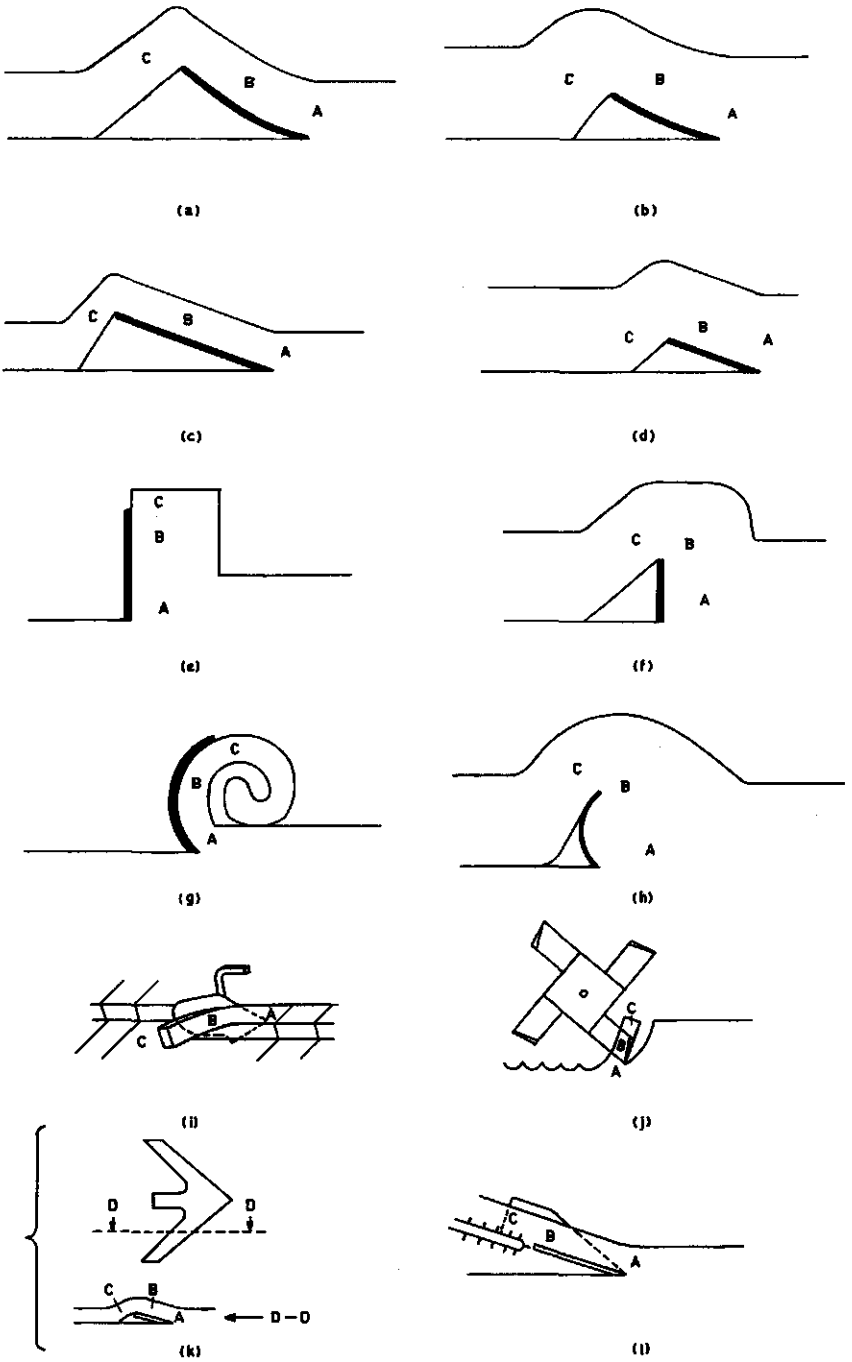

FIG. 9. Some plough-body shapes (A = intake process, B = main flow process, C = output process).

4.2. THE CURVED 2-DIMENSIONAL BLADE WITH SMALL CUTTING ANGLE AND SMALL WORKING DEPTH-BLADE HEIGHT RATIO

This blade is shown in Fig. 9a and has been treated in detail in (KOOLEN, 1972, 1973). Much of the following was first presented in these papers.

4.2.1. *The intake*

The different shapes of intake processes can be put into the following categories:

- intake by shear-plane failure: in the soil that is being taken in, failure surfaces occur and normal stresses act on (almost) all parts of these surfaces (Fig. 10a),
- intake by steady cutting: in the soil that is being taken in, failure surfaces do not (or seldom) occur (Fig. 10b),
- intake with open cracks: from the edge of the blade (share) cracks will develop, into which the share can penetrate like a wedge (Fig. 10c).

Intake by shear-plane failure. See Fig. 10a. The cutting edge of the tool tries

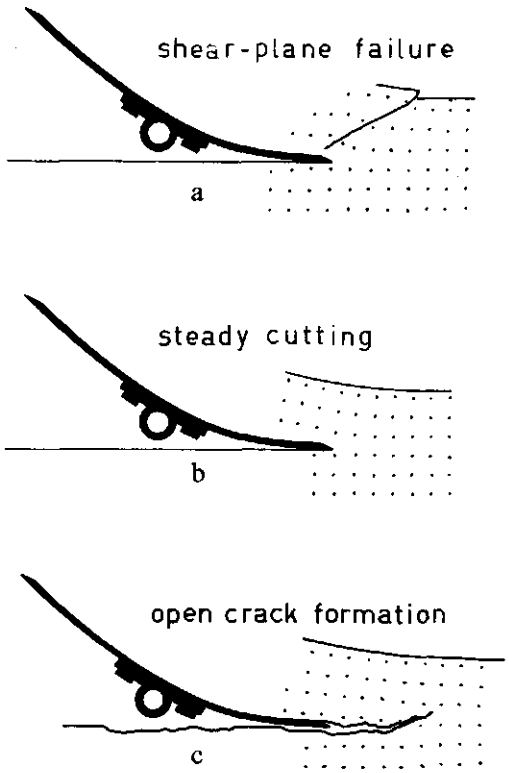

FIG. 10. Types of intake.

to push the soil upwards, thus inducing a field of increasing stress. As soon as the shear stress has become as large as soil shear strength (sum of soil cohesion and internal friction), a failure plane is initiated, which will extend very quickly up to the soil surface. The failure plane separates a soil lump moving upwards along the tool and the still firm soil. After soil lump separation, that is after overcoming cohesion and internal friction, cutting resistance falls until the pushing action of the cutting edge makes it rise again. Then the process is repeated and the following lump will be formed (SÖHNE, 1956).

Intake by steady cutting. See Fig. 10b. Each volume element of the soil being taken in deforms so as to enable the soil beam to follow the change in direction at the cutting edge without breaking or tearing.

Intake by open crack formation. See Fig. 10c. The cutting edge of the blade penetrates into the still firm soil, inducing a stress field in the soil. The field develops in such a way that, at a certain moment, a crack is initiated, which will extend in a near horizontal direction, thus clearing the path for the blade edge. The blade penetrates into the crack like a wedge, so that the crack is developed further. Direction of crack propagation is not stable. Several causes make the travelling crack turn off downwards or upwards more and more. Turning off can become so much as to inhibit the blade edge from following the crack opening any longer. Then the cutting edge must again penetrate into the still firm soil. At the same time crack front velocity decreases, and often becomes zero at a certain moment. With the starting of blade penetration in firm soil a new period of the process begins, which more or less resembles the previous period.

Hence, in the intake there is a cutting edge that sometimes penetrates firm soil and sometimes acts like a wedge, as well as a crack that usually continues to extend and the direction of which may vary. The edge action and the crack front action can interfere in such a way that the following phenomena can occur (Fig. 11): tongues in the bottom of the furrow, holes in the bottom of the furrow, slices left in the bottom of the furrow, slices left in the main flow.

4.2.2. *The main flow*

The basic shapes of the main flow are based on blade curve variation. The following shapes may be distinguished:

- blade with curvature increasing towards the end,
- blade with curvature decreasing towards the end,
- blade with constant curvature (arc of a circle).

4.2.2.1. Main flow in the case of blades with curvatures increasing towards the end

The soil from the intake process is transported to the output process by the main flow. During this main flow process the soil can also be changed to a certain extent. The shape of the soil-strip that is delivered to the main flow is determined by the intake process. If the intake process is pure steady cutting, the strip will be continuous. An intake process with shear-plane failure gives

FIG. 11. Tongues, holes and slices in the case of intake with open crack formation.

a strip of moving pieces separated by parallel failure planes. If open cracks are formed during the intake process, the main flow will normally receive a soil-strip that is more or less cracked at the lower part. Parts of the soil-strip over these cracks can be indicated as hinges. So 3 main types of soil-strip delivered to the main flow can be observed (Fig. 12):

I. unbroken strip,
II. strip of pieces connected by hinges,
III. strip of pieces moving along each other.

Soil-strip of type I. Here an unbroken soil-strip is delivered to the main flow. If there is an overall contact between the blade and the soil-strip, the whole strip must be deformed during its movement along the blade, because blade curvature is not constant. Sometimes contact between blade and soil can be lost. In that case tension cracks may develop in the lower part of the strip (Fig. 13).

Soil-strip of type II. If the soil-strip delivered to the main flow consists of pieces that are connected by hinges not much weaker than the pieces themselves, its behaviour will very much resemble that of an unbroken strip. If the hinges are much weaker than the pieces, every change in curvature will be absorbed entirely by the hinges and the pieces will move as rigid bodies along the blade. Because the curvature is increasing, the cracks under the hinges will be widened. Old crack fronts may become active again. Usually cracks that produce hinges run from the bottom of the strip in a forward and upward direction, and the pieces are pointed in this way. These points crumble during the main flow process especially on drier soils. Occasionally these points stay behind a little causing a certain rotation (Fig. 14).

Soil-strip of type III. If the intake process delivers a set of pieces moving parallel to each other, this parallel movement will be maintained on the blade, allowing pieces to keep parallel to each other when following the blade curve.

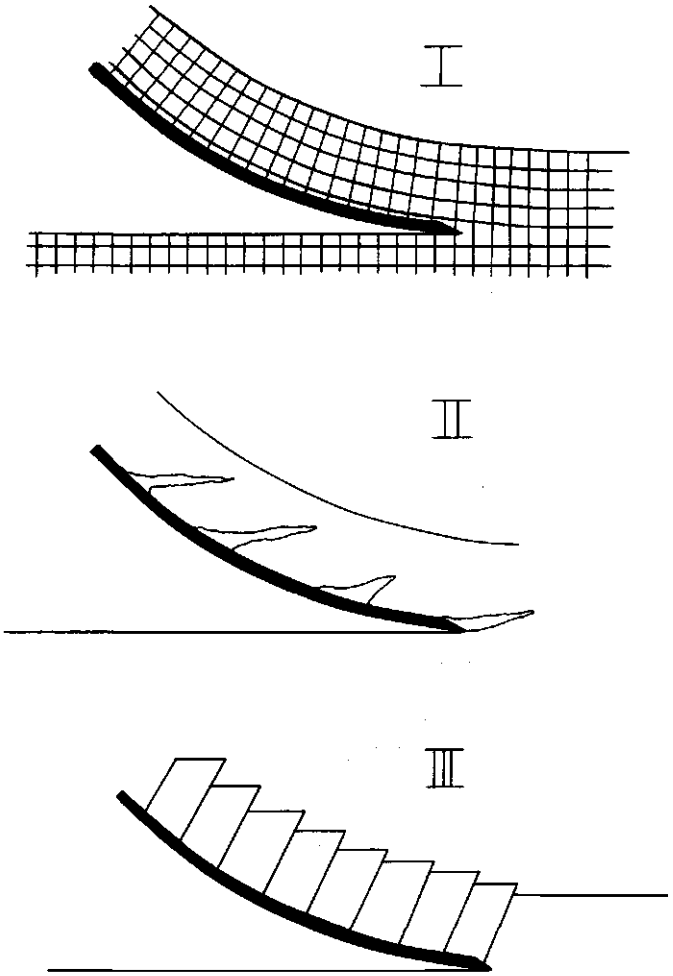

FIG. 12. Types of main flow.

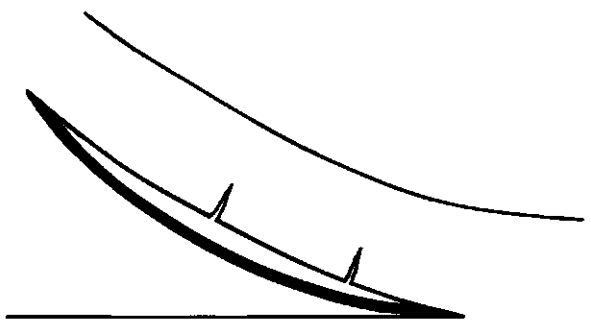

FIG. 13. Tensile cracking due to soil-tool contact being partly lost.

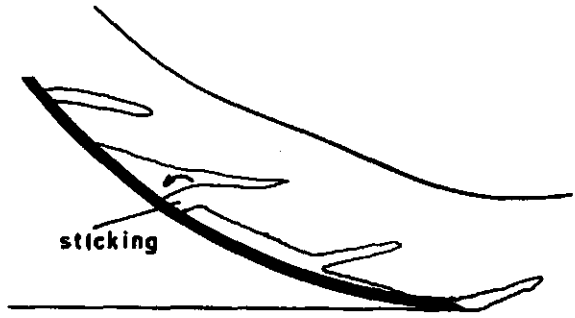

FIG. 14. Rotation of an adhering tongue.

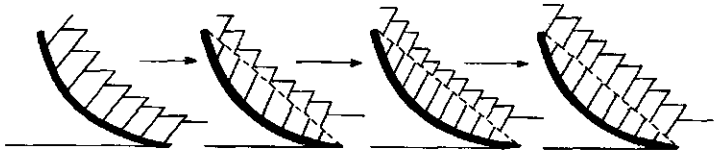

FIG. 15. Filling up of the hollow of the blade.

If binding forces inside the pieces on the curved blade are small, the bottom parts of these pieces will crumble and fill up the blade curvature. Then the blade is changed more or less into a plane plate and the pieces will not have to move parallel to each other any more (Fig. 15).

4.2.2.2. Main flow in the case of blades with curvatures decreasing towards the end

The above description of types I, II and III apply, on the understanding that, in the case of type II,

- cracks below hinges close as the strip travels over the blade,
- there is much less falling behind of pointed ends of soil pieces.

4.2.2.3. Main flow in the case of blades with a constant curvature

Here too, the above mentioned type III may occur. Although blade curve is constant, relative movements between successive pieces are maintained, allowing the pieces to follow the blade curvature without any rotation of the pieces. However, if the main flow receives an unbroken soil-strip or a strip composed of pieces connected with hinges, a process type will occur that does not involve any soil deformation when the soil beam follows the blade curve.

4.2.3. *The output*

The output process contains the changes after the soil-strip leaves the blade. If the soil-strip is extended further behind the end of the blade, the cross section over the end is stressed more and more. At a certain length this extending part

starts to break or to shear off. When the failure surface is completed, a piece of soil is formed, and this falls down freely. Normally these pieces have other dimensions than those formed by the intake process and the main flow. The free fall ends in a collision in the furrow where the piece joins previously formed pieces. At the same time the main flow produces the next piece and the process is repeated.

The length of the pieces formed in this breaking process depends on soil strength and the degree of weakening by the intake process and the main flow. This is illustrated in Fig. 16, which shows for several processes the pieces that are successively formed when the soil leaves the blade. In this figure the cracks that are formed during input and main flow are indicated by solid lines, and the cracks that are formed when the soil leaves the blade are indicated by broken lines. In Fig. 16a the intake process produced a few cracks but they did not weaken the soil-strip to the extent of influencing the position of the output cracks. This is opposite to Fig. 16b where intake and output are so closely related that output cracks nearly always coincide with input cracks. This is also the case in Fig. 16c. The relatively long length of output pieces in Fig. 16d can be explained by the high cohesion of this soil-strip. Nevertheless, output cracks have a certain preference for places where input cracks are present. In Fig. 16e there is a relationship between intake and output cracks in some places and no relationship at other spots. Obviously there is only a relationship if the intake crack is in a favourable position.

When a piece breaks off the strip, a rotation starts and, therefore, the piece has a certain angular speed when it starts falling. The value of the angular speed depends on the length of the piece, soil plasticity and the position of the output-

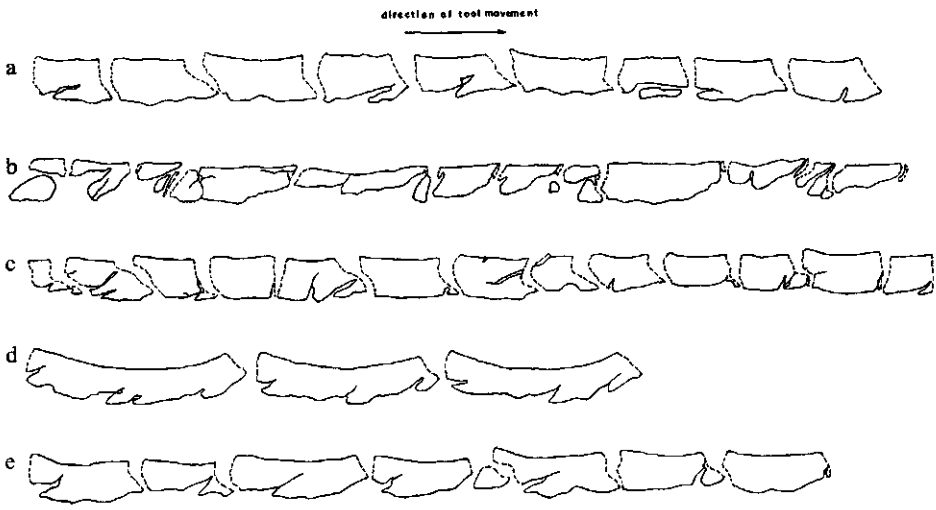

FIG. 16. Pieces that are successively formed when the soil leaves the blade (shown for several processes).

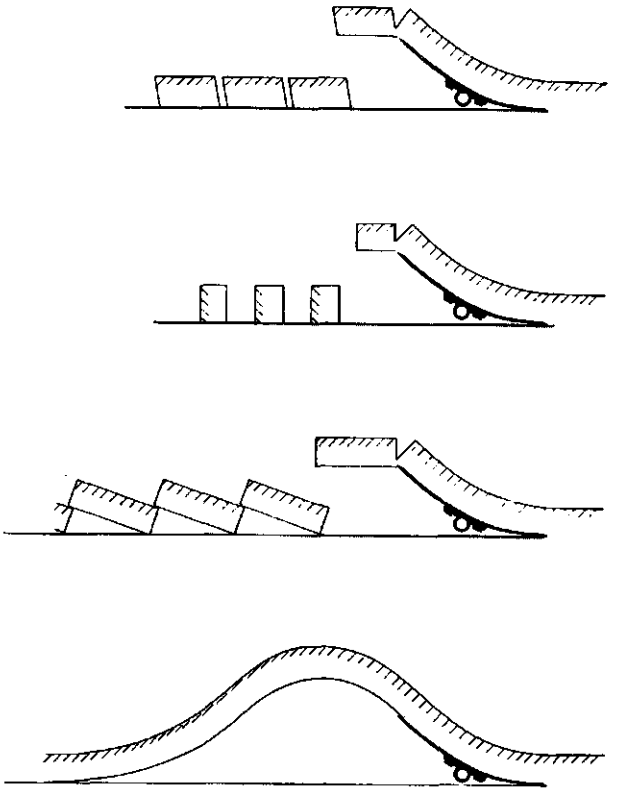

FIG. 17. Output processes (KOOLEN, 1972).

crack relative to the input-crack. This free fall of the piece ends in a collision with the bottom of the furrow or with foregoing pieces. If cohesion is low, the soil may crumble at this collision. The series of fallen pieces shows a geometry that is determined by the shape of the pieces and by angular speed obtained in the breaking process. Some types of this geometry are given in Fig. 17. The upper three cases present processes in which the velocities are very low. In the first case the soilstrip is compacted and deformed. At higher speeds the last output type of Fig. 17, which is well-known in practice, can be observed. Several pieces, not distinctly separated, are involved at the same time in the output process.

4.3. FURTHER PLOUGH-BODIES

4.3.1. *The curved 2-dimensional blade with small cutting angle and large working depth-blade height ratio*

If for the blade that has been discussed above (section 4.2.), the working depth is increased to a large working depth-blade height ratio (Fig. 18), then some important changes will occur:

- the main flow will become smaller in relation to the other process parts,
- the soil will have to curve more in the intake,
- the ratio between height of fall in the output and working depth will become smaller.

This blade (like all following plough-bodies) will be able to cause many of the phenomena discussed for the previous blade, but only observations from (NICHOLS et al., 1958) are available, showing intake by shear-plane failure. The same paper indicates the importance of the shape of the cutting edge for the process shape. It is illustrated in Fig. 19. Of course, such cutting edge effects will not be restricted to this type of blade.

4.3.2. *The plane 2-dimensional blade with small cutting angle and small working depth-blade height ratio*

Intake. The intake processes of this blade can be separated into the types defined in 4.2.:

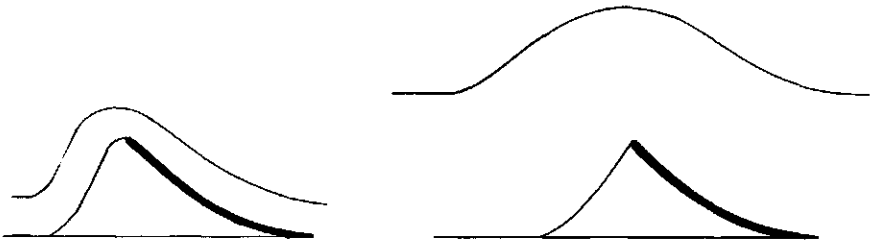

FIG. 18. Towards a larger working depth-blade height ratio.

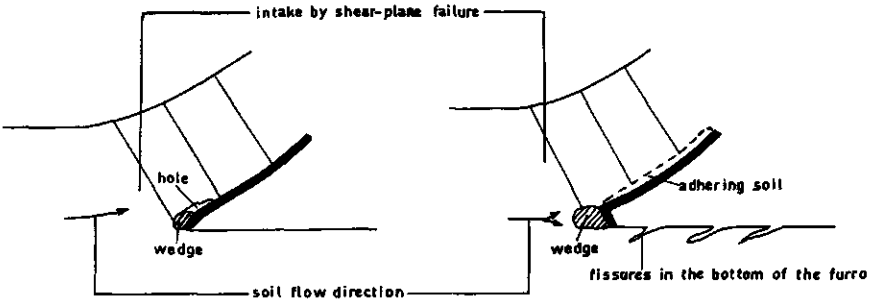

FIG. 19. Some cutting edge phenomena (NICHOLS et al., 1958).

- intake by shear-plane failure (SÖHNE, 1956; DREES, 1956; SELIG and NELSON, 1964; ELIJAH and WEBER, 1968),
- intake by steady cutting (SÖHNE, 1956; DREES, 1956; ELIJAH and WEBER, 1968),
- intake with open crack formation (SELIG and Nelson, 1964; KAWAMURA, 1952; DREES, 1956; ELIJAH and WEBER, 1968).

Main flow. In soil moving over a plane blade, changes are at a minimum. Nevertheless, some changes occur due to friction at the blade surface, as can be seen from (ELIJAH and WEBER, 1968). This paper presents stresses measured at the soil-blade interface. The paper reports that locations of stress moved along the tool. These locations sometimes suddenly disappeared, probably by rotation or pulverization of the soil. Quite often the highest stresses were not measured at the bottom of the tool. A stress transducer gave a zero signal for 20–80% of the time, the percentage being strongly dependent on soil type, and tending to increase with soil strength.

Output. For the output the reader is referred to 4.2.3.

4.3.3. *The plane 2-dimensional blade with small cutting angle and large working depth-blade height ratio*

If a plane blade with small cutting angle is changed from a small working depth-blade height ratio to a high working depth-blade height ratio, then
- the main flow will become smaller in relation to the other process parts,
- the height of fall-working depth ratio is decreased.

Diminishing the importance of the main flow influences the intake. For plane blades this is shown in (SELIG and NELSON, 1964). This paper presents the development of the process shape in the course of time from the very start of the tool for a plane blade with small working depth-blade height ratio. It appeared that at the start, where a main flow had not yet developed (so where the process corresponds with that described in 4.3.3.), the process shape differed from that occurring after some decimeters of tool travel, where a main flow and an output were present (corresponding with 4.3.2.).

All intake processes described in literature for plane 2-dimensional blades with small cutting angles and large working depth-blade height ratios can be divided into:
- intake by shear-plane failure (SÖHNE, 1956; SIEMENS et al., 1965; OLSON and WEBER, 1966),
- intake by steady cutting (SÖHNE, 1956; OLSON and WEBER, 1966),
- intake with open crack formation (KAWAMURA, 1952).

4.3.4. *A blade derived from 4.3.3.*

In the case of a plane blade with a small cutting angle and a large working depth-blade height ratio, that has a side running through an open furrow, the shape of the intake will follow the pattern indicated in Fig. 20 (SÖHNE, 1956), when the intake is assumed to be of the shear-plane failure type. There are additional cracks, being more or less parallel to the furrow.

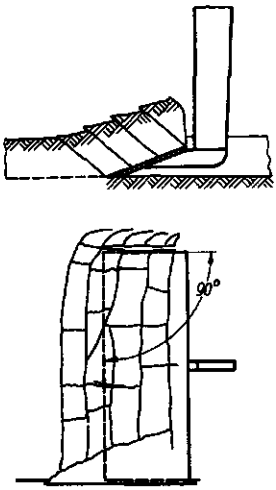

FIG. 20. Additional cracks due to one side of the blade travelling through a furrow (SÖHNE, 1956).

4.3.5. *Blades with small cutting angles versus blades with large cutting angles*

Blades with large cutting angles are rather similar to blades with small cutting angles, but it will be shown that there are also many differences, such as:

- intake by open crack formation is not likely to occur when the cutting angle is large,
- in the intake of a blade with a large cutting angle a soil wedge tends to form, which can be considered as being part of the blade,
- the outputs of blades with large cutting angles are not always directed backwards, but can occur in a forward direction.

4.3.6. *The curved 2-dimensional blade with large cutting angle and small working depth-blade height ratio*

Intake. DREES (1956) reports: 2 types of intake exist, namely intake by shear-plane failure and intake by steady cutting. Sometimes the intake is accompanied by cracks that start from the cutting edge and travel at an acute angle downward from the forward horizontal. These cracks can later be found in the bottom of the furrow.

Main flow. Depending on the type of intake involved, one of the two 'main flow' types that are presented in Fig. 21, will occur. Especially, in the case of this blade it is useful to realize that the length of the main flow cannot exceed a certain limit. Several reasons for this can be indicated.

- An obvious one is if the soil reaches the blade end. Then there is output as defined for the blades already discussed.
- Another cause involves a main flow that curls up, giving rise to a curled up soil beam in front of the main flow. Blade curvature can advance this action (DREES, 1956). See Fig. 22.

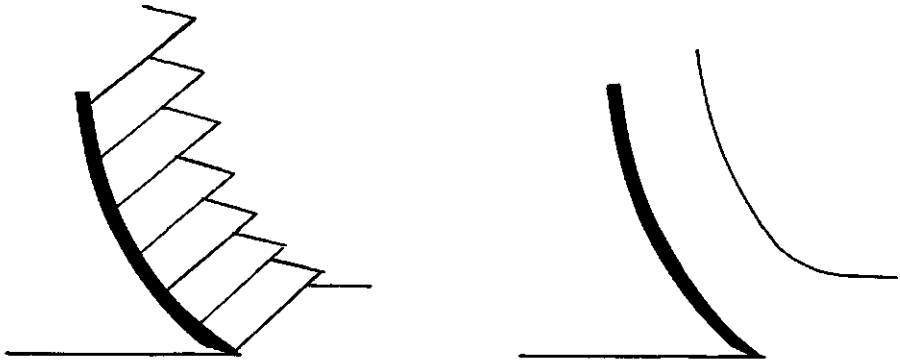

FIG. 21. 'Main flow' types at large cutting angles and backwards directed output.

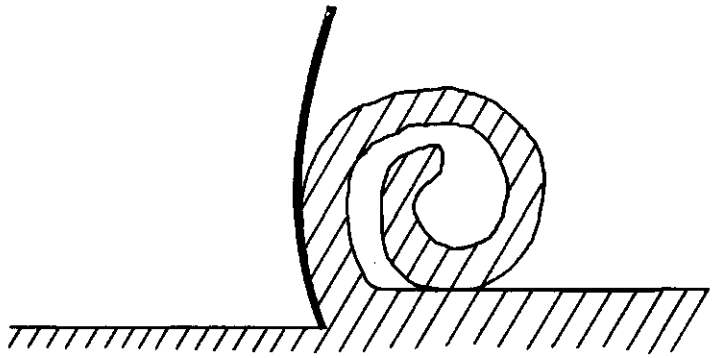

FIG. 22. Curling up.

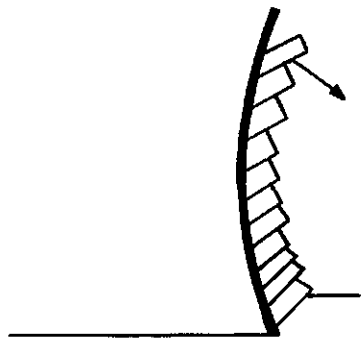

FIG. 23. Pieces falling forwards.

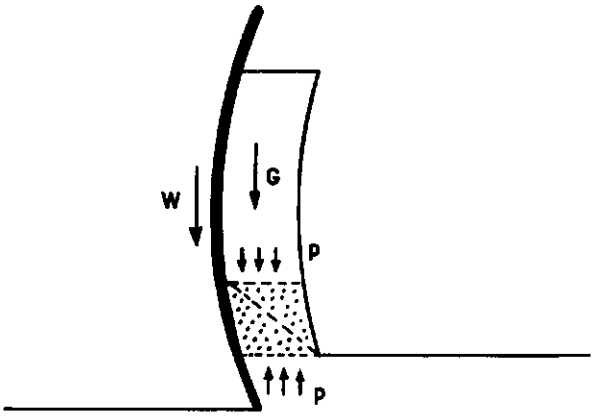

FIG. 24. Failure of the main flow.

– A third cause is represented in Fig. 23. The soil is bent forward so far, that because of the great beam inclination the soil fails or rolls, and will fall forward and downward (DREES, 1956).
– Fig. 24 demonstrates a last cause. Here, the length of the main flow is limited as shear strength of the soil in the first part of the main flow is reached. The shaded part of the soil is loaded by a stress p that originates from the blade-soil friction force W and the weight G of the soil which is on top of the shaded part. With the increase in main flow length the forces W and G increase, and so does p. If p becomes large enough to make the soil in the shaded part fail, a failure plane develops that nearly follows the broken line in the shaded area. The column over the broken line slides forward and downward, which can be considered to be be the output process. The process is repeated periodically, piling up an increasing amount of soil in front of the main flow. It should be noted that soil strength involved in such cases is often very low because of soil heterogeneity and the soil weakening that has occurred in the intake.

Output. If there is an output being directed backwards, then it will very much

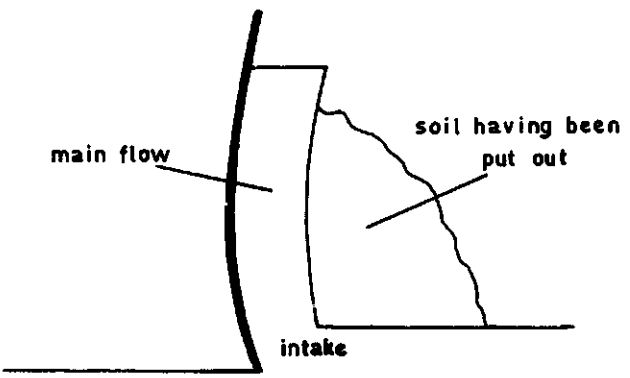

FIG. 25. Permanent influence of soil having been put out.

resemble that which is defined for the previous blades. In the case of forward output soil will fall in front of the blade to the top of the still firm soil (see Fig. 25), which has two significant consequences. Firstly, weight of the soil having been put out rests on the intake zone, and this additional load influences the shape of the intake process. Secondly, the main flow has to push forward the fallen soil like a bulldozer, which gives rise to a mutual influence between the main flow and the soil that has been put out.

4.3.7. *The curved 2-dimensional blade with large cutting angle and large working depth-blade height ratio*

Section 4.3.6. dealt with the curved 2-dimensional blade with a large cutting angle working at a small working depth-blade height ratio. If for this blade the working depth-blade height ratio is altered to a large value, then the following changes will occur:

- the main flow becomes comparatively much smaller,
- the soil must curve more at intake,
- although some soil may fall forward, output is always directed backwards, because in this case the main flow can hardly exert any bulldozing action.

According to OSMAN's observation (1964) there are two types of intake:

- intake by shear-plane failure,
- intake by steady cutting.

At strong blade curvatures the blade may be filled up with a soil body that has been immobilized and should be considered as part of the blade. See Fig. 26. In that case the blade acts like a plane blade with a cutting angle equal to α' and a soil-tool friction angle equal to the angle of internal soil friction.[1]

4.3.8. *The plane 2-dimensional blade with large cutting angle and small working depth-blade height ratio*

Sometimes a wedge tends to be formed, as can be deduced from work done by SELIG and NELSON (1964). Two types of intake can be distinguished:

[1] No distinction is made in this report between the angle of internal soil friction and the angle of sliding friction between two rigid bodies of soil.

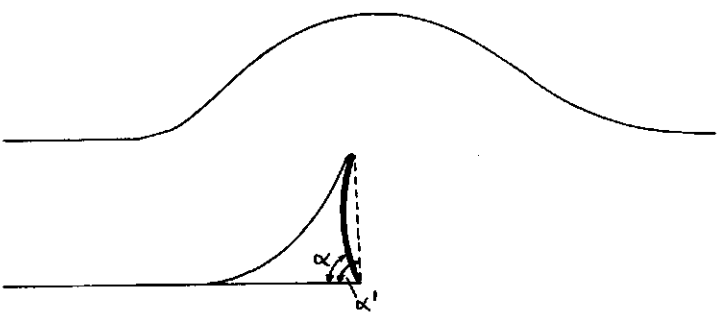

FIG. 26. A curved blade being filled up.

- intake by shear-plane failure (PAYNE, 1956; SELIG and NELSON, 1964; O'CALLAGHAN and FARRELLY, 1964),
- intake by steady cutting (4.3.9. provides evidence for this possibility).

Large cracks that travel forwards and downwards at an acute angle with the horizontal may develop from the blade cutting edge (SELIG and NELSON, 1964).

4.3.9. *The plane 2-dimensional blade with large cutting angle and large working depth-blade height ratio*

SIEMENS et al. (1965) report a tendency for wedges to be formed. Two types of intake appear to be possible:

- intake by shear-plane failure (OSMAN, 1964; SIEMENS et al., 1965; OLSON and WEBER, 1966),
- intake by steady cutting (OSMAN, 1964; OLSON and WEBER, 1966).

4.3.10. *More complicated plough-bodies*

Plough-bodies used in practice often have a more complicated shape than the 2-dimensional blades that have already been dealt with. For these more complicated plough-bodies only a few investigations into process shapes have been conducted, but it can be easily seen that many of the phenomena defined for the blades will also occur in the case of the more complicated plough-bodies, such as the mouldboard plough, blade of rotary tiller, sweep, potato harvester lifting blade, etc. Indeed, a good observer of tillage processes in practice is sometimes able to see phenomena such as: tongues in the bottom or in the wall

FIG. 27. Tongues in a furrow.

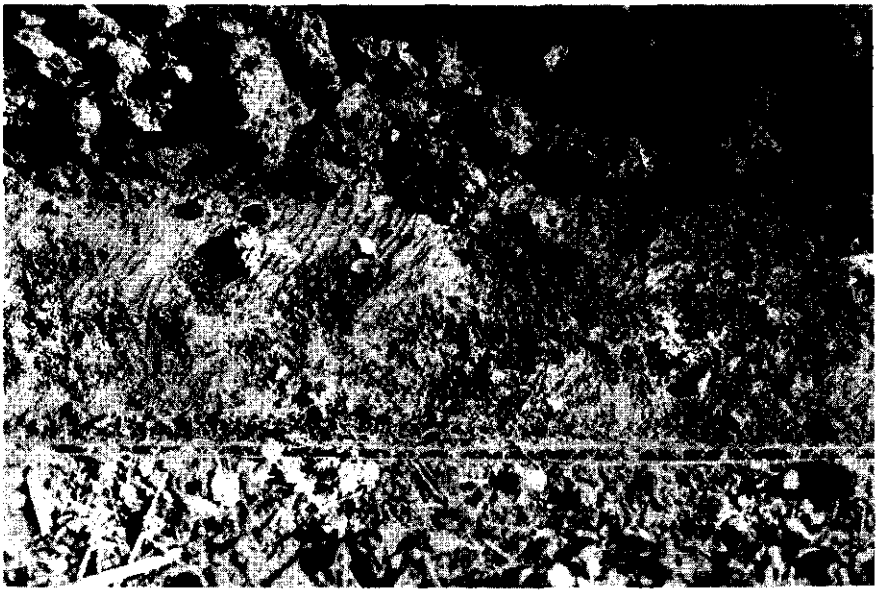

FIG. 28. Holes in a furrow bottom.

FIG. 29. A ploughed field exhibiting a very regular pattern.

of a furrow (Fig. 27), holes in a furrow bottom (Fig. 28), a strong regularity in the soil beam left by a mouldboard plough (Fig. 29).

CHASE (1942) made observations from sweeps that show the possibility of the main flow length being smaller than the tool length. He reports: 'If the blade is flat, it will slip through the soil disturbing it or the vegetation very little, as shown by Fig. 30a, but if the angle of the blade to the horizontal is too great, so much resistance to the movement of the earth over the blade is set up that the soil and trash jam together and cause not only a mixing of the mass but an uneven distribution on the fixed soil, and entirely too often a complete clogging of the gang of tillers (Fig. 30b).' The same paper reports the following on the significance of the cutting edge: 'Sweeps were also tried with the bevel side up and the same pitch for the body of the blade. We found this gave better penetration in hard ground, but also introduced a scouring problem in many fields

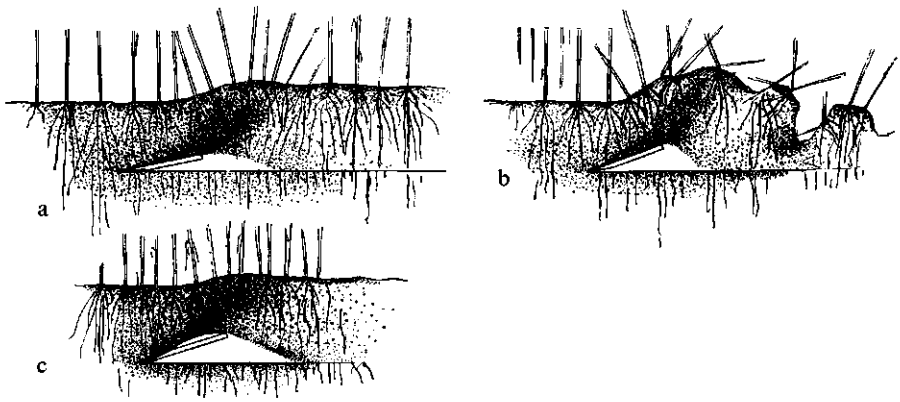

FIG. 30. Sweep phenomena (CHASE, 1942).

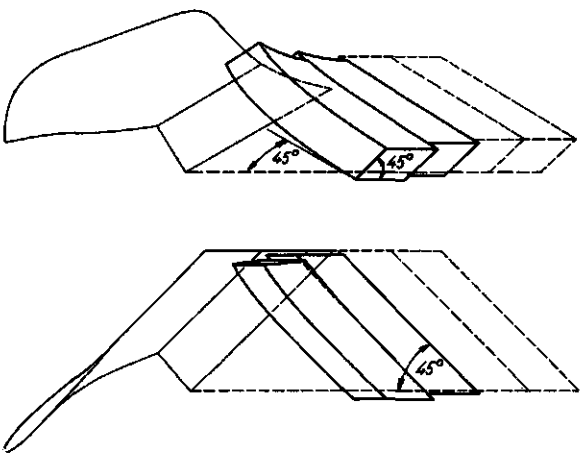

FIG. 31. Primary shear planes at mouldboard ploughing. (SÖHNE, 1956).

and especially when the ground had to be tilled the second time ater the first. Just at the rear of the break between the bend and the body of the blade is an area of reduced pressure (Fig. 30c), and unless the soil is in a very dry condition, it will adhere at this point and eventually cause choking'.

That the main flow has a limited length, also appears from the fact that lifting blades of potato harvesters may be choked. It is described in (HAWKINS, 1957).

For subsoilers NICHOLS and REAVES (1958) report wedge formation and indications for the possibility of shear-plane failure and steady cutting.

In (NICHOLS and REED, 1934) the process of mouldboard ploughing 'under normal conditions' is defined as follows. Near the plough-share shear-planes develop as Fig. 31 shows, which separate soil blocks. These planes are called primary shear-planes. As these blocks are travelling over the mouldboard failure planes (called secondary shear-planes) develop perpendicular to the primary planes. The formation of primary shear-planes described in this paper should be considered as intake by shear-plane failure and the formation of secondary shear-planes as a phenomenon belonging to the main flow.

Finally it should be noted that attempts to classify mouldboard shapes can be found in (SÖHNE and MÖLLER, 1962; HÉNIN et al., 1969; DALLEINNE and BILLOT, 1975).

5. CLOSING REMARKS ON SYSTEMATICS

When it is the intention to separate all process shapes (types) that tools or tool parts can induce into a classification system, use may be made of:
- a system based on process shapes,
- a system based on tool properties,
- a system being founded on process shapes as well as on tool properties.

The last alternative has been followed here.

A system based on process shapes. A start for a system based on process shapes is represented in Fig. 32. Firstly, a distinction has been made between loosening processes and load bearing processes, which are defined as: in loosening processes unstable deformation is most significant, and in load bearing processes stable deformation is most significant. According to these definitions processes with intakes by steady cutting must probably be considered as load bearing processes. In the first stage of the tillage process firm soil will be loosened, so this includes the intake processes of plough-bodies. The second stage involves further tillage tool action in soil already loosened, and comprises, for instance, main flow processes. As soon as the soil leaves the sphere of direct influence of the tool, the third tillage stage will start, under which output phenomena can thus be understood, for example soil pieces falling and the impact between soil pieces and the furrow bottom. If in the first stage the soil is highly confined, then a certain kind of stable deformation will be present, which may give rise to wedges as observed in the cases of steep tines and plough-

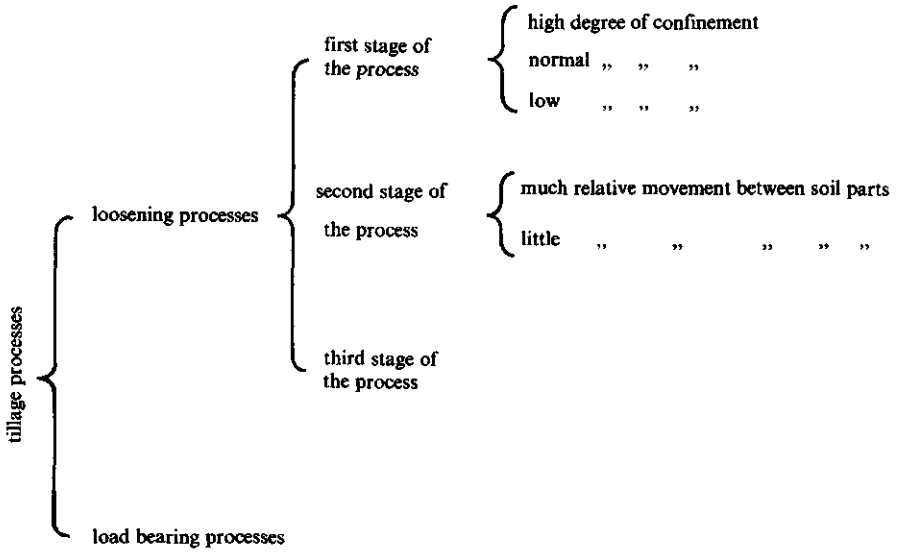

FIG. 32. Hypothetical classification system based on process types.

bodies with large cutting angles. At a normal degree of confinement this wedge formation does not occur. When there is a low degree of confinement, then many zero stresses or tensile stresses are present, which will be accompanied by open crack formation and further opening of cracks already initiated. Sometimes, the second process stage involves much relative movement between parts of soil, as in the main flow of many curved blades, and, possibly, between the separated soil clods being present at the front and at the sides of a tine. Relative movement between soil parts may also be insignificant as on a plane blade.

However, current knowledge of processes is still insufficient to design a thorough system based on process shapes. In addition, such a system would be difficult to handle in practical applications.

A system based on tool properties. It may be possible to develop a systematics based on tool properties such as:

- dimensions,
- contour,
- curvature of surface,
- position,
- working depth.

Such a system would probably involve a series of tools ranging from simple to very complicated. A great deal is known about processes of simple tools, which is in contrast to the situation concerning complicated tools, although it is the complicated tools that are important in practice. If a system based on tool properties is selected, then simple tools would be emphasized too much, and the similarity between simple and complicated tools would not be expressed. It is this similarity that helps us to understand the processes of complicated tools (compare, for instance, a plane tine with a wedge-shaped tool).

A system based on process shapes as well as on tool properties. The system followed in this report is outlined in Fig. 33. Here, loosening processes are defined as processes which *aim* at loosening the soil. So they also comprise processes that do not meet the intended aims. A tool shape is considered to be basic if it is able to induce processes that are rather general, and is not more complex than necessary for these general processes to occur. In order to keep the number of basic shapes as low as possible, they should change as the system extends further. In the case of plough-bodies, process parts (intake, main flow, output) have been distinguished for each basic tool shape. The process parts are related to tool parts, which can also have many shapes. Therefore, basic shapes in tool parts should also be selected. For instance, at the main flow of a curved blade such basic shapes may be: blades with a curvature that increases towards the end; blades with a constant curvature: blades with a curvature that decreases towards the end.

In making this outline the following considerations have been aimed at:

- the lowest division should separate all process types that a tool or tool part is able to induce. This links up best with the prediction methods that are most promising (see sections 6–9),
- processes that do not meet the intended aims, should also have our attention.

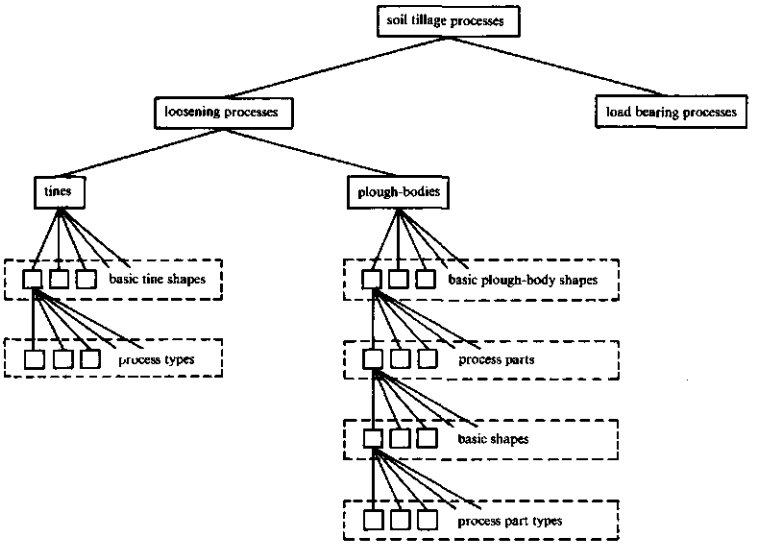

FIG. 33. Proposed classification system.

This may result, for instance, in a better understanding of soil workability limits,

- the classification system should allow the knowledge already available to be presented in such a way that the chance of the system being wrong when further knowledge is available is as small as possible,
- similarities should be highlighted in order to gain more insight into the more complicated processes, which are difficult to investigate,
- in the case of tines process parts cannot yet be distinguished, because current knowledge is too limited.

6. INTRODUCTORY REMARKS ON PREDICTABILITY

6.1. WHAT SHOULD BE PREDICTED?

An ideal situation would exist if, for each tillage process at any moment and any location in the process, the following could be predicted:

- the state of stress in the soil,
- the state of strain in the soil,
- the amount of displacement and rotation the soil sustained in the process before the moment considered,
- whether a failure surface or crack is present or not, and the state of movement of such a crack or failure surface.

In that case:

- the tillage results for each soil volume element that has been subjected to the process would be known in terms of amounts of deformation, rotation, displacement and failure,
- using integration procedures, the horizontal and vertical forces on the tool could be calculated from normal and shear stresses that are present along the tool face,
- there would be an adequate starting point in case we want to optimize the process further with respect to, for instance, tillage results, energy consumption, or tool shape feasibility in manufacturing.

Unfortunately, this ideal has still not been reached, and will not be reached in the near future either, because of the very complexity of tillage processes and of involved soil mechanical properties. However, in many cases it is still useful to be able to predict only an aspect of a process. A few of these aspects follow below.

It is very important to be able to predict the type of process involved in a certain tillage operation. Presumably, workability limits (limits identifying soil conditions that allow tillage results to be satisfactory), which are important in practice, correspond with changes in process type. Research into changes in process type with a view to tillage results is very limited, probably because the necessity of distinguishing process types is still hardly recognized.

The ability of predicting changes in process type is also important for the predictability of aspects like draught force etc. Generally, prediction methods for predicting draught force are only valid for one process type. In tests for draught force prediction method verification many disappointments must have arisen, due to distinct process types not being recognized (sometimes testing the method on another process type than that for which the prediction method was established). Only very recently has the idea grown that, in the case of draught force predictions, one must also define the process type to which the prediction method is intended to apply (SPRINKLE et al., 1970; PANWAR et al., 1973).

Other significant aspects we should be able to predict are the horizontal and vertical forces on a tool without any further specification of the normal and shear stresses on the tool. A number of methods available for this assume arbitrary failure patterns. These methods have a reasonable success, which may be surprising since the assumed failure patterns are often incorrect and conflicting (WITNEY, 1968; OSMAN, 1964; COOK and REECE, 1966; WHITMORE, 1968). The surprise is less when examining the rising limit analysis theories, which discuss the degree of freedom allowed in selecting failure patterns for resistance calculations (YONG, 1973; SMITS, 1973; CHEN, 1975).

Further important aspects that should be considered for prediction are the undesired local tillage effects, like puddling at the bottom of a furrow, or an undesirable final arrangement of soil parts. Prediction of such aspects is likely to be simpler because it mainly involves a process part only. Examples of solutions are hardly known.

Finally it should be noted that the ability of predicting an aspect not being directly useful, is also significant, because it may form an element in the further construction of the arsenal of predicting methods.

6.2. TO WHAT ACCURACY SHOULD WE PREDICT?

In predicting a soil tillage process aspect the question of what would be the consequence of an inaccuracy in the prediction will be encountered. The significance of such an inaccuracy should be indicated in terms of the loss of profit or the rise in costs, due to the inaccuracy in the aspect prediction. Far from all aspects have been investigated to such an extent that they can be related to profit or costs. At the moment it is only possible for the aspects: draught forces and workability.

For ploughing costs to be at a minimum, ZOZ (1974) presents graphs that allow the determination of tractor weight and power from factors such as: acreage to be ploughed annually, ploughing depth, specific ploughing draught, fuel costs, labour costs, etc. For United Kingdom conditions and with 200 acres to be ploughed annually the following can be read from the graphs: in the case of a specific draught of 8 psi (at zero speed), the total ploughing costs per acre is minimum ($\pm$ 5.5 dollars) if use is made of a tractor with the specifications

power: 115 pto hp
weight: 127 lb/pto hp

If a specific draught was predicted as 9 psi for this soil with a true specific draught of 8 psi, (thus involving a prediction error of 12.5%) then, due to the erronous prediction, the following tractor would have been selected from ZOZ' graphs:

power: 125 pto hp
weight: 129 lb/pto hp

This selection would increase the total ploughing costs per acre. According to ZOZ' graphs this increase in costs is probably much less than 5%.

BUISHAND (1973) presents a graph in which the pod yield of butter-beans (*Phaseolus vulgaris L.*) has been plotted against sowing date. This graph shows that pod yield may decrease by $\pm 10\%$ when, due to an erronous workability prediction, tillage and sowing dates are delayed by 1 day. On the other hand, we know that the yields of many crops are unaffected by the sowing date. Very little is know yet about losses of profit due to tilling too early.

From the few examples presented it can be concluded that the accuracy required in predicting will differ for the different aspects.

6.3. FROM WHAT SHOULD WE PREDICT?

Aspects of a tillage process can only be predicted provided information is available concerning the tool, the soil-tool system, and the soil. Tools may be characterized by shape, dimensions, position, surface condition. Information concerning the soil-tool system may be: working depth, forward speed. As opposed to the information of the tool and the soil-tool system, the pertinent information of the soil is still difficult to define. Therefore, any soil characteristic that may be related to tillage process aspects, should be considered to serve as a basis in predicting. These soil characteristics can be divided into:

- relationships between 'treatment' and 'behaviour' of soil,
- properties used in soil science,
- mechanical properties,
- aspects of characterization processes.

Relationships between 'treatment' and 'behaviour' of the soil. Soil behaviour in a tillage process will depend on the treatment to which the soil has been subjected prior to the tillage process in question. That treatment may be composed of a series of:

- tillage operations,
- wettings,
- dryings,
- warmings,
- coolings,
- thixotropic processes (changes within the soil in the course of time, not due to an external cause).

Measures of soil behaviour in tillage are, for example,

- draught force needed,
- data reflecting soil pulverization, deformation, compaction, displacement.

Knowledge of the relationships between soil treatment and behaviour may provide a basis for the prediction of process behaviour in those cases where previous soil treatment is known.

Properties used in soil science. Soil science uses a number of quantities to characterize soil as a material, and to define transport processes within the soil. Among them the following should be considered for the purpose of tillage process prediction (KOOLEN, 1976):

- texture,
- number of soil particles in a unit of volume, which complements porosity,
- the distribution of soil particles in space, related to pore-size distribution,
- the volumetric moisture content (cm^3/cm^3),
- soil-water distribution within the soil,
- the bonds at points of contact between solid particles not arising from soil moisture tension,
- distribution of these bonds.

These quantities relate directly to soil strength (KOENIGS, 1961; SCOTT, 1963; TOWNER and CHILDS, 1972). The above quantities are connected with the following quantities, which can often be measured more easily, or which are more widely known:

- soil porosity,
- soil moisture content as a percentage of dry weight,
- water retention,
- measures of soil structure and stability.

Mechanical properties. Soil loosening processes in tillage are such that the investigation of them may be considered as research into mechanics, for mechanics is the science that studies the *movements* of material systems in the broadest sense. Indeed, we may use quantities like:

- specific mass of the soil,
- cohesion,
- angle of internal friction,
- adhesion,
- angle of external friction,
- spring constant,
- damping constant.

The above quantities arise from 'rigid body' mechanics. However, observations tell us that, prior to tillage, soil is also like a continuous deformable material, and useful quantities may therefore also be taken from mechanics of 'deformable solids'. This brings us to the following quantities:

- elastic modulus,
- modulus of compressibility,
- Poisson's ratio,
- shear modulus,
- notch sensitivity factor,
- rate of propagation of elastic waves in soil,
- yield strength,
- coefficient of viscosity,
- further rheological material constants.

It is not true that the mechanical properties mentioned are always most useful for our purpose, because mechanical behaviour of soil is more complex than that of those materials for which mechanics was mainly developed. When the definition of the pertinent soil mechanical properties is intended, it is advisable to follow a more general method that basically stems from mechanics of

deformable solids. In this science a mechanics problem is usually reduced to the solution of the following set of equations:
- equations of equilibrium,
- boundary conditions,
- constitutive equations.

For soil tillage processes the constitutive equations are equivalent to soil mechanical properties. In this sense, the mechanical properties can be assumed to comprise the geometrical changes (compaction, deformation, failure) that a small soil volume element will show when loaded by stresses p_1, p_2, p_3 (see Fig. 34), and this for all possible values of p_1, p_2 and p_3. A number of special cases from this range of geometrical changes have got special attention, because of reasons such as:
- measuring being comparatively easy,
- great usefulness in theoretical analyses,
- representing a salient point in the range.

Each of the following tests involves such a special case:
- compaction test using a hydrostatic stress ($p_1 = p_2 = p_3$) (DEXTER and TANNER, 1973; DEXTER and TANNER, 1974),
- uni-axial compression test (KOOLEN, 1974),
- triaxial test at constant p_3 (BISHOP and HENKEL, 1964),
- triaxial test at constant p_m ($p_m = (p_1 + p_2 + p_3)/3$) (BAILEY and VANDENBERG, 1968; BAILEY, 1971; BAILEY, 1973; DUNLAP and WEBER, 1971),
- unconfined compression test (KAROL, 1960),
- tensile test (FARRELL et al., 1967).

Above, the tests are ranked according to the degree of sample confinement during testing. The sample confinement is highest in the first test, and lowest in the tensile test. Tests involving a low degree of sample confinement are significant for soil loosening processes, whereas tests with a high degree of confinement are significant for load bearing processes.

Finally it should be noted that, although mechanical properties can easily be

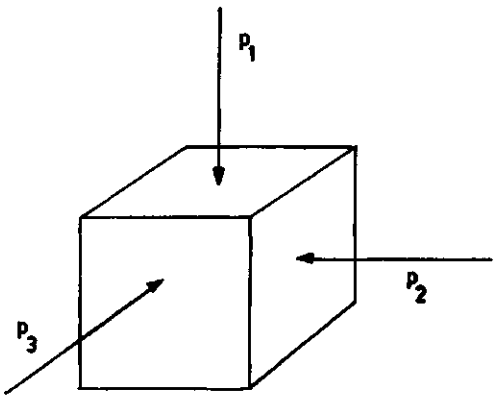

FIG. 34. A loaded soil volume element.

defined in theory, their determinations involve many problems, because they are difficult to measure. These measuring difficulties arise from the involved preparation of the samples on which should be measured, the comparatively large strains in the sample during a test and the great influence the strain rate has on the test results.

Characterization processes. When measuring a soil mechanical property in the sense of constitutive equations, it would be ideal if, at any moment, the state of stress and the state of strain did not vary within the sample. This ideal will almost never be reached, due to measuring problems. As the ideal is approached less closely, the character of the measurement will be more like that of a tillage process. Measurements which strongly exhibit this, will be indicated here as 'characterization processes'. Their process-aspects are relatively easy to measure in most cases. Examples of characterization processes are:

- cone penetrometer test (FREITAG et al., 1970),
- plate penetration test (FREITAG et al., 1970),
- determination of the Atterberg consistency limits (KAROL, 1960),
- drop shatter test (FARRELL et al., 1967).

From the above it can be seen that there is no distinct boundary between mechanical property measurements and measuring aspects of characterization processes.

6.4. HOW SHOULD WE PREDICT?

Predicting tillage process aspects from a set of soil and tool characteristics can only be possible providing there is a method of prediction that is suited to the characteristics and process aspects in question. Although variation among such predicting methods may be great, two general types can be distinguished:

- methods that are mainly based on observations of relationships between characteristics and process-aspects,
- methods that are mainly based on knowledge of the mechanism of the process under consideration.

7. PREDICTION METHODS MAINLY BASED ON OBSERVATIONS OF RELATIONSHIPS BETWEEN CHARACTERISTICS AND PROCESS-ASPECTS

The main feature of these methods is that they involve the assumption of any process aspect y being dependent on characteristics $x_1, \ldots\ldots x_n$ of soil, tool and soil-tool system, which may be formulated as:

$$y = f(x_1, \ldots\ldots x_n),$$

where f is the prediction function, defined for given ranges of x_i (the region given by these ranges will be subsequently referred to as the field of application of f). Characteristics x_i should be so as to satisfy the following requirements:
- the function must be unique,
- sensitivity of y to any x_i should be appropriate,
- no superfluous characteristics x_i should be involved.

The function is unique if for each set $(x_1, \ldots\ldots x_n)$ it only predicts one value of y. This is not the case, for instance, when the set $x_1, \ldots\ldots x_n$ does not involve all those soil mechanical properties that are pertinent in the process and may vary within the field of application. Then, additional characteristics should be taken into account, in the hope that they represent the mechanical properties which have been overlooked. Scale model research has revealed many sets $x_1, \ldots\ldots x_n$ involving functions which are not unique.

The sensitivity of y to x_i may be represented by the differential quotient (dy/dx_i). When this quotient is large, the function can only be unique if a high accuracy is achieved in measuring x_i. This quotient can indeed be high, as will appear for example from (FARRELL et al., 1967). In this paper, results of unconfined compression tests are presented in the form:

$$\text{unconfined compressive strength} = f(\text{moisture content}),$$

the function being measured on a loam soil that was compacted at 14% moisture content, then saturated, and finally dried to the testing moisture contents. At 2% moisture content the unconfined compressive strength equalled 14 bar, and dy/dx was

$$\frac{\text{d (unconfined compressive strength)}}{\text{d (moisture content)}} = 4.5 \text{ bar per \% moisture content}$$

If a quotient dy/dx_i is small, x_i is apparently of little importance and can better be left out of consideration, because a prediction method will generally be more simple as the number of x_i is smaller.

When it is the intention to develop a prediction method of the type under discussion, it must be decided on which particular characteristics x_i will have to be chosen. That decision may depend on many and various considerations. Some of them are discussed below.

1. The consideration that mechanical processes such as loosening processes are mainly determined by soil mechanical properties. However true that may be in itself, this consideration has often lead to great disappointments in the past. Common reasons for this were:
   - using a set $x_1, \ldots . x_n$ that does not allow the function to be unique,
   - under-estimating the influence of speed on the results of mechanical property measurements,
   - the inability of measuring soil mechanical properties adequately.
2. The assumption that the pertinent soil mechanical properties in their turn are completely determined by soil physical properties. If this is true, then process properties (aspects) are unique functions of soil physical properties. Use of soil physical characteristics may be advantageous because they will be comparatively easy to measure. Texture, porosity, and moisture content are well-known soil physical characteristics. Probably there are some cases in which soil mechanical properties are unique functions of texture, porosity and moisture content. It may be true for pure sand that has been untouched long enough to allow local soil moisture suction variations to disappear (TOWNER and CHILDS, 1972).
3. The consideration that characterization processes may be preferred because of the advantage that their aspects can be quite easily measured. This approach seems to be promising, as may be concluded from the success the cone index determination has in predicting the aspects of load-bearing processes (GILL and VAN DEN BERG, 1967). Until now the use of characterization processes has been limited to the prediction of a process aspect from the result of a single characterization process. Using a prediction method based on more characterization processes will be a logical development, an example being:

$$\text{process aspect } y = \text{f (result of characterization process no. 1, result of characterization process no. 2)}$$

In that case the characterization processes should be selected in such a way that they reflect soil mechanical properties that differ from each other.

In general, developing a prediction method will be easier as the number of characteristics x_i is smaller. Two methods for decreasing that number should be mentioned.

a) Decreasing the number of characteristics x_i by making a less general statement of the problem. In that case one or more x_i are in fact assumed to be constant. Of course it will imply that then the prediction method can only be applied where the x_i in question equal those constant values. Characteristics that may be kept constant, are, for example:
   - working depth: in agricultural practice a 'most normal' working depth for a tool type often exists,

- travelling speed: for the travelling speed as well there may be a value that is typical of agricultural practice,
- shape of the tool,
- soil type: a prediction method being, for example, only applicable to sandy soils, will be more simple than a universal prediction method.

b) Decreasing the number of variables by using Buckingham's Pi-theorem.

Supposing that for a process, the following relation exists between a process aspect y and characteristics x_i:

$$y = f(x_1, \ldots\ldots, x_n),$$

and that the number of dimensions in which y and x_i can be measured are equal to b, this theorem states that the above function can be reduced to:

$$Y = F(X_1, \ldots\ldots, X_{n-b}),$$

with the only restriction being that Y and X_i are dimensionless and independent (MURPHY, 1950). Methods for calculating Y and X_i from y and x_i are given in (MURPHY, 1950). As force, length and time are often the pertinent dimensions in loosening processes, b will equal 3, and, by using the theorem, the number of quantities that determine y can be reduced by 3. It will be illustrated with the following example. In (SPRINKLE et al., 1970) it is stated that the draught force of plane blades at a fixed length to width ratio, will satisfy:

$$D = f(v, g, d, \alpha, \phi, \delta, c, \gamma),$$

where D = draught force
v = travelling speed
g = acceleration of gravity
d = working depth
α = cutting angle
ϕ = angle of internal soil friction
δ = angle of soil-metal friction
c = soil cohesion
γ = bulk density of the soil

These quantities involve the dimensions of force, length and time. The sum of those dimensions is three and therefore, according to the Pi-theorem, the 8 characteristics can be reduced to 5 quantities, provided these quantities are dimensionless and independent. The following formula satisfies this:

$$\frac{D}{\gamma \cdot d^3} = F\left(\frac{v^2}{g \cdot d}, \alpha, \phi, \delta, \frac{c}{\gamma \cdot d}\right)$$

Quantities such as those present in this formula are called Pi-terms. It should be noted that Pi-terms may have the disadvantage of being complex and difficult to imagine.

Prediction methods that are mainly based on observations of relationships between characteristics and process aspects, may be divided into:
- comparative methods,
- methods using empirical formulae or graphs.

7.1. Comparative methods

The assumption of a process aspect y depending on characteristics $x_1, \ldots . x_n$ of soil and tool, may be formulated as:

$$y = f(x_1, \ldots ., x_n),$$

where f is the way in which y depends on $x_1, \ldots . x_n$. When f is unknown, the above equation can still be used as a prediction method, for, if it has once been observed that at certain values of $x_1, \ldots . x_n$ a certain value of y occurs, then it is true that, when those particular values of $x_1, \ldots . x_n$ again occur, the particular y-value is also again attained. Methods based on this will be called comparative methods. Some of them follow now.

7.1.1. *The opinion of the experienced farmer*

An experienced farmer has had to make many decisions concerning soil loosening tillage processes in practice. He remembers relationships between process aspects and characteristics concerning soil and tool. These relationships will usually be specific for a certain piece of land. The characteristics concerning the soil are composed of those which can be sensory perceived, and of the treatments to which the soil has been subjected. However, it must be stated that this experience often does not suffice, for it does happen that a farmer readjusts or even stops a tillage process, depending on his opinion of its desired effects.

7.1.2. *The soil tillage record*

The experience method may be improved by:
- supporting the memory by making notes,
- a shift from the (subjective) sensory perceptions to (objective) observations that can be quantified.

It seems logical that on the farms a soil tillage record will thus develop from the experience method. Such a soil tillage record may be composed of notes concerning:
- quantifiable soil characteristics that have been determined just prior to a tillage operation,
- process aspects of tillage operations that have been carried out,
- the treatments to which the soil has been subjected.

When a farm consists of pieces of land that differ from each other, such a record may be kept for each piece individually.

That such a record may be useful, is shown from the fact that soil workability

limits are sometimes considered to coincide with certain soil moisture suction values (BOELS and WIND, 1975; WIND, 1976). FLORESCUE and CANARACHE (1973) report a start of a record in which the process aspect is the draught-soil moisture content relationship in ploughing. Starting points for Dutch conditions can be found in (KUIPERS, 1959).

7.1.3. *Using the fact that mechanically equal soils exhibit equal behaviour*

Because it must be true that mechanically equal soils exhibit equal behaviour, the following prediction method can be applied. For a series of standard soils a number of mechanical properties and/or aspects of characterization processes are measured on each soil. These properties and/or characterization processes should be selected so as to allow each important feature of the soil mechanical behaviour to be reflected in at least one of these measured properties and/or characterization processes. For each standard, the pertinent aspects of the tillage process to be predicted are subsequently determined by experiments. For any other soil where the tillage process in question is to be predicted, the same mechanical properties and aspects of characterization processes are measured to select the standard soil which most resembles the soil under consideration. The tillage process aspects of this soil can now be predicted as being equal to the tillage process aspects measured in the standard soil which resembles it the most.

That mechanically equal soils indeed exhibit equal behaviour in tillage, is demonstrated in the following experiment. For 3 different soil types (Wageningen silty clay loam, Lexkesveer loam, Schinnen silt loam) two soil blocks

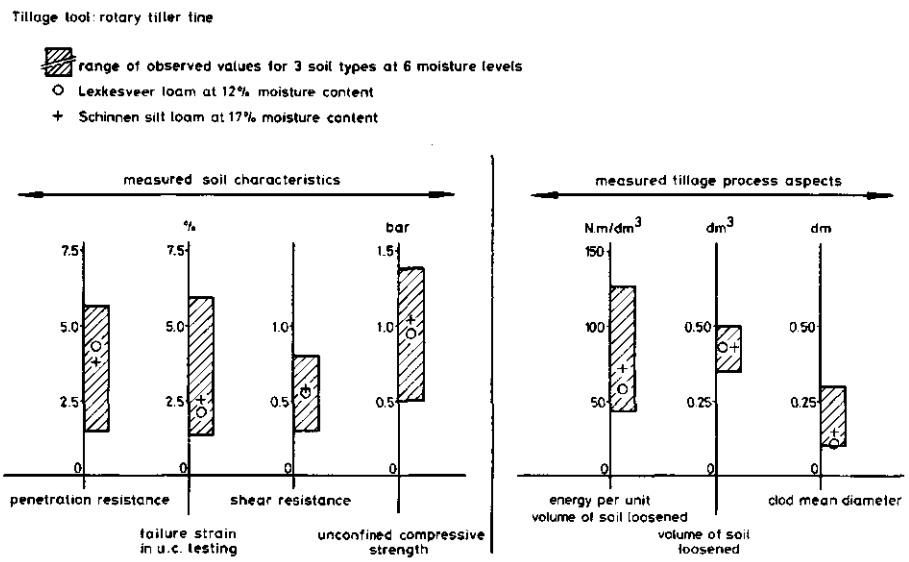

FIG. 35. Equal mechanical properties provide equal processes.

were prepared at 6 moisture levels, giving 36 soil blocks in total. For each soil block the following characteristics were measured:

- shear strength, using the torvane (N.N., 1971),
- penetration resistance, using the pocket penetrometer (N.N., 1971),
- unconfined compressive strength,
- the amount of strain needed to produce failure in the unconfined compression test.

The left part of Fig. 35 presents the ranges of these measuring results together with the results for Lexkesveer loam at 12% moisture content and for Schinnen silt loam at 17% moisture content. This shows that these two soil conditions may be considered to be mechanically equal. Subsequently, each soil block was subjected to a tillage process in a pendulum type impact machine using a tine striking through the soil like a rotary tiller tool (see Fig. 36). For each tillage process:

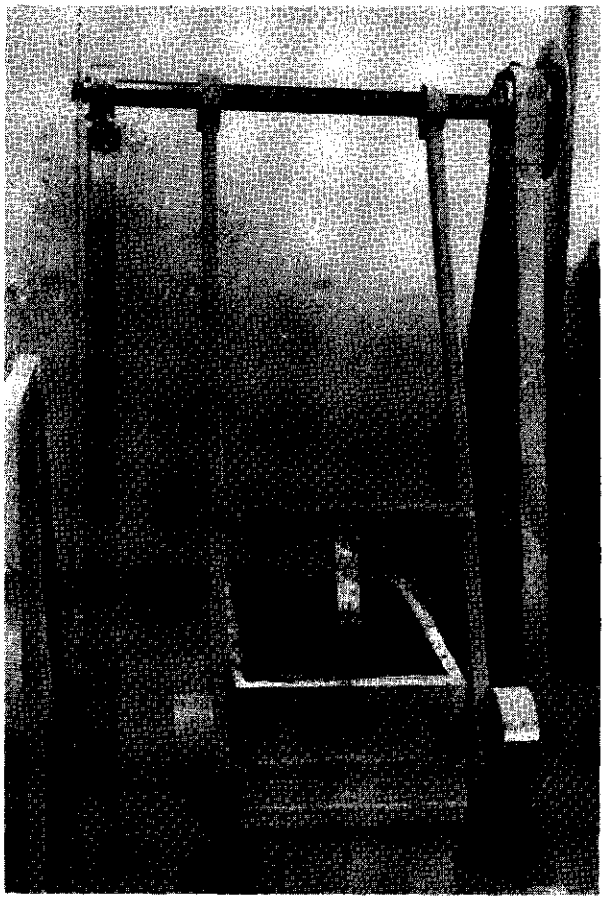

FIG. 36. Pendulum type impact machine.

– the energy consumption,
– the volume of the soil loosened,
– the mean aggregate size of the soil loosened,
were measured. The right part of Fig. 35 presents the ranges for these measuring results, along with the results for the two mechanically equal soil conditions mentioned above. It clearly demonstrates that mechanically equal soil conditions also exhibit equal process aspect values.

7.1.4. *Rules of thumb for plough designers*

A plough-bottom that is to be satisfactory in practice, still cannot be designed on theoretical consideration only, and therefore plough designers often start from characteristics of existing ploughs that have already proved to be useful. Investigations into the characteristics of such plough-bottoms resulted in rules of thumb, which now serve the plough designer. Such rules of thumb are reported in (SÖHNE and MÖLLER, 1962).

7.1.5. *Scale model testing*

Scale model testing is also a comparative method. It will be illustrated with a (very simple) example, which has the following field of application:
– bulldozer blades having a given shape, a given height-width ratio and a given cutting depth-height ratio,
– negligible velocity effects, thus excluding the dimension of time,
– soils, the mechanical behaviour of which can fully be defined by: cohesion, angle of internal soil friction, angle of soil-metal friction, bulk density.

For this field of application it may be stated that

$$D = \mathrm{F}\,(l, \gamma, c, \phi, \delta),$$

where D = horizontal pushing force at maximum blade load,
l = blade width,
γ = soil bulk density,
c = soil cohesion,
ϕ = angle of internal soil friction,
δ = angle of soil-metal friction.

Using the Pi-theorem this expression can be reduced to

$$\frac{D}{c \cdot l^2} = \mathrm{f}\left(\frac{c}{\gamma \cdot l}, \phi, \delta\right)$$

Within the field of application we now consider 2 bulldozer blades, which will be labelled 'prototype' (index p) and 'scale model' (index s), respectively. The prototype is intended to operate under practical conditions (with known values of $l, \gamma, c, \phi, \delta$), with a D-value that is unknown. We want D to be known, but, due to the large blade size, it would be very expensive to measure D on the prototype. The scale model on the other hand is very small but is well suited for

the determination of D. Using the last formula and designing the scale model so as to satisfy

$$\left(\frac{c}{\gamma \cdot l}\right)_s = \left(\frac{c}{\gamma \cdot l}\right)_p$$
$$\phi_s = \phi_p$$
$$\delta_s = \delta_p$$

we achieve:

$$\left(\frac{D}{c \cdot l^2}\right)_s = \left(\frac{D}{c \cdot l^2}\right)_p$$

Using this equality, D for the prototype can be calculated from a D measured on the scale model. The design condition

$$\left(\frac{c}{\gamma \cdot l}\right)_s = \left(\frac{c}{\gamma \cdot l}\right)_p$$

requires the scale model soil to be different from the prototype soil, as may be seen after rearranging to

$$\frac{\left(\frac{c}{\gamma}\right)_s}{\left(\frac{c}{\gamma}\right)_p} = \frac{l_s}{l_p}, \text{ which is not equal to 1.}$$

Scale models are often run in artificial soils (oil-mineral mixtures), because artificial soils can exhibit the desired low c-values and have mechanical properties that do not vary much with time.

Further information on scale model testing can be found in (WISMER et al., 1976). Finally, it should be noted that scale model research in soil has been primarily developed in laboratories of industrial enterprises such as Caterpillar Tractor Co. For obvious reasons, these laboratories are not eager to publish their knowledge.

7.1.6. *The use of draught-moisture content relationships*

FLORESCU and CANARACHE (1973) report that a general draft requirement map has been made for Rumania. In this map the Rumanian soils are divided into 6 categories. Within each category the draught-moisture content relationships involved in ploughing are roughly the same. The Ministry of Agriculture of Rumania uses this map to determine where tractors, ploughs, fuel etc. must be distributed.

7.1.7. *Suitability tests*

The suitability of implements in practice may be determined by testing one or several types of implement in one or several practical environments (POESSE and VAN OUWERKERK, 1967; SPRONG, 1972). In this case predictability is mainly limited to the (implicit) assumption that a certain tool used in a certain way in a certain practical environment always involves one and the same tillage process.

It is possible that there is a consistent relationship in the suitability test results between a process aspect and one or more tool, soil, or soil-tool characteristics; for instance, a consistent relationship between ploughing draught and the lateral directional angle at the end of a mouldboard. Such relationships may be presented by means of empirical formulae, or graphs, which will be discussed below. Note that the quality of this 'by-product' of suitability testing cannot be expected to be very high, because the aims, and therefore also the testing methods, in suitability testing greatly differ from those in determining the empirical formulae or graphs.

7.2. THE USE OF EMPIRICAL FORMULAE OR GRAPHS

The methods using empirical formulae or graphs also start from the assumption that a process aspect y is dependent on characteristics $x_1, \ldots . x_n$:

$$y = f(x_1, \ldots ., x_n)$$

Here, f represents the way in which y depends on $x_1, \ldots . x_n$. In the methods under discussion f is known to such an extent that y can be calculated for any arbitrary $x_1, \ldots . x_n$ (within certain limits). f may be given in the form of a formula or a graph.

When f is given as a formula, the knowledge of f will be based on:

1. assuming a general formula that incorporates $x_1, \ldots . x_n$ as well as one or more (yet unknown) constants,
2. determining these constants empirically by measuring y for different sets $x_1, \ldots . x_n$.

When f is given as a graph, the knowledge of f will be based on:

1. assuming a graph shape,
2. drawing the graph from measurements of y at different sets $x_1, \ldots . x_n$.

Some examples of empirical formulae and graphs are presented below.

7.2.1. *The profile of a furrow made by a tine*

WILLATT and WILLIS (1965) present prediction formulae for the (upper) width b and the area A of a section through a furrow (boundary between still firm soil and loosened soil) made by a tine. These prediction formulae have been tested for:

– plane vertical tines and curved tines,

- soils ranging from sandy loams to clays and located in wheat growing areas of New South Wales,
- working depths between 2 and 7 in.,
- 2 in. tine width,
- a travelling speed of 4–5 ft/sec,
- process type A (see section 3.1.1.).

The following characteristics were involved:

- tine width w,
- working depth d.

No influence of soil type or moisture content was seen from the measurements. Assuming:

- a trapezoidal section shape as indicated in Fig. 37,
- a constant inclination of the non-horizontal sides,

a general prediction formula has been established as:

$$b = k_1 \cdot d + w,$$

where k_1, is a constant. For measured values of b and d linear regression computed k_1 as 2.42 In the case of the section area A the assumptions allow:

$$A = k_2 \cdot d^2 + w \cdot d$$

where k_2 is a constant. From measured values of A and d it has been calculated that $k_2 = 1.03$.

7.2.2. *Ploughing draught as affected by soil moisture content*

Total draught K of a drawn plough may be predicted using a method that has the following field of application:

- all current types of drawn mouldboard ploughs,
- 'normal' ploughing speed,
- limited to one piece of land.

The characteristics are:

- soil moisture content in percentage of weight (m),

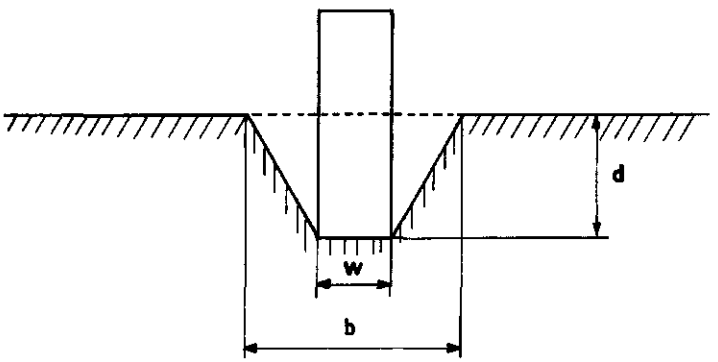

FIG. 37. Section of a furrow made by a tine.

- ploughing width (b),
- ploughing depth (d).

A general formula for K is assumed to be:

$$\frac{K}{b \cdot d} = k_1 - k_2 \cdot m + k_3 \cdot m^2,$$

where k_1, k_2 and k_3 are positive constants. This is the formula of a parabola with its vertex being a minimum value. The soil moisture content present at this minimum is called optimum moisture content. Constants k_1, k_2 and k_3 must be determined empirically by measuring plough draughts on the piece of land in question at different moisture contents (BAKHTIN et al., 1968; OMETTO, 1970; FLORESCU and CANARACHE, 1973).

With this method it should be noted that the assumption of a parabolic relationship having a minimum value quite often appears to be untrue. In some cases the relationship between K and m involves a parabola with a maximum value (BAKHTIN et al., 1968). Also, the relationship may be a decreasing function in the range of moisture contents that are relevant in practice (OMETTO, 1970). This has been confirmed by CANARACHE (personal communication) stating that on many occasions, the soil has to be moistened artificially if measurements in the rising part of the parabola are wanted. The function is not fully unique, for ploughing resistance is also affected by mouldboard shape, ploughing speed, soil bulk density, soil structure, all being allowed to vary within the field of application (POESSE and VAN OUWERKERK, 1967).

7.2.3. *Ploughing draught as affected by speed*

Draught K of a body of a mouldboard plough may be predicted by the method known as Gorjatchkin's formula, which was published in Gorjatchkin's book 'Uber Streichbleche' in 1898 (VORNKAHL, 1967). The field of application is very limited, namely:

- one mouldboard type,
- one piece of land in a particular condition.

The characteristics are:

- working width (b) of the plough-body,
- working depth (d) of the plough-body,
- ploughing speed (v).

Probably on the basis of his knowledge of fluid mechanics Gorjatchkin stated the following general formula:

$$\frac{K}{b \cdot d} = z + \varepsilon \cdot v^2,$$

where z and ε are constants which must be determined from K-measurements for different values of b, d and v. The method has been adopted by many in-

vestigators (SÖHNE, 1960; SÖHNE, 1962; POESSE and VAN OUWERKERK, 1967; BERNACKI, 1963; ZOZ, 1974).

Sometimes the accuracy of the formula leaves much to be desired. This would especially be the case for the heavier soils (POESSE and VAN OUWERKERK, 1967). An additional constant x may be used to increase the accuracy:

$$\frac{K}{b \cdot d} = z + \varepsilon \cdot v^x,$$

with the constants z, ε and x to be determined from measurements (TELISCHI et al., 1956). Some investigators tried to enlarge the field of application by using:

$$\frac{K}{b \cdot d} = z + c \cdot (1 - \cos \phi) \cdot v^2,$$

where z and c are constants. It would apply to any series of mouldboards that only differ in side angle ϕ at the trailing edge. According to SÖHNE (1960) and BERNACKI (1963) this seems to be true, but POESSE and VAN OUWERKERK (1967) could not observe any relationship between K and ϕ. Finally, it may be noted that VORNKAHL (1967) applied Gorjatchkin's formula to tines.

7.2.4. *Ploughing draught in USA conditions*

The ASAE cooperative standards program (Agricultural engineers yearbook 1976, ASAE, St. Joseph, Michigan) includes the following information (ASAE Data: ASAE D230.2) concerning ploughing draught. The field of application can be defined as:

- all mouldboard ploughs currently in use in the United States of America,
- all arable land of the USA.

The characteristics are:

- soil type,
- travelling speed,
- ploughing width,
- ploughing depth.

For this field of application and these characteristics the ASAE has established a graph by assembling available measuring data. From this graph ploughing draught can easily be read. See Fig. 38. Because, on one hand, the field of application is quite large, and, on the other hand, the number of characteristics is small, the degree of uniqueness cannot be very high.

7.2.5. *Draught of plane blades and tines operating in a saturated clay*

WISMER and LUTH (1972) present a method that predicts draught force of plane tines and blades within the following field of application:

- a specific saturated clay, irrespective of its packing state,
- plane steel tines and blades having a specific surface finish.

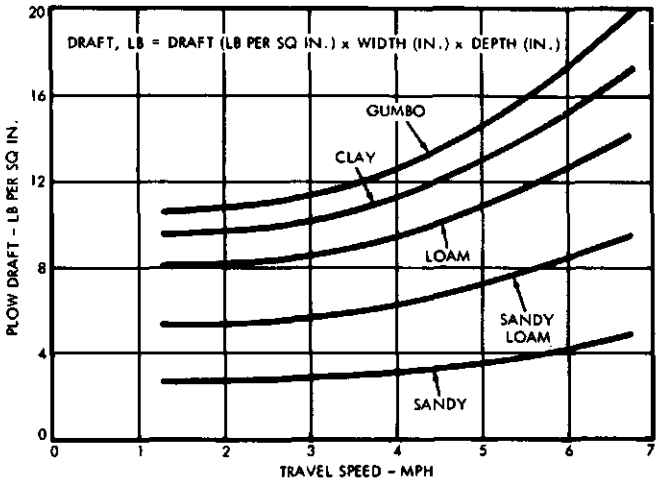

FIG. 38. ASAE data on plough draughts (NN, 1975).

The following characteristics were selected:
- tool width b,
- tool length l,
- tool operating depth z,
- cutting angle α (radials),
- operating velocity v,
- cohesive c,
- internal friction angle ϕ,
- unit weight γ,
- shear rate factor β,
- acceleration of gravity g,
- coefficient of soil to metal friction μ.

Application of Buckingham's Pi-theorem resulted in the following equation:

$$\frac{F}{\gamma \cdot l^3} = \mathrm{f}\left(\frac{L_1}{L_2}, \frac{L_1}{L_3}, \alpha, \frac{v^2}{g \cdot L}, \mu, \phi, \frac{c}{\gamma \cdot L}, \beta\right)$$

where F is draught force and L represents unspecified length variables of the tool (according to the Pi-theorem, the L's can be interchanged and mixed, the only requirement being that the terms remain dimensionless and that the L_1/L_2 and L_1/L_3 terms are not identical). From measurements on the clay in question it was shown that the packing state did not affect ϕ and μ, so these characteristics could be left out of consideration. Preliminary research justified the quantities $c/(\gamma \cdot L)$ and β to be replaced by one quantity:

$$\frac{CI}{\gamma \cdot z} \cdot \beta,$$

where CI is the cone index of the clay, determined according to a standard method. In this way

$$\frac{F}{\gamma \cdot L^3} = f\left(\frac{L_1}{L_2}, \frac{L_1}{L_3}, \alpha, \frac{v^2}{g \cdot L}, \frac{CI}{\gamma \cdot z} \cdot \beta\right)$$

was obtained. Further tests, in which the relationship for each independent quantity with the dependent quantity was determined at constant values of the other independent quantities, showed that the following general formula might satisfy:

$$\frac{F}{\gamma \cdot b \cdot z^{0.5} \cdot l^{1.5}} = \alpha^{k_1} \cdot \left(\frac{z}{l \cdot \sin \alpha}\right)^{k_2} \cdot \left[\left(\frac{CI}{\gamma \cdot z} \cdot \beta\right)^{k_3} \cdot \left\{k_4 \cdot \left(\frac{z}{b}\right)^{k_5} + k_6\right\} + k_7 \cdot \frac{v^2}{g \cdot l}\right]$$

Consequently, k_1, through k_6 were calculated from measuring data by multiple regression. This resulted in the following prediction formula:

$$\frac{F}{\gamma \cdot b \cdot z^{0.5} \cdot l^{1.5}} = \alpha^{1.15} \cdot \left(\frac{z}{l \cdot \sin \alpha}\right)^{1.21} \cdot \left[\left(\frac{CI}{\gamma \cdot z} \cdot \beta\right)^{1.21} \cdot \left\{0.055 \cdot \left(\frac{z}{b}\right)^{0.78} + 0.065\right\} + 0.64 \cdot \frac{v^2}{g \cdot l}\right]$$

Regarding the accuracy, the standard error of estimate of $F = 43$ lb. F varied from 17 to 550 lb and the standard error of estimate expressed as a percentage of the mean was 20%. This is a good result in view of the fact that the prediction formula is intended to apply to:

- plane tines with small cutting angles,
- plane tines with large cutting angles,
- plane blades with small cutting angles and small working depth-blade height ratios,
- plane blades with large cutting angles and small working depth-blade height ratios,
- plane blades with small cutting angles and large working depth-blade height ratios,
- plane blades with large cutting angles and large working depth-blade height ratios.

8. PREDICTION METHODS MAINLY BASED ON KNOWLEDGE OF THE MECHANISM OF THE PROCESS UNDER CONSIDERATION

These methods assume that the process under consideration is equivalent to a hypothetical process which proceeds according to a particular hypothetical mechanism. On the basis of this mechanism, values of process aspects can be derived from values of characteristics. Usually, such a hypothetical mechanism is composed of assumed failure patterns, compaction patterns, deformation patterns, and/or displacement (movement) patterns. To establish such a mechanism, exploratory research is required. In particular, observations on processes performed under simplified conditions are useful.

For a hypothetical mechanism, process aspects can be calculated using conditions stated in mechanics. These conditions are:

- the condition of equilibrium of forces in the mechanism,
- conditions reflecting the characteristics of the soil simulated in the mechanism. These are for example: a stress-volume change relationship, a stress-strain relationship, those stress states that produce soil failure, information on the friction forces that the soil can develop,
- the so-called boundary conditions. They involve all further conditions, imposed on the mechanism, and that must be satisfied at any moment. For instance, the values of travelling speed and tool-operating depth.

Any method based on a hypothetical mechanism involves the following three features (which may easily be confused):

- the effectiveness of the method,
- the compatibility of the mechanism,
- the degree to which the hypothetical mechanism resembles the mechanism to be simulated.

A method is *effective* in the prediction of a process aspect if for any arbitrary set characteristics within the field of application its mechanism predicts a value of this process aspect which matches a measured value. Method effectiveness has to be determined experimentally. A mechanism is *compatible* if it can be physically realized and is able to function as it has been hypothesized. It is illustrated by the following example: if a hypothetical mechanism involves a frictional force in a contact surface between two soil lumps, and it has been hypothesized that this frictional force is proportional to the normal force in the contact surface, then the mechanism is not compatible when this normal force is a tensile force. Many hypothesized mechanisms involve local incompatibility, which is considered insignificant in most cases, for instance at soil lump and tool edges. Incompatibility of the mechanism for some values of characteristics may reduce the field of application, but it has also appeared that sometimes an incompatibility does not seriously affect effectiveness (WITNEY, 1966). A hypothetical mechanism *resembles* the mechanism to be simulated if both

mechanisms involve the same forces and movements. Almost always the hypothetical mechanism differs from the real mechanism that is to be simulated, because the latter mechanism is so complex. Fortunately, large differences between hypothesized and real mechanisms need not be a serious drawback on the effectiveness of the hypothesized mechanism (WITNEY, 1968).

When a method involves a hypothetical mechanism being nearly equal to the mechanism that is to be simulated, it will be called an *exact* method. When this is not the case, the method will be called *approximate*.

8.1. APPROXIMATE METHODS

Some examples of approximate methods follow below.

8.1.1. *Mechanisms composed of rigid soil bodies which may shear along each other*

Söhne's model (SÖHNE, 1956) is an example of a hypothetical mechanism that is composed of rigid soil bodies which may shear along each other. It applies to plane blades with small cutting angles. See Fig. 39. Line q, r denotes a potential failure plane in which the force due to cohesion and the frictional force are fully developed.

B = weight of soil body,
C = cohesive force,
K = force due to soil acceleration,
R = the normal force that the blade exerts on the soil plus the frictional force accompanying this normal force,
D = reaction force of the still firm soil,

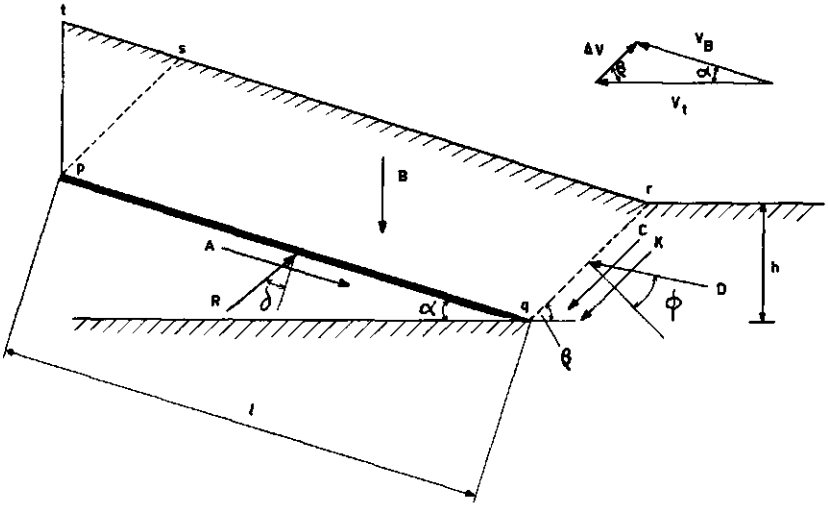

FIG. 39. Söhne's model.

A = adhesive force,
l = blade length,
ϕ = angle of internal soil friction,
α = cutting angle,
β = shear angle, which has been assumed to be 45° in the model,
δ = angle of soil-metal friction.

It follows from the vector diagram:

$$\Delta V = V_t \cdot \frac{\sin \alpha}{\sin (\alpha + \beta)} \qquad (V_t = \text{travelling speed})$$

The acceleration force can be calculated from ΔV: soil particle acceleration takes place during a time interval Δt, so mean acceleration is $\Delta V/\Delta t$. The soil mass being accelerated at one moment equals $\rho \cdot b \cdot h \cdot V_t \cdot \Delta t$, where b = blade width, ρ = bulk density, and h = working depth. Using the previous formula we then obtain:

$$K = (\rho \cdot b \cdot h \cdot V_t \cdot \Delta t) \cdot \frac{\Delta V}{\Delta t} = \frac{\sin \alpha}{\sin (\alpha + \beta)} \cdot \rho \cdot b \cdot h \cdot V_t^2$$

It can be further derived that:

$$C = \frac{h \cdot c}{\sin \beta} \qquad (c = \text{cohesion}),$$

$$A = l \cdot a \qquad (a = \text{adhesion}),$$

$$B = \rho \cdot g \cdot l \cdot h \cdot \frac{\sin (\alpha + \beta)}{\sin \beta} + \frac{1}{2} \cdot \rho \cdot g \cdot h^2 \cdot \frac{\sin (\alpha + \beta) \cdot \cos \beta}{\sin^2 \beta \cdot \cos \alpha}$$

In this formula, the last term accounts for the soil in s, t, p and the last but one for the soil in p, q, r, s.

There are two forces of Fig. 39 still unknown, namely R and D. Using the equilibrium conditions in horizontal and vertical directions, two equations can be formed, which allow R and D to be calculated. Finally A and R can be combined to find blade resistance. The horizontal component of this resistance is the blade draught.

Several such mechanisms, composed of rigid soil bodies, are known:
- for tines (PAYNE, 1959; O'CALLAGHAN, 1967; HETTIARATCHI and REECE, 1967),
- for plane blades with large cutting angles and large working depth-blade height ratios (OSMAN, 1964; HETTIARATCHI et al., 1966),
- for bulldozer blades (COOK and REECE, 1966).

8.1.2. *Draught of a curved blade with a large working depth-blade height ratio*

OSMAN (1964) states: draught of a curved blade (left part of Fig. 40) having a large working depth-blade height ratio will lie between the draught that would occur if the blade were to be replaced by the plane blade of Fig. 40 with a soil-metal friction angle equal to that of the curved blade, and the draught that would occur if the blade were to be replaced by such a plane blade with a soil-metal friction angle equal to the internal soil friction angle.

8.1.3. *A criterion to distinguish tines from blades*

In section 3 it was mentioned that a soil wedge is often present in front of a tine. It has the shape of a standing prism. If the tine width were to be continually increased or the working depth decreased, then the standing prism would disappear at a certain moment, and it can be stated (PAYNE, 1956) that the tine has then been changed into a plough-body (plough-bodies may also be accompanied by soil wedges, but they look like lying prisms). From (PAYNE, 1956; PAYNE and TANNER, 1959; O'CALLAGHAN and FARRELLY, 1964; O'CALLAGHAN and MCCULLEN, 1965) it is shown that the boundary between straight tines without profile and plane blades can be formulated as:

$$\frac{\text{working depth}}{\text{tool width}} \approx 0.5 - 2.5$$

The proof of this is complex and involves classical soil mechanics theories.

8.2. EXACT METHODS

Some examples of exact methods are presented below.

8.2.1. *Application of the mathematical theory of plasticity*

On some locations in loosening processes there may be soil in a plastic state, which can be treated by one of the methods available in the mathematical theory of plasticity (SMITS, 1973; BUTTERFIELD and ANDRAWES, 1972; YONG,

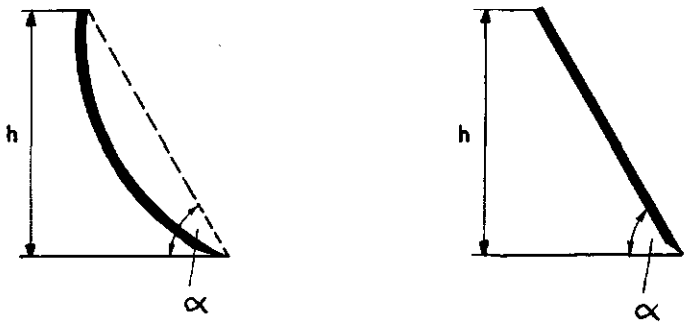

FIG. 40. Refers to Osman's hypothesis.

1973; CHEN, 1975). Although this theory comprises a huge amount of knowledge, only the literature will be referred to here because its application in soil loosening processes is very limited.

8.2.2. *Vertical force on plane blades and straight tines without profile*

For plane blades and straight tines without profile we can calculate the ratio:

$$\frac{\text{vertical force on the tool } (F_v)}{\text{horizontal force on the tool } (F_h)},$$

if the following ratio is known:

$$\frac{\text{tangential force on the tool } (F_t)}{\text{normal force on the tool } (F_n)}$$

Such calculations may use the next prediction formula (See Fig. 41):

$$\frac{F_v}{F_h} = \operatorname{cotan}\left(\alpha + \arctan\left(\frac{F_t}{F_n}\right)\right),$$

which can easily be obtained by elementary calculus.

Both F_t and F_n are composed of 2 parts:

$F_t = F'_t + F''_t$,

$F_n = F'_n + F''_n$,

where:

- F'_n and F'_t are components of the force at the cutting edge that tries to push the tool upward. This force is not negligible when the cutting edge is blunt or in soils exhibiting significant elastic recovery (PAYNE and TANNER, 1959),
- F''_n is the normal force that the soil exerts on the tool surface,
- F''_t is the friction force between the soil and the tool surface.

Provided a soil flow along the blade not involving any sideways soil movement exists, then:

$$F''_t = F''_n \cdot \tan \delta,$$

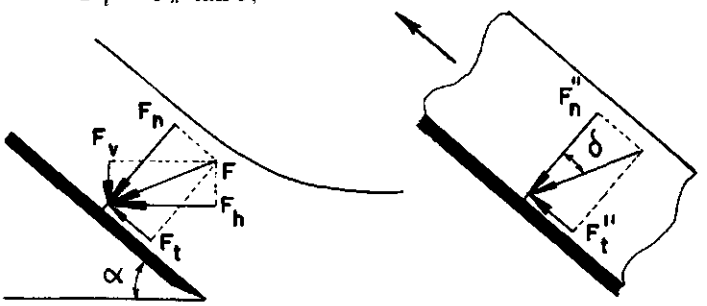

FIG. 41. Refers to the calculation of the vertical force-horizontal force ratio in the case of straight tines and plane blades.

where δ denotes the soil-metal friction angle (See Fig. 41), which can be measured rather accuretely by using one of the several measuring apparatuses available.

Sometimes there is no soil flow, but a soil wedge that is more or less stationary, so that:

$$F''_t < F''_n \cdot \tan \delta$$

At cutting angles larger than 90° the soil wedge may tend to move downwards. In that case F''_t changes direction, but, because the subsoil prevents the wedge from travelling downwards it is still true that $F''_t < F''_n \cdot \tan \delta$ (PAYNE and TANNER, 1959). When soil flow direction involves any sideways component, it is true that the friction force equals $F''_n \cdot \tan \delta$, but the friction force direction does not resemble the F''_t direction any more, which means that F''_t is only a component of the friction force, so smaller than $F''_n \cdot \tan \delta$ Hence, provided

- the cutting edge is sharp,
- there is not much elastic recovery,
- a soil flow is maintained, not involving a significant sideways component,

$F_t/F_n = F''_t/F''_n = \tan \delta$, which allows arctan (F_t/F_n) in the prediction formula to be substituted by δ. The result is a much simpler prediction formula, namely:

$$\frac{F_v}{F_h} = \text{cotan } (\alpha + \delta)$$

9. CLOSING REMARKS ON PREDICTABILITY

Two classes of prediction methods have been presented in sections 7 and 8:
- methods mainly based on relationships between characteristics and process aspects,
- methods mainly based on knowledge of the mechanism of a process.

The former class was discussed at great length, the latter, on the other hand, only very briefly. The reason for this being that the former class is likely to be much more promising. Within this class there are methods in which the high complexity of soil loosening processes is not a drawback. It is this complexity that impedes the development of the second class of methods. Perhaps it can be stated that the latter class serves the former. An understanding of the mechanism allows better choices concerning characteristics, fields of application and general formulae to be made. Within the former group the most promising methods will probably be those that meet potential users needs the most. Soil tillage records and rules of thumb for designers have good prospects.

It is the wish that this introduction to predictability, together with a well-matched systematics, will contribute to the effectiveness in establishing new and better prediction methods.

10. A STUDY OF A 2-DIMENSIONAL CURVED BLADE WITH A SMALL CUTTING ANGLE AND A SMALL WORKING DEPTH-BLADE HEIGHT RATIO

10.1. INTRODUCTION

The 2-dimensional curved blade with a small cutting angle and a small working depth-blade height ratio plays a basic role in the systematics presented in sections 2–5. The treatment of a number of plough-bodies could be greatly simplified by referring to this particular blade, and knowledge of plough-body processes will make tine processes more readily understood. The blade in question is useful in the systematics because of the following factors:

1. A 2-dimensional blade is characterized by: an infinite width, a cutting edge that is horizontal and perpendicular to the direction of travel, and a blade shape that does not vary across the width. When the blade operates in soil that is reasonably homogeneous, then the shape of the process involved will also scarcely vary across the tool width. Therefore, the study of such a process can be restricted to studying one vertical section of the process, parallel to the direction of travel. It is not necessary to consider the third space dimension. The process shape present at any given moment can be recorded adequately by drawing such a vertical section. Two-dimensional flows also played an important role in the development of fluid mechanics (SHAMES, 1962).
2. A tool usually has a two-fold action, namely a soil loosening action, and a further tool action. This has been recognized for many years, as can be seen from the names of the tool parts listed below:
   - share and mouldboard in the case of ploughs,
   - cutting edge and mouldboard in the case of bulldozer blades,
   - cutting edge and bowl in the case of scrapers,
   - chisel and shrank in the case of tines.

   For the blade in question loosening and further action can easily be distinguished from each other, because the working depth-blade height ratio is small.
3. Excessive soil pulverization can interfere with process studies. In particular, large cutting angles may involve intensive and irregular pulverization (JOHNSON et al., 1969). Therefore, process studies are simpler as the tool cutting edge becomes smaller.
4. Further tillage action depends on blade curvature and is at a minimum when the blade is flat. In that case the soil moves like a rigid body over the tool. A curved blade induces significant further tillage action.
5. The process of different tools exhibit many similarities. For instance, it can be expected that processes occurring within the width of a tine, look like plough-body processes, thus like processes of 2-dimensional blades. Knowledge of blade processes can therefore be a help in studying tine processes.

At the Tillage Laboratory of the Agricultural University in Wageningen

process studies were made using a 2-dimensional blade with a small cutting angle and a small working depth-blade height ratio (KOOLEN, 1972, 1973). Several results of this investigation have already been reported in the systematics presented in section 4.2. This will be looked at in more detail in the following sections.

10.2. MEANS TO ANALYSIS

In order to develop a systematics of process types for the blade, and in support of process aspect prediction method development, observations from such processes will be necessary. It is useful in this respect to distinguish between:

- conducting such processes,
- recording such processes,
- transforming recorded processes to a form that is more accessible to analysis.

10.2.1. *General remarks on conducting of processes for research purposes*

Two-dimensional blade processes in the strict sense cannot be physically realized because of the infinite width, but they can be simulated by tillage processes involving one or more sections which look like sections of a true 2-dimensional process. In such simulation processes, these sections may be process sides, but, equally, they may be selected somewhere within the process. Some such processes are outlined in the following Figs:

42a (ELYAH and WEBER, 1968),
42b (SIEMENS et al., 1965; OLSON and WEBER, 1966; NICHOLS et al., 1958),
42c (KAWAMURA, 1952; STEFANELLI, 1968; ROWE and BARNES, 1961),
42d (SELIG and NELSON, 1964; KRAUSE, 1973; CHANCELLOR and SCHMIDT, 1962; GILL, 1969),
42e (SÖHNE, 1956),
42f (used here).

Simulation processes should be conducted at optimum conditions for the intended purpose. These conditions relate to:

- soil homogeneity,
- control of working depth, travelling speed etc.,
- process accessability for the determination of movement patterns, forces etc.
- reproducibility of soil conditions,
- the occasional need for simulating such processes in large numbers at a high rate.

Because of these implications it is often thought that tillage processes involved in exploratory research do not resemble practical tillage processes.

10.2.2. *The experimental set up and the tested soils*

A test run comprised the following: Natural soil was sieved through a 10 mm screen (occasionally after a freezing treatment), adjusted to the desired moisture

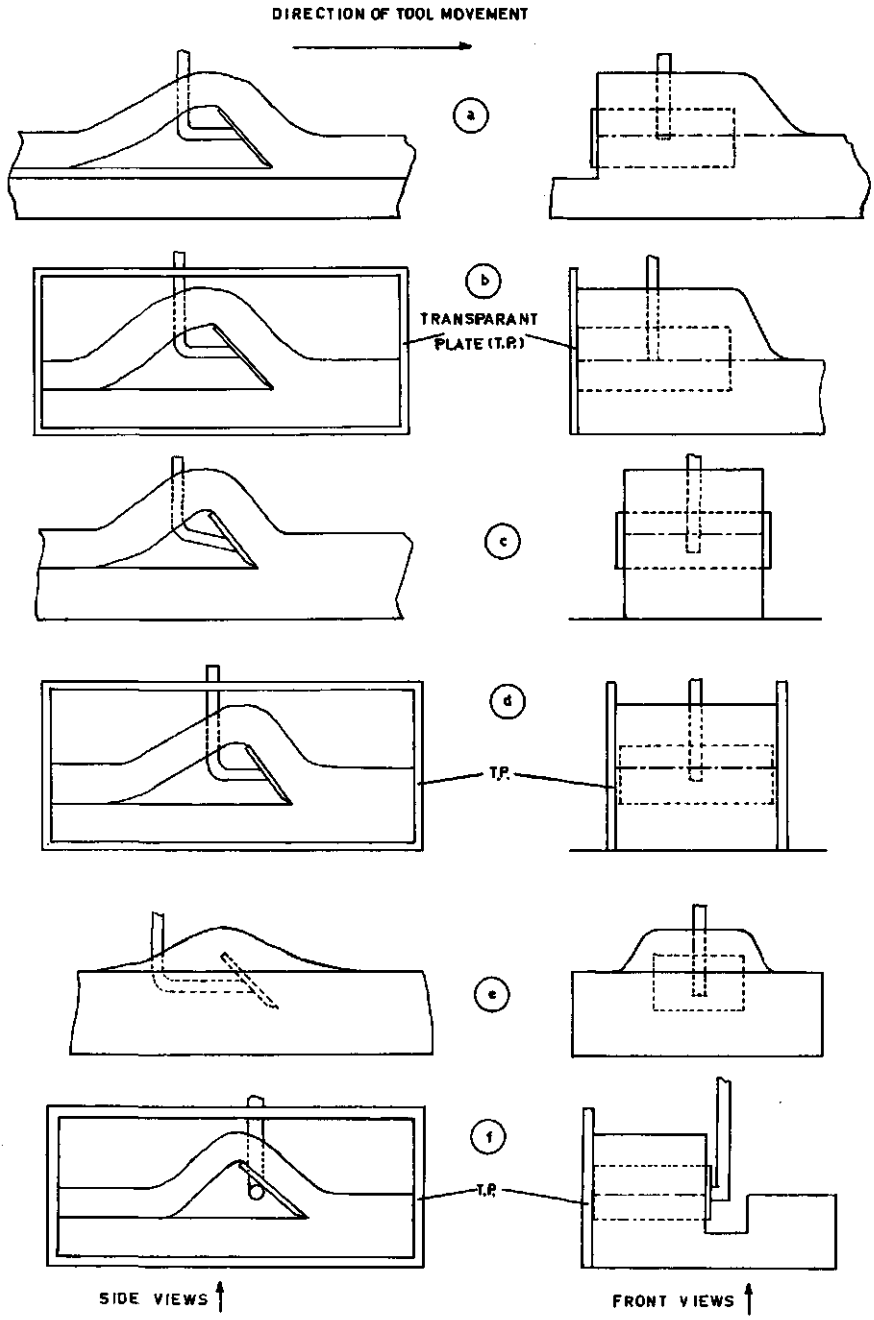

FIG. 42. Simulation processes.

content, equilibrated and uniformly distributed in a soil bin (length 150 cm, width 50 cm, height 21 cm). The desired soil porosity was then adjusted in a hydraulic compression machine, using a large compression plate (about 150×50 cm^2) that just fits into the bin. The soil bin was stored for some time to equilibrate again. The soil bin was then moved by a mobile crane to the testing room, where it was placed on a table under an overhead carriage that could be propelled along rails by an electric motor. Tools and model tools could be attached to this carriage. After removing bin sides, moisture content and bulk density determination, levelling of the soil surface, removal of all the soil outside the blade path, and applying markers, the blade test run was accomplished. During the run the soil movement was filmed.

Soils tested. Four soil types, described in Table II, were investigated under various conditions of water content and pore space as indicated in Table III. These conditions were selected from Fig. 43 (only a schematic figure is given here, because scaling of the axes and shapes of the curves are dependent on soil type). Water content and pore space are the main characteristics of soil prepared as described above. Any condition of pore space and water content that is possible in these tests on pre-compacted soil should lie in the area enclosed by curves A, B and C. Curve A indicates saturated soil. Conditions given by curve B will be obtained when pressure in the compaction machine is at a maximum (2.5 bar). Points above C indicate soil having such a low strength that non-scouring will occur. The exact location of C is not known. (Non-scouring may particularly occur with this type of implement at low travelling speeds). The intended conditions were selected so that they cover the shaded area in Fig.

TABLE II. Soil description.

Soil	% of minerals			% of soil			Moisture content at $pF2 = 100$ cm suction (%)
	$< 2\mu$	2–16μ	16–50μ	Humus	$CaCO_3$		
Wageningen, silty clay loam	36	27	21	2.3	3.3	7.4	27.3
Lexkesveer, loam	15	12	17	1.6	10.4	7.2	20.2
Schinnen, silt loam	17	14	57	2.1	2.9	7.2	27.2
Ede, sand	3.5	2.5	4.5	3.6	–	4.4	17.4

TABLE III. Water content and pore space of soils tested. WC = water content (%). P = pore space (%).

Soil	Wageningen		Lexkesveer		Schinnen		Ede	
	WC	P	WC	P	WC	P	WC	P
Series								
1	27.3	45.2	20.2	40.0	25.9	43.3	17.3	41.1
2	27.0	50.8	19.5	44.3	27.7	48.5	17.5	43.9
3	25.9	54.9	19.6	51.6	25.9	51.2	17.6	49.5
4	22.4	46.9	15.6	41.5	21.6	42.8	13.9	42.1
5	17.7	49.8	12.4	42.4	18.0	44.0	10.9	43.9

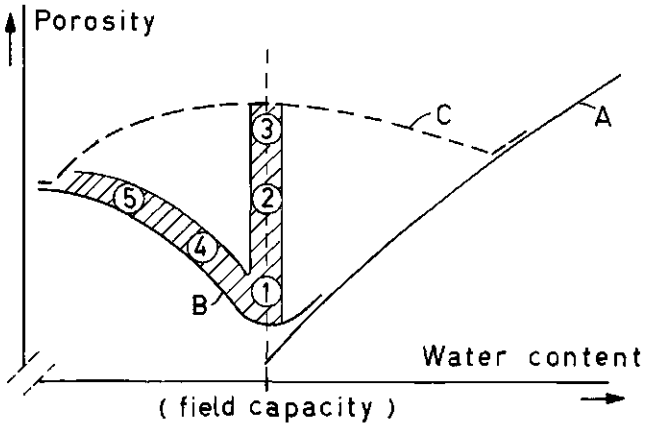

FIG. 43. The conditions of porosity and water content in the experiments.

43. Numbers enclosed by circles refer to the test series from Table III. Non-scouring occurred to a certain extent in W5 (Wageningen series 5), E5, L3, E3. These represent two loose soils and two less loose but drier soils.

The next sections of this report will be easier to understand if the reader is aware that the numbers referring to the soil conditions have the following meanings:

1 = high moisture content, high compaction pressure
2 = high moisture content, intermediate compaction pressure
3 = high moisture content, low compaction pressure
4 = intermediate moisture content, high compaction pressure
5 = low moisture content, high compaction pressure.

Soil preparation. As previously mentioned, soil preparation involves sieving, (occasionally) freezing, and adding water. To obtain an equal soil moisture distribution, water was added to 5 kg soil portions, after which all portions were mixed together. The soil mass was then left to equilibrate for at least one day. A special feature of this preparation was that for each test a large soil mass ($\pm$ 200 kg) had to be moistened to a high accurancy and without the formation of soil lumps. In the first place, it should be noted that the soil cone formed during the sieving operation is not homogeneous because the larger aggregates mainly gather at the outer part of the cone. This sorting effect may cause errors in the moisture content determination, because, in a mass of aggregates, the larger ones are on the whole, drier than the smaller ones. If a large soil mass is equilibrated too long, then the height difference (i.e. soil moisture suction difference) between the top and bottom of the mass causes an unequal soil moisture distribution with the higher moisture contents occurring in the lower soil. Wetness of the lower soil with, at the same time, the upper soil acting as a consolidation pressure, will increase the risk of clod formation in the lower soil.

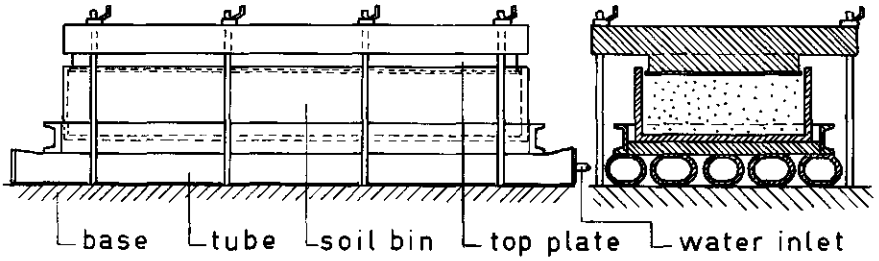

FIG. 44. Soil compaction equipment.

Bin preparation. The soil bin was 150 cm long and 50 cm wide. Bin walls were removable. The bin was filled very carefully with loose soil. After the soil had been smoothed, the desired porosity was adjusted using a compression machine. This machine utilizes 120 mm diameter flexible tubes as seen in Fig. 44. Prior to loading these tubes are empty and therefore flattened. When the bin is placed on the tubes, the top plate is positioned so that it is level with the soil surface, and rigidly attached to the base. The tubes are then filled with water under pressure which causes soil compaction. To obtain the desired final soil height, pressing can be repeated for different top plate positions. Normal tap-water pressure is 3 atmospheres and this allows a maximum compaction pressure of 2.5 kg/cm^2. In order to test the soil homogeneity achieved, 100 cm^3 core samples were taken from one prepared bin, the soil height of which being 14 cm. The results are tabulated in Table IV. In soil bin technology, these results are considered to be very satisfactory.

The curved blade. A picture of the blade is shown in Fig. 45. It was 20 cm wide, 7.5 cm high, and had a horizontal length of 16 cm. The intake angle (angle of the leading edge) and the output angle (angle of the trailing edge) were 5° and 45°, respectively. In selecting these angles the fact that higher output angles would increase the risk of choking, and that the difference between the

TABLE IV. Core sampling data from one soil bin. Lexkesveer loam. Bin dimensions 150 × 50 × 14 cm^3. $\bar{x}$ and $\bar{y}$ are mean values of x and y respectively. S = standard deviation.

	Porosity x (%)				Water content y (%)			
	number in sample	$\bar{x}$	S_x	$S_{\bar{x}}$	number in sample	$\bar{y}$	S_y	$S_{\bar{y}}$
Upper half	90	44.59	0.57	0.060	90	20.53	0.15	0.015
Lower half	90	43.44	0.50	0.052	90	20.82	0.13	0.013
Border of the upper half	38	44.30	0.49	0.079	–	–	–	–
Center part of the upper half	52	44.80	0.53	0.073	–	–	–	–
Whole soil mass	180	44.01	0.79	0.058	180	20.67	0.20	0.014

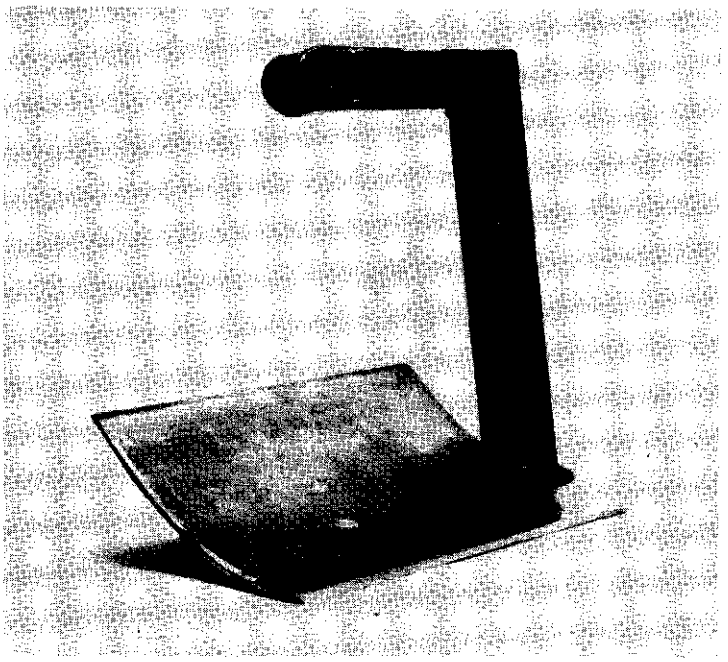

FIG. 45. The tool.

two angles should be as large as possible to obtain significant blade curvature effects was taken into consideration. Fig. 46 indicates blade shape. This shape is made up of two parts of third order parabolas the coefficients of which are calculated from selected values of a, b, c, γ and δ. Blade thickness was 3 mm and the leading and trailing edges were bevelled as shown in Fig. 46 (the bevel side at the leading edge was at an angle of 25° to the direction of travel). The blade, being made of steel, was kept free of rust using a steelwire brush.

Preparation of the soil strip to be tested and the experimental set-up. The complete experimental set-up is shown in Fig. 47. A small top layer with a

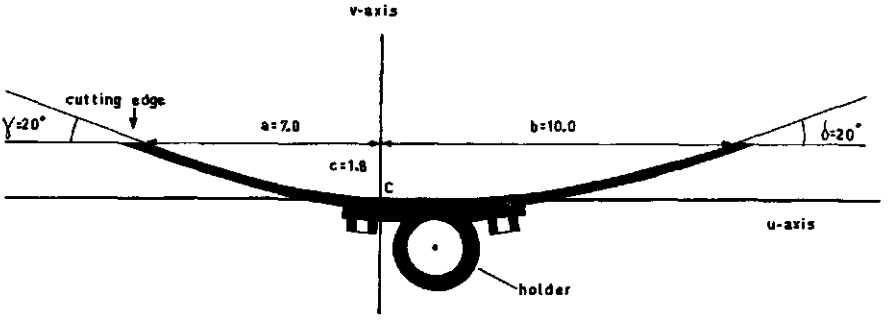

— unit of length : cm
— in C the blade is tangential to the u-axis
— the blade satisfies $v = 0{,}0586\,u^2 + 0{,}0031\,u^3$ when $-7.0 \leqslant u \leqslant 0$
$v = 0{,}0176\,u^2 + 0{,}00004\,u^3$ when $0 \leqslant u \leqslant 10{,}0$

FIG. 46. Blade shape.

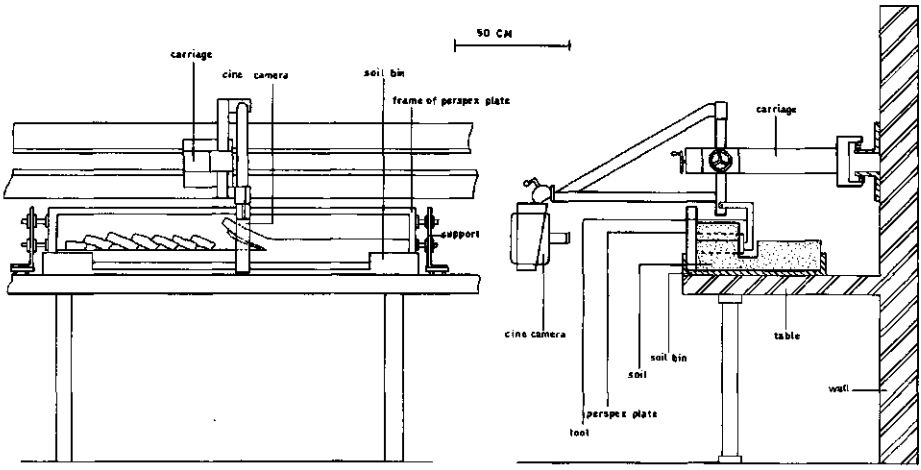

FIG. 47. The experimental set-up.

thickness of about 1 cm was removed from the soil to obtain a flat horizontal surface. A vertical soil layer of 5 cm thickness was removed at a side in order to, firstly, make room for the transparant perspex plate, and, secondly, to remove any soil that was possibly disturbed by wall influences in soil bin compaction. In addition, a trench was made in the soil block to make way for the tool bar mounted on the left side of the blade. As can be seen from the figure, the bin was wide enough for two test runs. The width of the soil to be treated by the blade was 18 cm and the distance between the blade and the perspex plate 1–2 mm. Generally, working depth was 3 cm and travelling speed 32 cm/sec. To minimize friction between the perspex plate and the soil involved in the tillage process the plate was greased with a silicone lubricant. Before positioning the perspex plate a point grid was painted on the soil side. A cine camera was mounted to the carriage so that it could film perpendicularly to the perspex plate.

10.2.3. *General remarks on process recording*

In order to gain full understanding of a process the following measurements can be taken from that process:

- determination of soil particle movements,
- determination of forces exerted on, or within, the soil.

Forces. Force measurements may be:

- measurement of the force that a tool or a tool part exerts on the soil (ELIJAH and WEBER, 1968; WISMER and LUTH, 1972).
- measurement of the stress at specific places on the tool surface (ELIJAH and WEBER, 1968),
- measurement of the stress at specific places within the soil (NOVIKOV, 1967).

Tool force masurements have only a limited use because such a measured force, firstly, is an integral quantity, and, secondly, can only be determined at

the tool face. Stress measurements within the soil involve tremendous technical problems in the case of loosening processes. Stress measurements at the tool surface can be accomplished rather easily but are confined to a rather small part of the process.

Movements. Measurements of displacements, compactions, deformations, failure plane formations, velocities, and accelerations may be indicated as movement measurements. Such measurements can be greatly facilitated by using marker points within or on an outer surface of the soil mass, preferably arranged in a regular pattern.

Examples of markers that may be applied within a soil mass, are:
- layers of paint (SÖHNE, 1956),
- marking pins (GILL, 1967, 1969),
- lead spheres (CHANCELLOR and SCHMIDT, 1962).

In the case of paint layers or pins, the tool is suddenly stopped as soon as it enters the marked region of the soil, and soil will then be removed to allow the new marker positions to be measured. In the case of lead spheres it is possible to record the process development in time by taking a series of X-rays through the soil that is being treated.

Paths of markers applied to a side of a soil flow can be observed by the naked eye during the entire tillage process. Examples are:
- strings of wet paper (TANNER, 1960),
- line grid of chalk (SIEMENS et al., 1965),
- line grid of paint (ELIJAH and WEBER, 1968),
- line grid of powdered carbon (KIM and STALEY, 1973),
- point-grid of painted dots (used here).

The movements of these markers may be recorded by taking photographs or cine films.

10.2.4. *Marking and filming in the experiments*

A cine camera which could film perpendicularly to the perspex plate was mounted on the carriage in the experimental set-up (Fig. 47). In this way films could be obtained in which the tool has a fixed position and in which the soil flows over the tool at an initial speed equal to the travelling speed of the carriage. A 16 mm Paillard Bolex camera was used and the film rate adjusted to 64 frames per sec. Thus, as forward speed was 32 cm/sec, shots could be taken at intervals of 5 mm tool travel. Using a 10 mm object-lens and a film distance of 50 cm the width of the filmed area is 40 cm, which was just sufficient to include the tool and all soil in the tool sphere of influence. The lighting was also mounted on the carriage.

In preparing the experimental set-up for a test run the soil 'wall' to be filmed was obtained by removing a vertical soil layer. The wall should be finished so as to give a smooth surface without any cracks etc. that might interfere with the study of the process type. In removing the outer soil layer an adequate finish was obtained by using an electric powered jigsaw. Such a saw leaves a homogeneous surface, as opposed to a knife. After sawing a point grid was applied

to the wall over its whole length, using a perforated mould and a paint sprayer. The paint was moisture-resistant and quick drying. The grid mesh width was 1 cm. The perspex plate was rigidly attached to the table so that the plate just touched the soil wall without exerting any pressure. The perspex plate was provided with a line grid with 1 cm meshes. These lines were on the plate side that faces the soil so that refraction of light could not cause distortion errors when comparing the marking points with the lines. When transforming the films, the line grid, which was also visible in the films, was used to eliminate adjusting and distortion errors. Such errors may arise from refraction of light through the perspex plate, erroneous positionning of the camera or projector, and distortion caused by their optics.

10.2.5. *General remarks on transforming recorded processes to a more accessible form*

The kinematics of a 2-dimensional process can largely be recorded by film in which the time intervals between frames are small in comparison with the time that elapses during the formation of a failure surface, a deformation, or a mixing effect. In fact, such a film is a 3-dimensional quantity: a series (1 dimension) of 2-dimensional pictures. The interpretation of film material will be made more difficult by this, and will, therefore, often involve the selection of information that can be presented 2-dimensionally.

Instantaneous pictures. An instantaneous picture of a process gives an impression of the movement, compaction and deformation of the soil, and of the way in which the soil breaks. As the process varies more in the course of time, one instantaneous picture will be less suited to give a complete impression, and it would be better to consider a series of instantaneous pictures ranging over an entire period of the process. Additional information may be presented in an instantaneous picture: for instance, the indication of areas with much movement and areas with little movement (NICHOLS et al., 1958), or the presentation of velocity vector diagrams (SÖHNE, 1956).

Paths, velocities and accelerations of a point. Using successive film frames the flow path of a soil particle can be constructed, being the path along which the particle will travel as the tillage process progresses. A flow path of a particle may be particle path relative to the tool, or to the untouched soil. In the former case the tool is considered to be fixed, with the still untouched soil in front of the tool flowing towards the tool. In the latter case the still untouched soil is considered to be fixed, with the tool moving.

Velocity vectors and/or acceleration vectors may be drawn along a flow path.

Fields of flow paths, velocity or acceleration fields. A drawing representing the flow paths of more soil particles will be called a field of flow paths (SIEMENS et al., 1965). For the situation at any given moment the velocity vectors of more soil particles can be given, which may be called a velocity field representation. Similarly, acceleration fields can exist.

The deformation of a soil volume element in a given time interval. If the mesh

size of an applied marking grid is small enough, then each mesh may be considered to represent a soil volume element. Mesh size should be chosen small enough so that the state of strain of a mesh is always representative for all points near the mesh. This is true if all those points have almost equal states of strain; then the strain near the mesh will be called homogeneous. In a tillage operation this homogeneity means that opposite mesh sides remain almost straight and parallel. On the other hand, a strain analysis is only feasible if the mesh is still large enough to allow accurate measuring of the changes in both lengths of the mesh sides and angles between mesh sides that have occurred in the time interval considered.

From these dimensional changes the strain to which the soil element has been subjected in this given time interval can be calculated. This strain may be expressed as:

- mean change in length of the horizontal mesh sides,
- mean change in length of the vertical mesh sides,
- mean change of the mesh angles.

Because the interpretation of these three quantities is difficult, they are usually converted to:

- the direction in which maximum elongation occurred,
- the value of the maximum elongation,
- the value of the maximum shortening (the direction of which is always perpendicular to the direction of the maximum elongation).

In addition, the change of the area of the soil element is often expressed explicitly and the (rigid body) rotation of the element in the given time interval may be given. For reasons of simplicity these calculations usually follow the theory of small strains (FORD, 1963).

When the chosen time interval in which the strain is to be calculated is small enough, a strain rate can be derived. In that case, the accuracy of the measurements taken from the mesh must be very high.

Strain fields. Strain calculations for more meshes can be combined to strain fields (CHANCELLOR and SCHMIDT, 1962). YONG (1969) gives a strain rate field for the process under a rolling wheel.

Information concerning stresses. A strain analysis for a soil element can also give information on the stress to which the element was subjected during the time interval under consideration. This is because the direction of the maximum stress is assumed to coincide with the direction of the maximum shortening. Special methods have been developed to determine the direction of maximum stress from dimensional changes of a mesh, for instance:

- Haefeli's method (BEKKER, 1956),
- Moiré analysis (KIM and STALEY, 1973),
- a method presented in pp. 410–413 of (HETÉNYI, 1950) which allows the determination of the maximum stress direction from length changes of the sides and one diagonal of a mesh.

10.2.6. *Transforming the films from the experiments*

For a preliminary examination the films from the experimental set-up of

Fig. 47 were projected using a 'Bell and Howell' time and motion analyzer. For the actual transformation a 'Proti' 16 mm film reader was used. This film reader could project two successive frames at about the original object size at the same time. In this way, a soil particle could always be recovered in subsequent pictures. The reader had a horizontal screen.

On the whole, each transformation method started with film projection using the film reader. Some methods developed for the described testing procedure are presented below.

Representation of an instantaneous picture. A frame of a cine film taken from a process is an instantaneous picture. The picture could be copied by projecting it onto the horizontal film reader screen which had been covered with tracing paper. The tracing paper had the same line grid as that of the filmed perspex plate. In this way adjustment and distortion errors of the camera and the reader could be eliminated when tracing a projected picture. Fig. 48 presents a traced film picture (from Schinnen series 2), including the markers applied to the soil (a point grid).

N.B. Essentially, for each point grid mesh in Fig. 48, it is possible to calculate the strain that has occurred between the time at which the soil was still untouched, and the time at which Fig. 48 was shot. For this purpose:

- the point grid in the figure should be measured,
- it should be assumed that, in the underformed state, the grid was composed of horizontal and vertical rows of points being 1 cm apart.

However, it was deduced that, due to errors, the following standard deviations occurred in a mesh strain analysis:

- horizontal strain (mean relative change in length of the mesh sides that were initially horizontal): 2.9%,
- vertical strain (mean relative change in length of the mesh sides that were initially vertical): 4.7%,
- angular strain: 3.2°,
- relative change in mesh area: 5.4%,
- rigid body rotation: 1.7°.

These standard deviations were due to errors like:

- inaccuracies in applying the point grid,
- inaccuracies in tracing the film picture,

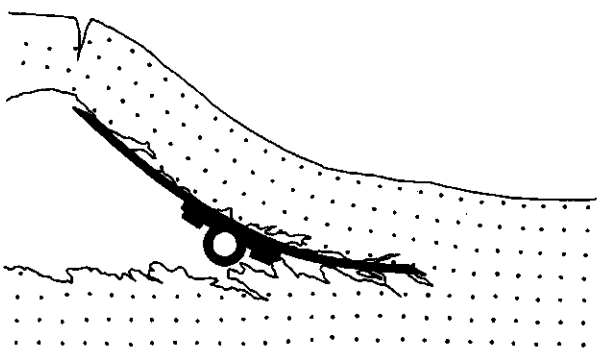

FIG. 48. A traced film picture (Schinnen series 2).

– inaccuracies in measuring the traced point grid.

The given standard deviations are too large to be able to perform a strain analysis with sufficient accuracy.

Failure films. For each tillage process the failure planes and cutting planes that developed during the process were traced on tracing paper that had already been provided with a drawing of the soil wall in the untouched state, including the untouched point grid. Here also, tracing occurred on the film reader screen. A picture, obtained in this way, is called a failure film. The top of Fig. 49 is part of such a failure film. Line AB is the original surface of the soil. Planes of cut are smooth, generally straight lines, failure surfaces normally show a strong variation in direction. There may be a difference between the real failure surface and the picture because parts of a failure surface may not be visible on the process-film. This is particularly uncertain for the final part of the failure surface. Incidentally, crumbling processes may make failure and cut processes less clear. In fact the failure film represents the total effect of a treatment after the elimination of rotation, translation and deformation of the soil. Because these eliminated processes are still small during the intake process, whereas the formation of failure surfaces is already very important at this moment, failure films are especially suited to describe the intake process.

Crack propagation films. The crack front at a certain moment is the end of the failure surface where cracking is still occurring or where it last stopped. During treatment crack fronts move onwards, or stop or new fronts are formed. On moving fronts soil particles are normally roughly in their original position. Therefore, it is possible to design a graph underneath the failure film to indicate

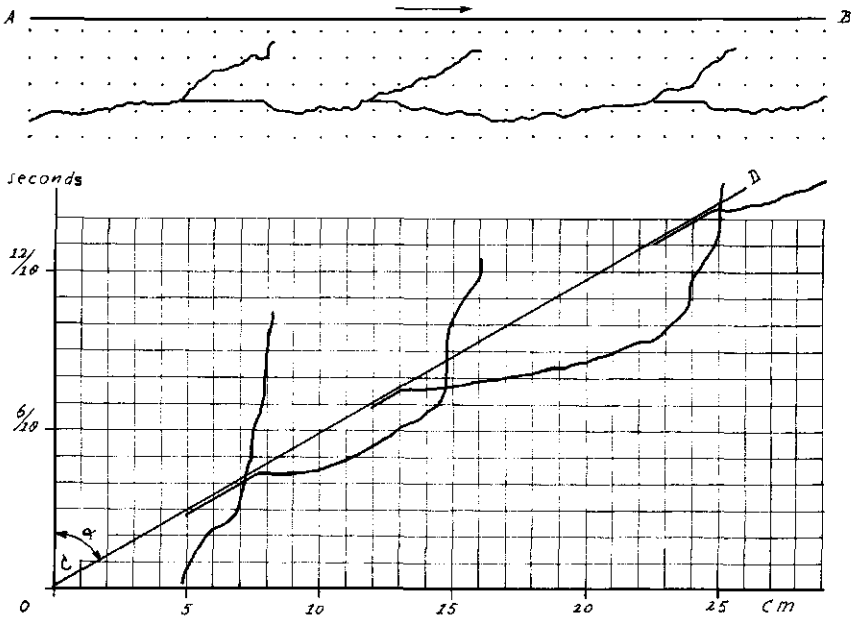

FIG. 49. A failure film and a crack propagation film (Lexkesveer series 1).

the propagation of these crack fronts. On the vertical axis a timescale is indicated and on the horizontal axis the horizontal projection of the position of the crack front in the failure film. An example is given in Fig. 49 (bottom). Line CD indicates the movement of the share (the cutting edge); the travelling speed of the share can be derived from tan α. The other curves show the relation between time and horizontal displacement of the crack fronts. These curves are called crack propagation graphs; CD is called share graph. Share graph and crack propagation graph will coincide when the share cuts and when a crack front is situated straight over or under the share. The direction of a crack propagation graph is vertical when a crack is completed and when a vertical crack is formed. Points not on a share graph indicate, that at the time under consideration, the crack front was ahead of or behind the share. The speed of propagation of the crack front at a certain moment can be derived from the inclination of the crack propagation graph. If the inclination of the crack propagation graph is smaller than the inclination of the share graph, it means that the crack front was moved at a higher speed than the travelling speed of the share. On the other hand, the horizontal speed of a crack front is small where the crack propagation graph is steep. In fact these crack velocities are mean values for a time interval between 2 pictures of the film. The value is more reliable if the position of the failure surface can be measured more accurately.

Indicator films. When in a process part or in a region of a process part the soil does not deform or break further, then it can be assumed that the soil beam coming from that process part will be 'frozen' to obtain a soil beam which is still exactly the same as it was in the process part in question. Such a 'frozen' soil beam can be rather easily traced from a film projected on the film reader screen, and is called an indicator film because it indicates the process shape at a given place on or near the tool. An indicator film can represent an entire tilled soil beam, so that the process shape variation can be expressed to some degree. It is very useful in studies of process developments near the place of indication.

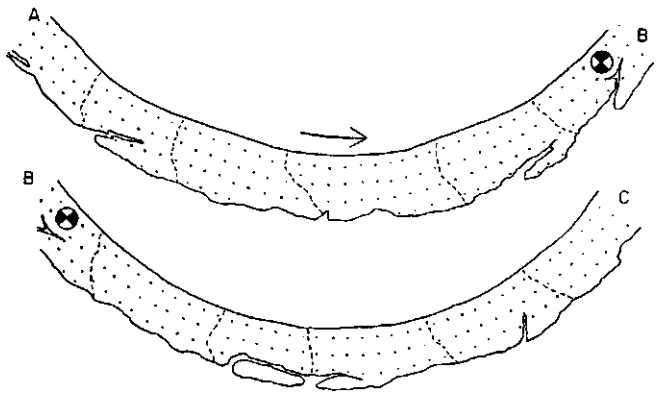

FIG. 50. An indicator film (Schinnen series 3) (KOOLEN, 1972).

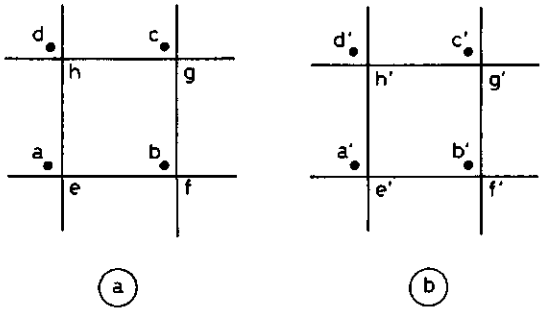

FIG. 51. Refers to the determination of small linear strains.

Fig. 50 shows an indicator film taken from above the trailing end of the curved blade (Schinnen series 3). This figure also shows output cracks, represented by broken lines.

Determination of small linear strains. Fig. 51a shows a small part (under load or having been loaded previously) of an instantaneous tillage process picture that has been traced onto blank tracing paper, using the film reader. Points a, b, c and d represent a mesh of the point grid. The lines passing through e, f, g and h give a mesh of the line grid on the perspex plate, which is also present in the film. Changes in length that occurred in this region between the time at which the picture was shot and the time at which the region was still not loaded, can be determined as follows:

A picture in which the region can be considered to be without a load is recovered from the film of the process. The region, in this state without a load, is traced from that picture. Assuming that Fig. 51b has been obtained in this way; because of lens distortions etc. mesh e, f, g, h does not have the same dimensions as e', f', g', h', and the difference between a, b, c, d and a', b', c', d' cannot be solely attributed to true soil deformation, but also includes lens distortion etc. However, if deformations are small, the following applies to the relative change in length in the direction r (ε_r):

$$(\varepsilon_r)_{\text{due to true soil deformation}} = (\varepsilon_r)_{\text{measured deformation}} - (\varepsilon_r)_{\text{line grid on plate}}$$

Applying this to the diagonal a c, for example, we obtain:

$$(\varepsilon_{ac})_{\text{due to true soil deformation}} = \frac{ac - a'c'}{a'c'} - \frac{eg - e'g'}{e'g'}$$

Hence, by measuring a c, a'c', e g and e'g' from the figures it is possible to calculate ε_{ac}, due to true soil deformation.

When applying this method the accuracy has often been increased by considering the corner points of a square of 4 meshes, rather than the corner points of one mesh. Sometimes comparable film pictures have been considered to be duplications, allowing averaging procedures to be used.

10.3.1. *Some instantaneous pictures*

In many of the experiments the intake appeared to be of the open crack formation type. In this case, share penetration into still firm soil will end in the formation of an open crack. The share can often enter the crack like a wedge, making the crack develop further. When the crack turns off, for instance up-

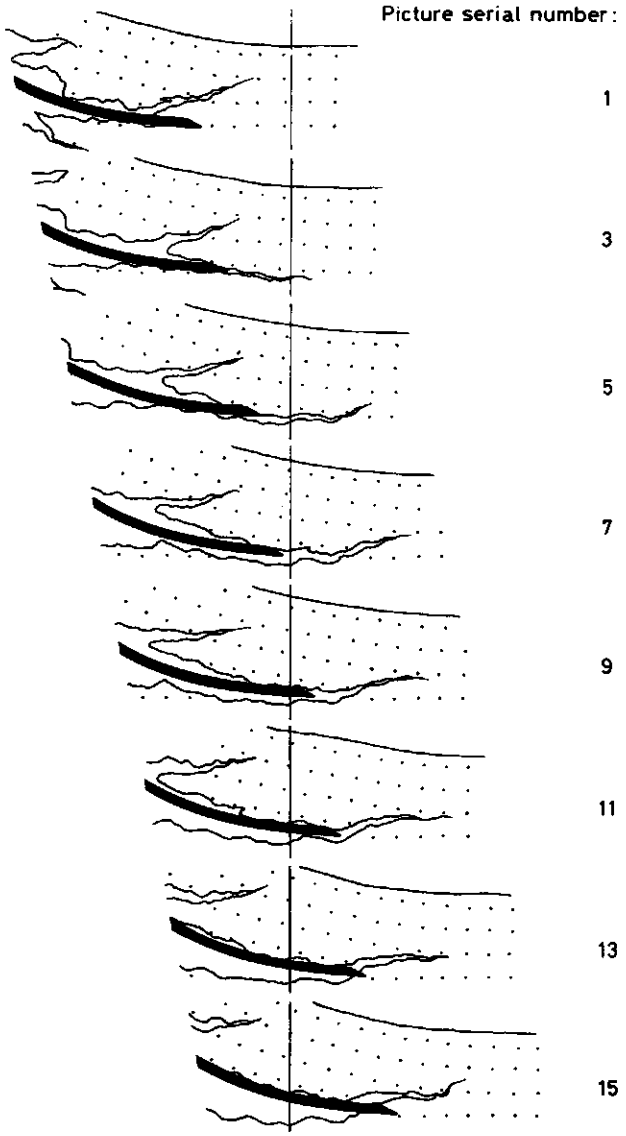

FIG. 52. Series of instantaneous pictures (L1).

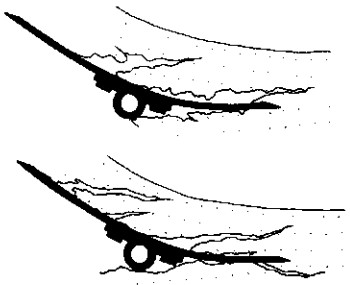

FIG. 53. Pictures from W3 (a) and L2 (b).

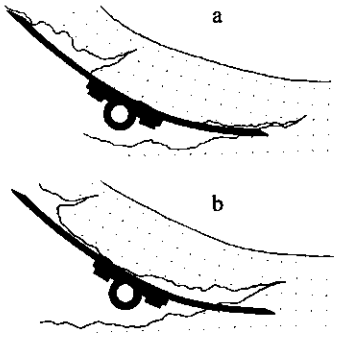

FIG. 54. Pictures from L1.

wards, then, at a given time, the share will encounter still firm soil again, after which another crack will be formed at the share point. Fig. 52 shows such a crack formation by means of a series of instantaneous pictures. Fig. 53 gives some pictures shot at situations where the share point has penetrated still firm soil so far that new cracking will start immediately. Fig. 54a shows the share starting to penetrate still firm soil, and Fig. 54b shows the situation in which the share has progressed so far that a new crack will occur immediately.

A multitude of cracking process forms are possible. These forms depend on:
- penetration length necessary to produce cracking,
- direction of crack propagation,
- any turning off upwards or downwards of such a cracking,
- the place at which cracking stops,
- crack propagation velocity.

10.3.2. *Some failure films and crack propagation films*

Failure films and crack propagation films from a number of experiments are discussed below.

Lexkesveer series 1. Fig. 55 is from process-film: 'Lexkesveer series 1' (Table III). The failure film starts with a crack ahead of the share front and at a greater depth than the nominal working depth. The entire soil-strip moves over the blade and therefore the share front is not cutting. The crack moves upwards and then, at one place, the depth of the crack will be less than the depth of the share. When the share reaches this point cutting will start. If we proceed in the crack propagation graph from point A to the right, we find that at this moment the crack front is about 4 cm ahead of the share and that the horizontal component of the crack velocity has been reduced to about zero. Real working depth of the share at the moment where cutting starts is very small. Along with the cutting a process is started that will bring the unbroken soil into a position where initiation of a crack is reached. After a cut of about 3 cm this condition is reached and cracking starts at an initial speed of 125 cm/sec which is much higher than the travelling speed of the share (about 32 cm/sec). Initially, the cracking proceeds in a downward direction and the depth of the soil-strip

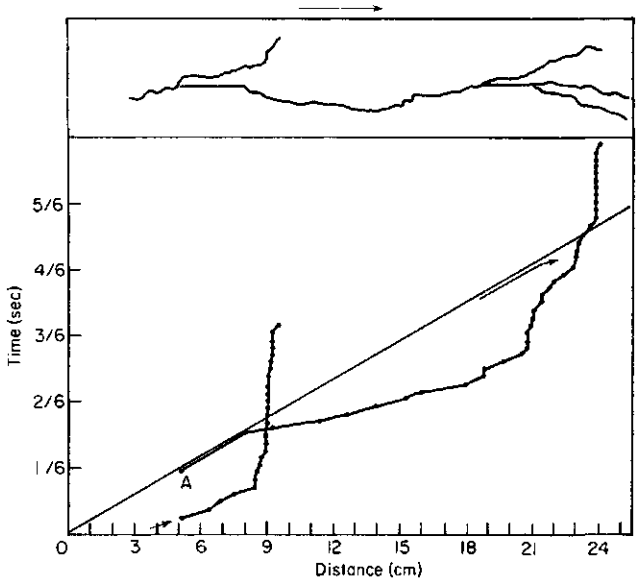

FIG. 55. An intake process of L1 (KOOLEN, 1972).

moving upwards is larger than the working depth of the share. Crack velocity decreases, and when this speed has dropped to the level of the share speed, the crack front is a maximum distance of 6 cm ahead of the share. The direction of propagation has now turned upwards and therefore cutting will have to start at a certain moment. From this picture it appears that when the share is cutting there is still another active (moving) crack front present. Sometimes 2 crack fronts are active at the same time. In these cases the oldest active front is a phenomenon belonging to the main flow.

Fig. 56 represents a greater part of the L1 experiment. It can be seen from this that crack development is always preceded by about 2 cm share penetration into firm soil. The cracks usually start in a downward direction, later turn off upwards, and stop close to the soil surface. Crack velocity does not resemble share velocity very much and the maximum distance between the share and the crack front is large When the share has to penetrate firm soil again, crack propagation generally stops. Where firm soil is penetrated, the working depth is equal to its nominal value, but where cracking occurs the crack may reach lower, as far as $\pm$ 1 cm; this is the way in which holes are formed in the furrow bottom.

For this experiment the place of application of the force exerted by the blade on the soil being taken in was determined (this place is actually the place of contact between the blade and the soil being taken in). These places are indicated by the shaded area. Turning off of a crack nearly always coincides with a change in the place of application in a direction away from the share.

Lexkesveer series 2. See Fig. 57. Penetrating firm soil occurs in a compara-

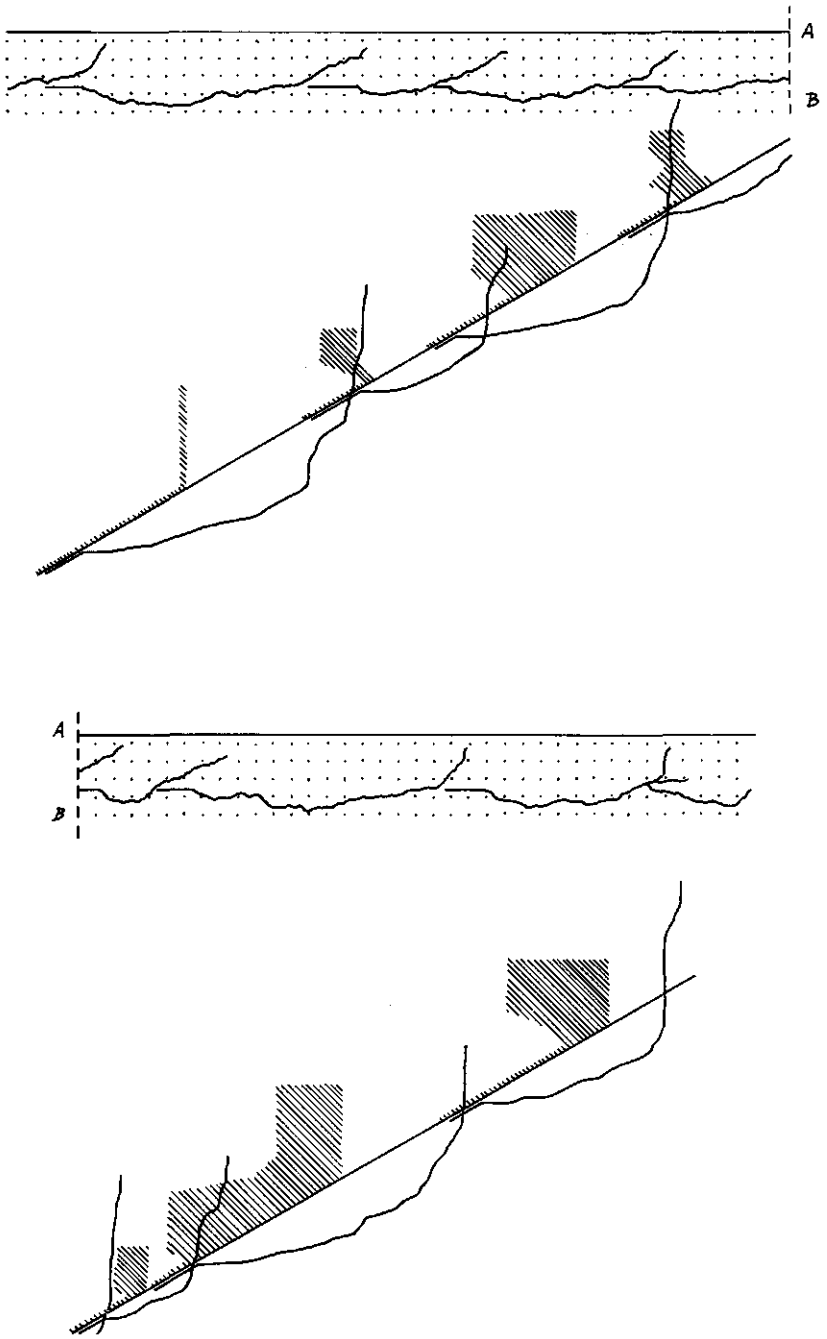

FIG. 56. Lexkesveer series 1.

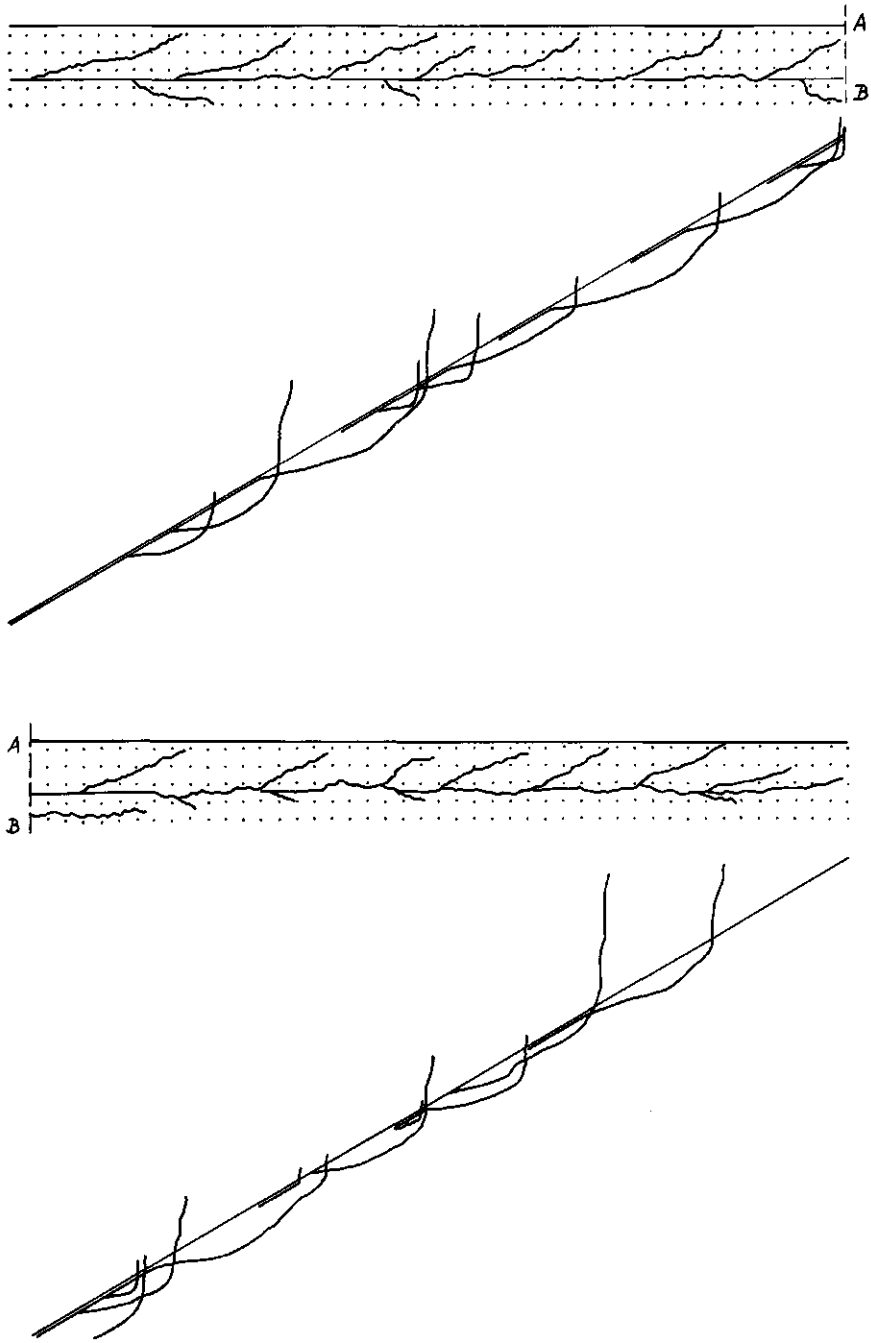

FIG. 57. Lexkesveer series 2.

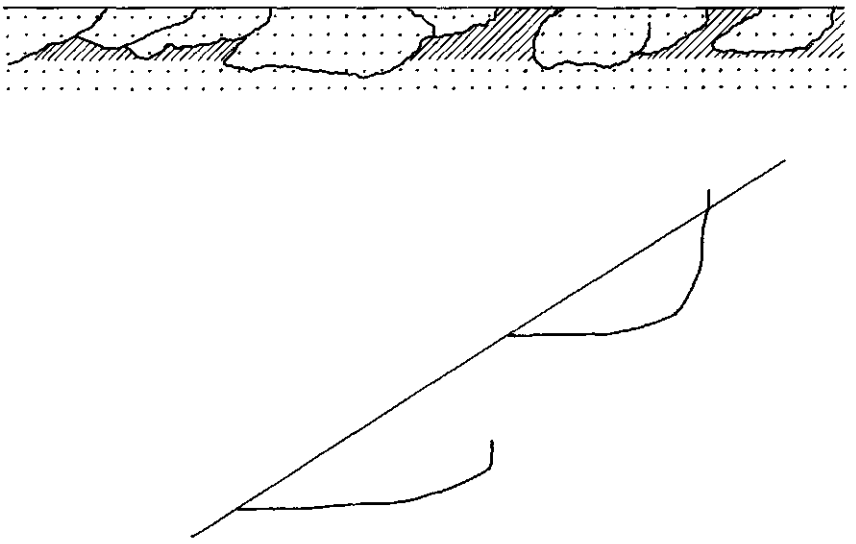

FIG. 58. Lexkesveer series 5.

tively large part of the film. The cracks may start in a downward or upward direction. In these cases the share keeps penetrating firm soil after the initiation of a crack. Cracks can also start in a horizontal direction, thus clearing the path for the share. The downward starting cracks form tongues in the furrow bottom. The upward starting cracks end just below the soil surface. Cracks starting horizontally, turn off upwards later, and also stop just below the surface. There is some fork formation (splitting of a running crack into two running cracks). In comparison with L1 there is more resemblance between share speed and crack front velocity, and the distance between share and crack front is less. When a new crack starts to develop the extension of the previous crack stops. Working depth almost equals nominal working depth. Because penetration of firm soil and horizontal cracking alternates, and because of tongue formation, the furrow bottom is composed of smooth parts (cutting planes), rough parts (crack planes) and fissures (bottom sides of tongues).

Lexkesveer series 5. In the shaded parts of the failure film of Fig. 58 the soil is highly pulverized. The larger pieces are torn out without any firm soil penetration. These cracks start in a downward direction, but the share can still enter them. Later the cracks turn off upwards and run right up to the surface. There is very little resemblance between share speed and crack front velocity, and the maximum distance between the share and the crack front is large. When large pieces are formed, working depth exceeds its nominal value, and holes will be left in the furrow bottom.

Wageningen series 1. See Fig. 59. Firm soil is nearly always being penetrated. If any cracking occurs, then the crack front is always very close to the share and the cracks do not reach far into the soil beam.

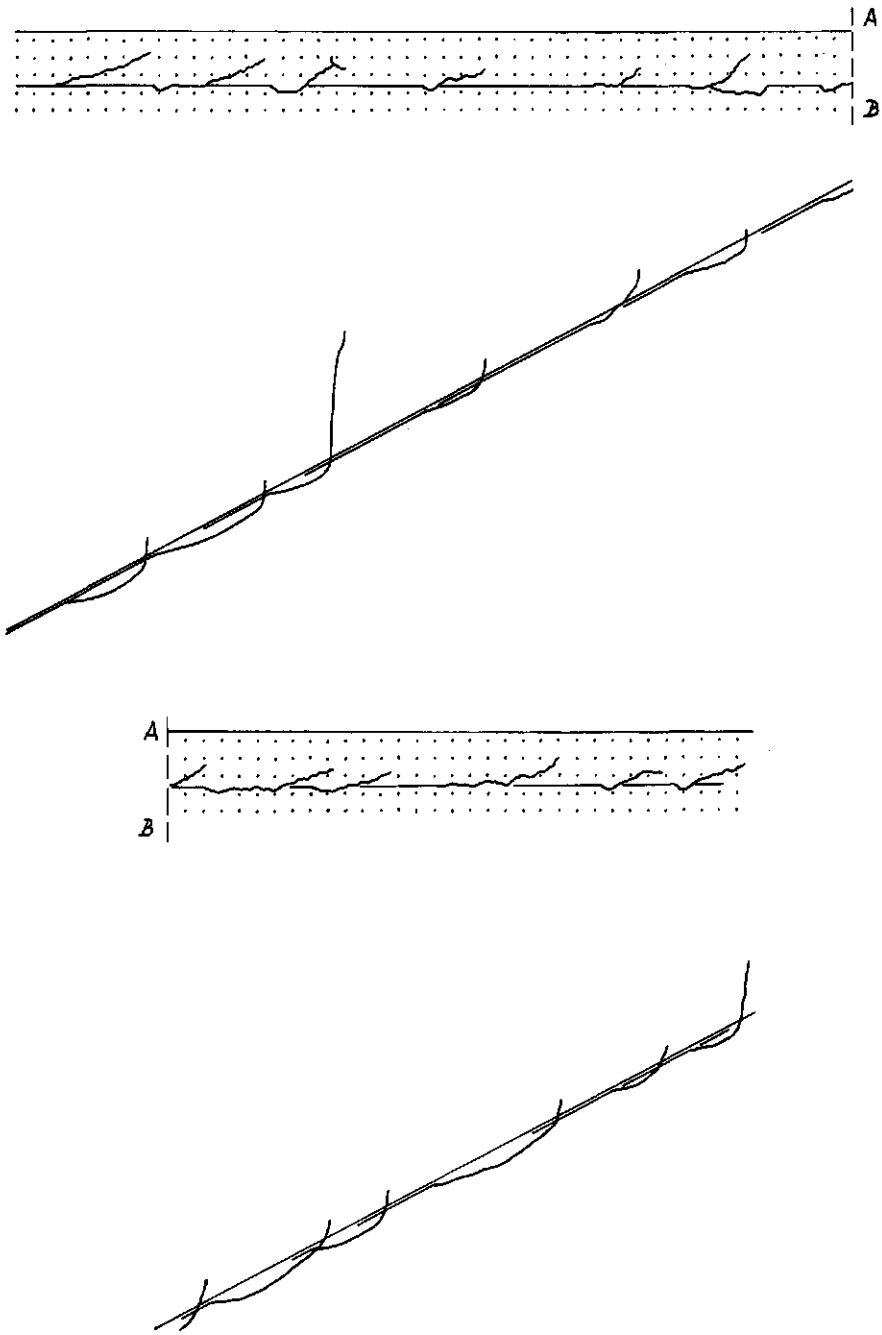

FIG. 59. Wageningen series 1.

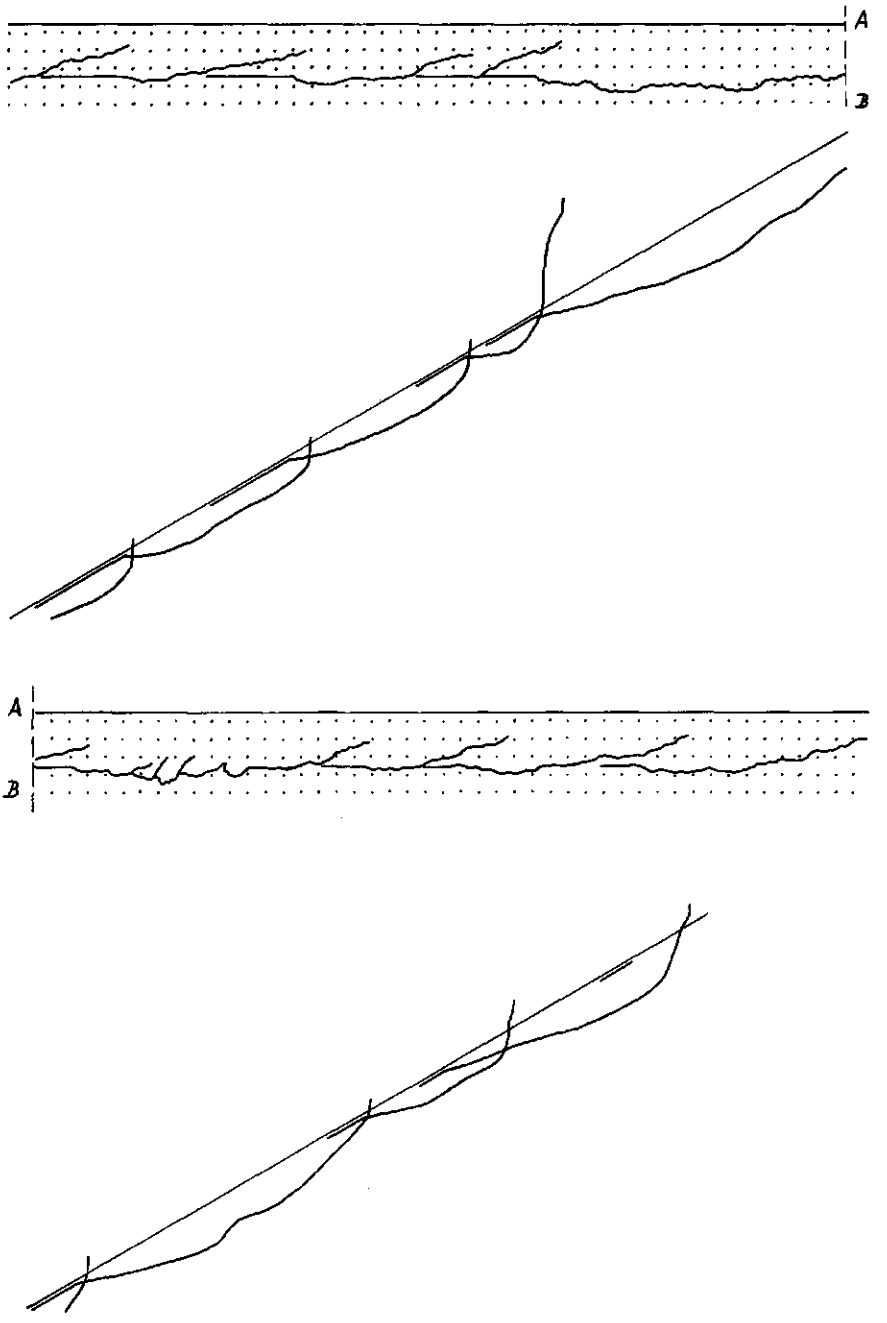

FIG. 60. Wageningen series 3.

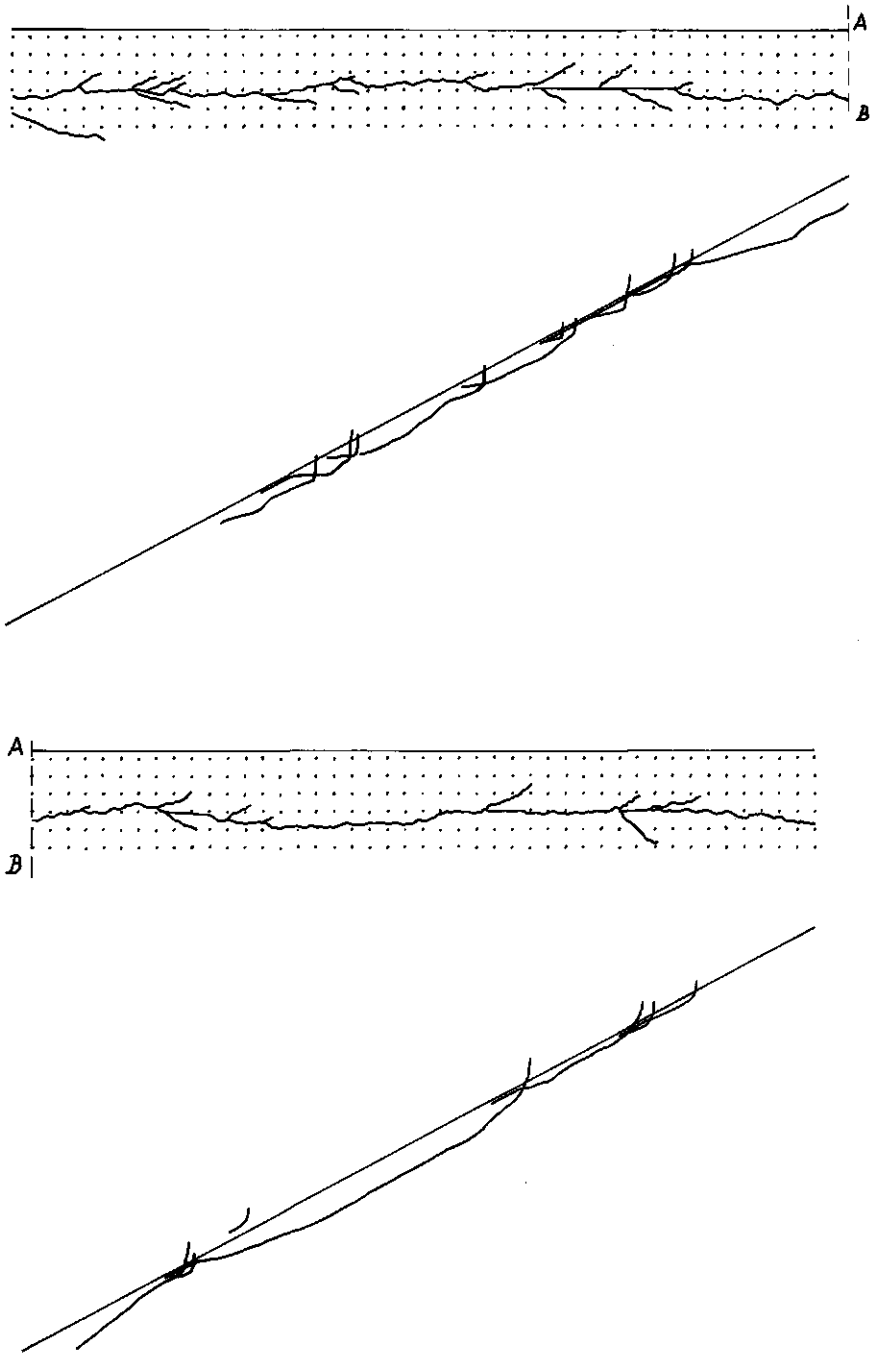

FIG. 61. Schinnen series 1.

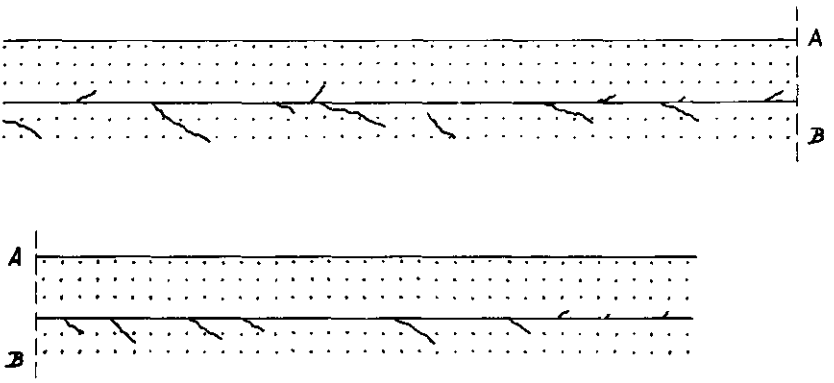

FIG. 62. Schinnen series 2.

Wageningen series 3. Prior to crack development the share has to penetrate a few centimetres into firm soil (Fig. 60). Cracks start in a nearly horizontal direction, turn off upwards later, and stop in the centre part of the soil beam. Crack front velocity somewhat resembles share speed, and there is a fair distance between the share and the front. When a new crack starts to develop, the extension of the previous one stops. Working depth often equals its nominal value. Sometimes it is larger, giving rise to holes in the furrow bottom.

Schinnen series 1. As shown in Fig. 61 there is comparatively little penetration of firm soil. Some cracks start in an upward or downward direction to such an extent that the share is unable to enter them. There are also cracks that start horizontally and clear the path for the share. These cracks may turn off downwards or upwards later. No cracks are present in the upper part of the soil beam. On some locations there is fork formation. Crack front velocity resembles share speed, and the distance between share and crack front is small. Cracking stops as soon as a new crack starts to develop. Due to the soil in front of the blade being pushed upwards, and due to hole formation, working depth usually exceeds it nominal value.

Schinnen series 2. Only a failure film is given from this experiment (Fig. 62). The blade penetrates firm soil all the time. Sometimes cracks appear which start in a non-horizontal direction. These occasionally run upwards, but usually downwards. The soil beam is left almost unbroken. A great deal of tongue formation is present. Because of soil being pushed upwards the working depth is greater than the nominal working depth.

Schinnen series 3. Fig. 63 shows that there is usually a few centimeters penetration of firm soil before cracking starts. Some cracks start in an almost horizontal direction, then turn off upwards and stop in the centre part of the soil beam. Other cracks start in a downward direction, still allowing the share to enter them. In these cases, the blade pushes the soil above the crack forwards and upwards, the crack being extended still further. Nevertheless, at a certain moment the blade must penetrate firm soil again, and downward crack exten-

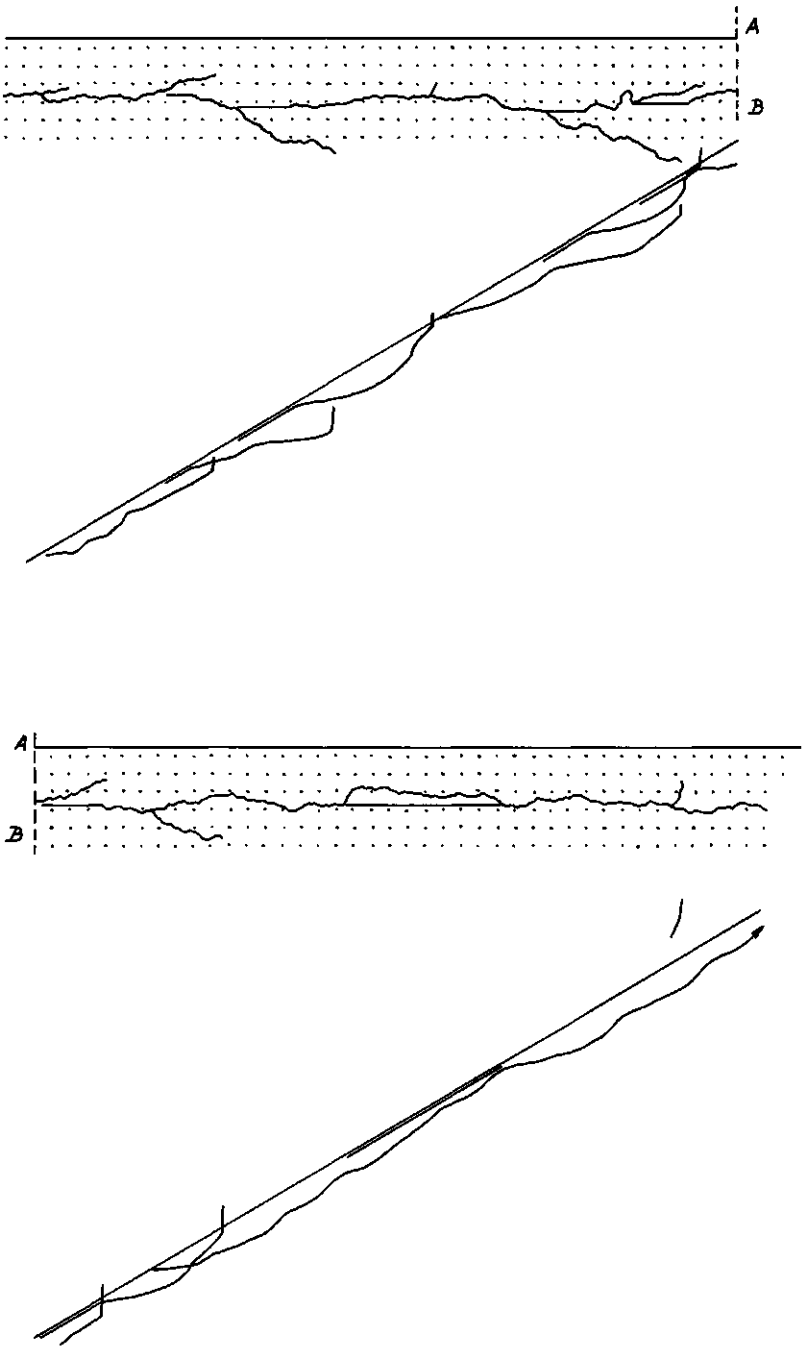

FIG. 63. Schinnen series 3.

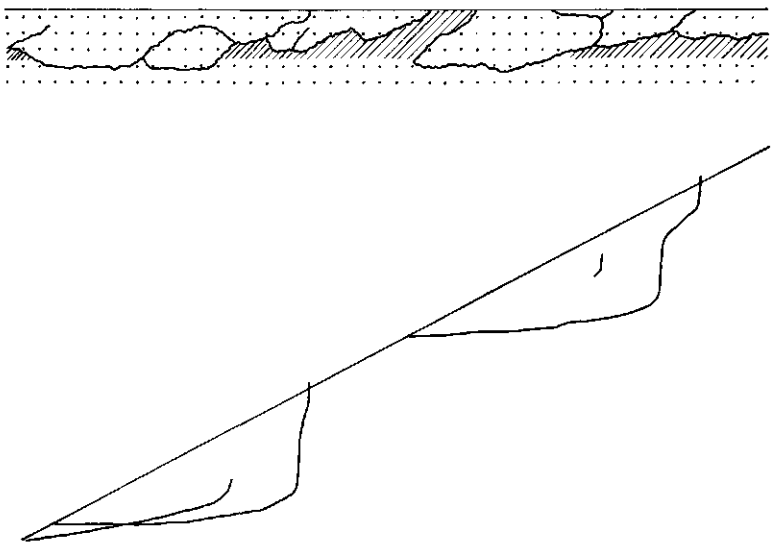

FIG. 64. Schinnen series 5.

sion stops. There is not much correlation between penetrating firm soil on the one hand and cracks coming to rest on the other. Crack front velocity resembles share speed and the distance between the share and the crack front is small. Working depth fluctuates strongly and often exceeds nominal working depth due to pushing action of the blade. Sometimes horizontal crack formation takes place somewhat higher than nominal working depth. In that case the share 'planes' as it were the lower crack surface, separating small soil parts. One slice in the soil beam can be seen in the failure film. It is caused by a horizontal crack running much higher than working depth, which later suddenly turned off downward, allowing the share to enter the crack again.

Schinnen series 5. This picture very much resembles that of L5 (compare Fig. 64 with Fig. 58).

Ede series 1. See Fig. 65. Penetrating firm soil almost always only takes place where slices in the soil beam are being formed. Cracking usually starts in a horizontal direction, turns off upwards later, and stops under the soil surface. In one case a crack travels downwards. Crack front velocity resembles share speed and there is a fair distance between the share and the crack front. Working depth is almost equal to nominal working depth.

Ede series 2. The picture (Fig. 66) shows a crack running more or less steadily and almost horizontally, with rather constant distance between the share and the front, and rather constant crack front velocity (being almost equal to share speed). The distance between share and crack front is large. Sometimes a crack that will develop in a forward and upward direction is initiated, occasionally due to fork formation. When the depth of cracking is somewhat less than share depth, the share is planing. When it is somewhat greater, holes are formed in the

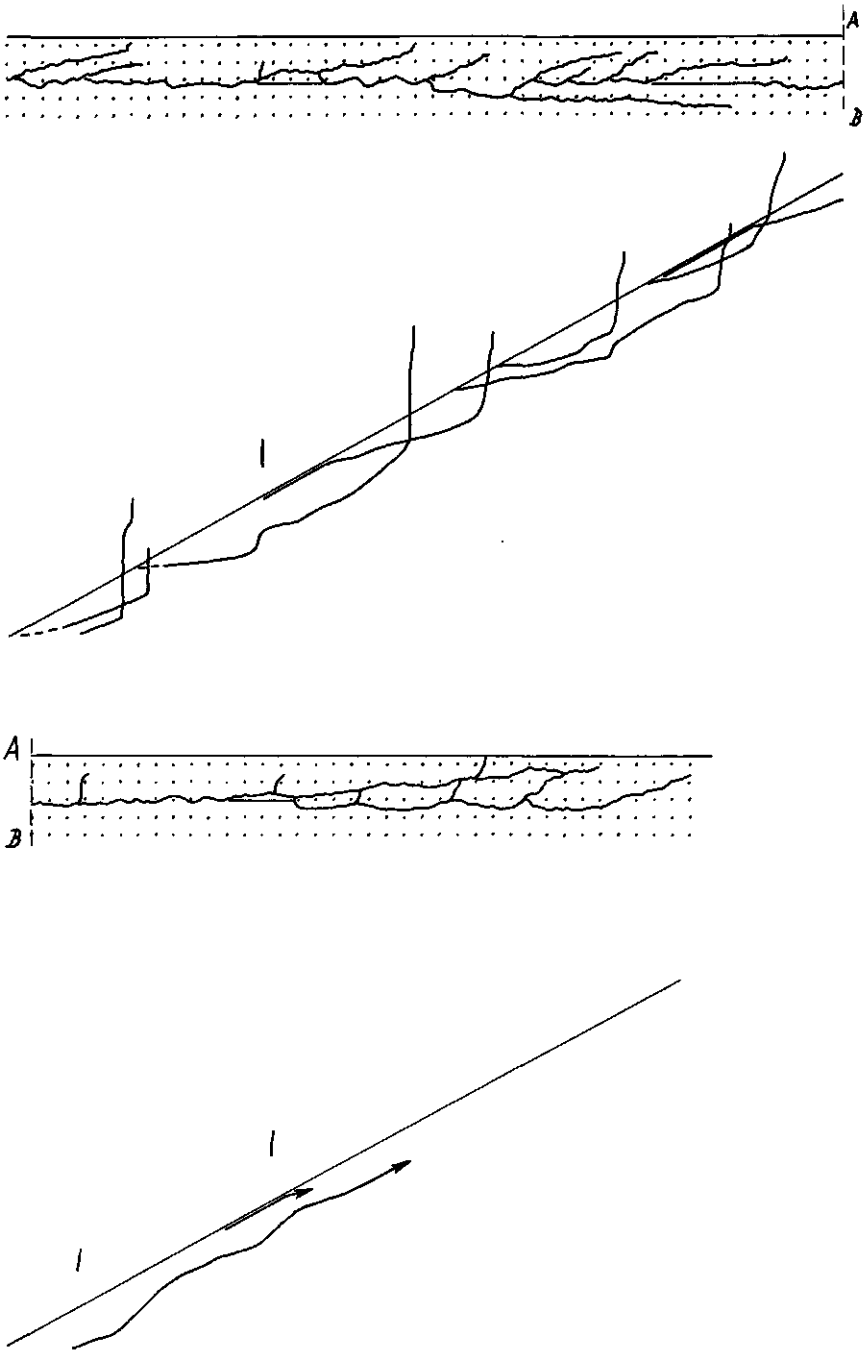

FIG. 65. Ede series 1.

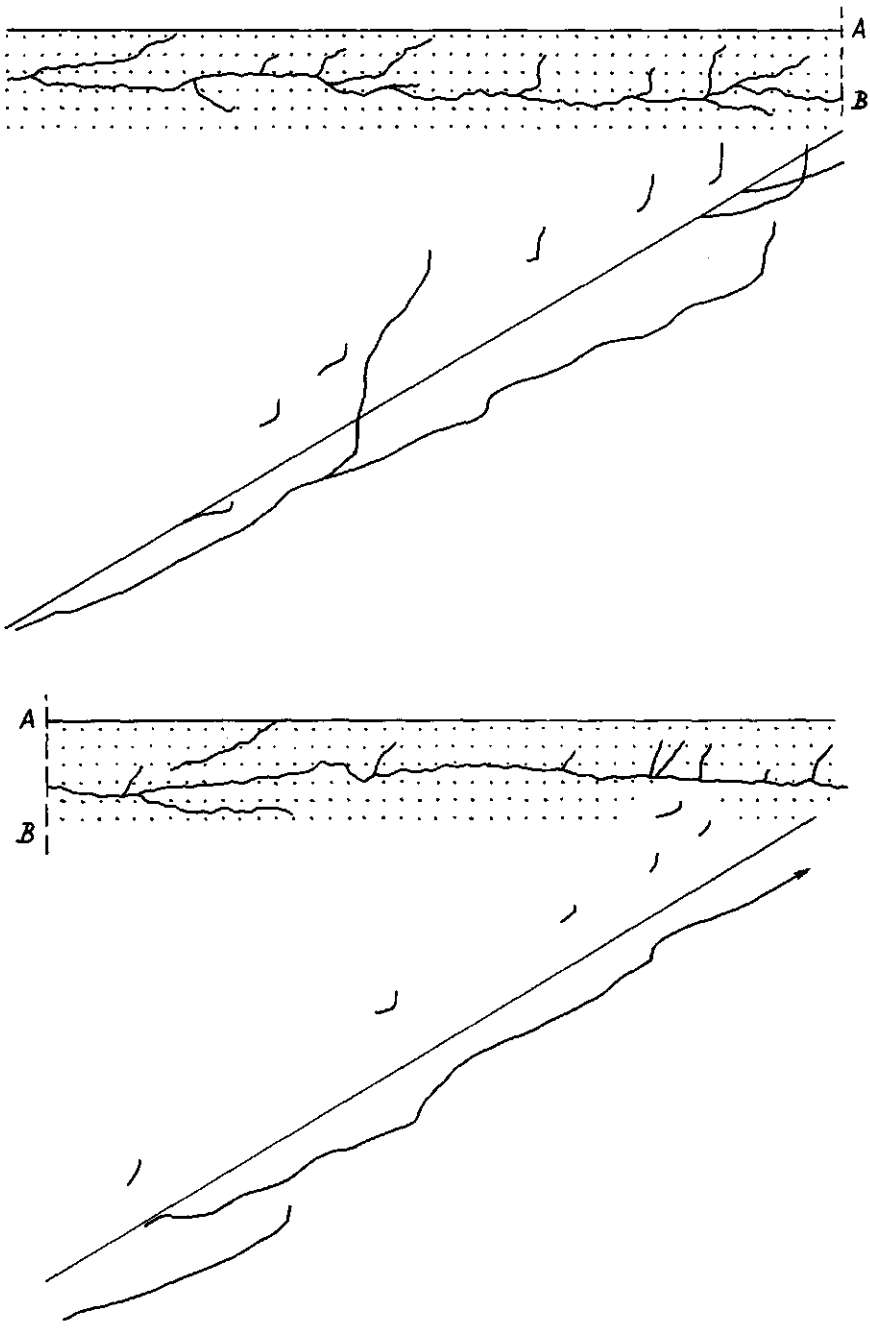

FIG. 66. Ede series 2.

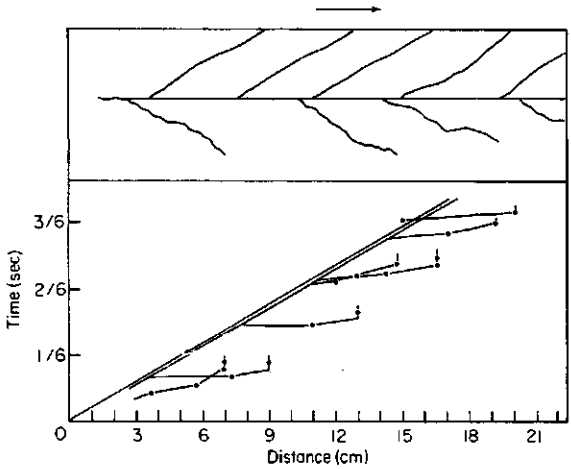

FIG. 67. Ede series 3. (KOOLEN, 1972).

furrow bottom. The small vertical cracks in the lower part of the soil beam develop in the main flow.

Ede series 3. Fig. 67. The share always penetrates firm soil, at the same time generating, with high regularity, failure planes that are directed upwards at an acute angle to the horizontal. These failure planes are parallel to each other and run right up to the soil surface. There is occasional downward cracking, giving rise to tongues. Crack front velocity is much higher than share speed.

10.3.3. *Classification of the intake processes*

The intake processes of the experiments have been divided into the following categories (which are defined in section 4.2.1.):

- intake by shear-plane failure,
- intake by steady cutting,
- intake with open cracks.

Failure films given in Figs. 59 (W1) and 62 (S2) were considered to be 'intakes by steady cutting'. Fig. 67 (E3) was classified as 'intake by shear-plane failure'. The rest of the presented failure films were called 'intakes with open cracks'. Table V gives the complete classification of the intakes. This shows that open crack formation occurred most frequently. Open crack formation may be sub-divided according to Fig. 68. Often, several of the phenomena mentioned in this figure occur in one experiment.

10.3.4. *Distance between the share and the crack front, crack length, and their quotient*

For the intakes with open crack formation the following quantities have been determined from the cracks that have ends with an upward direction.

l_{max} = length of the horizontal projection of the distance between the posi-

TABLE V. Intake processes.

Soil	Wageningen	Lexkesveer	Schinnen	Ede
Series				
1	steady cutting	open cracks	open cracks	open cracks
2	open cracks	open cracks	steady cutting	open cracks
3	open cracks	shear-plane failure	open cracks	shear-plane failure
4	open cracks	open cracks	open cracks	open cracks
5	open cracks	open cracks	open cracks	open cracks

tion where the crack was initiated and the position where the crack front came to rest.

h_{max} = length of the horizontal projection of the distance between crack front and share at the time that this distance is maximum.

These quantities were directly measured from film projections on the film reader screen. Table VI gives their mean values. In a few tests the failure patterns was indistinct thus preventing reliable determination of those quantities.

When discussing the failure films and the crack propagation films attention was also given to the degree of resemblance between share speed and crack front velocity. This was visually estimated from the degree to which the 'crack graphs' were parallel to the 'share graph'. A quantitative measure of this resemblance is provided by the quotient of the mean value of h_{max} and the mean value of l_{max}, which quotient will be denoted by F. Using Fig. 69, the following physical meaning can be assigned to F. Fig. 69 shows 3 intake processes with

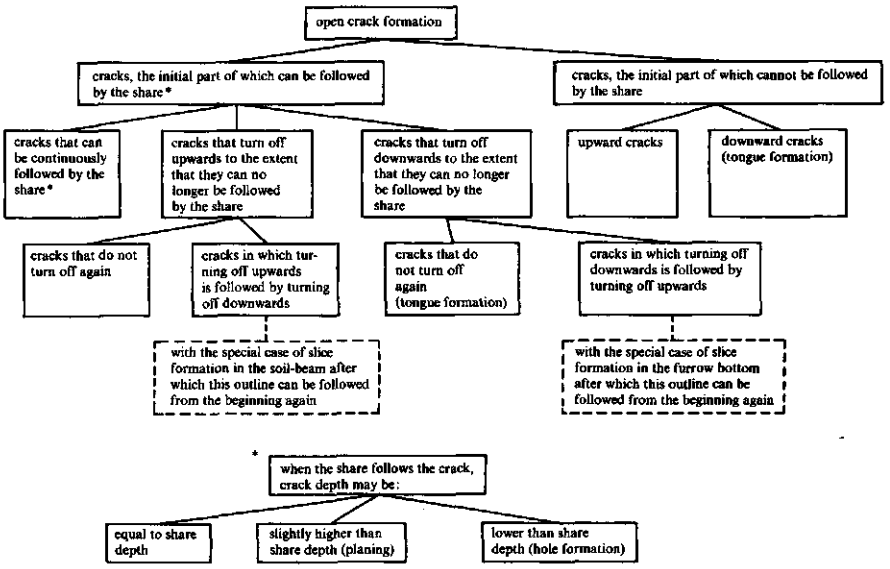

FIG. 68. Open crack phenomena.

TABLE VI. Mean values of the (projected) maximum crack length (l_{max}), the (projected) maximum distance between share and crack front (h_{max}), and their quotient (F).

Intakes with open cracks	Mean values of l_{max} (cm)	Mean values of h_{max} (cm)	F
W3	–	–	–
W4	7.3	5.5	0.75
L1	11.6	4.7	0.40
L2	7.8	2.9	0.37
L4	9.7	6.6	0.69
L5	10.2	7.7	0.76
S1	9.5	2.2	0.23
S3	13.7	3.1	0.23
S4	8.2	4.4	0.54
S5	–	–	–
E1	13.8	3.9	0.28
E2	27.1	6.8	0.25
E4	–	–	–
E5	–	–	–

open cracks. The first process demonstrates a theoretical one exhibiting:
- cracking that continues to travel in a horizontal direction,
- crack front velocity that always equals tool velocity.

These facts keep h constant; crack length l continues to increase and ratio

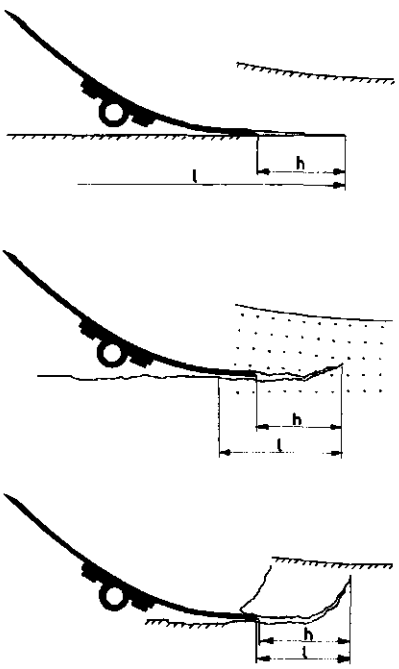

FIG. 69. Intake processes with open crack formation.

$h:l$ will attain values close to zero. The third example is also theoretical and demonstrates a process in which:
- crack formation has turned upwards,
- crack front velocities much higher than tool velocity have occurred, and now

$$\frac{h_{max}}{l_{max}}$$

approaches one. The second picture is typical of observed intake processes with open cracks and the ratio h_{max} to l_{max} obtains a value between zero and one. Hence, the F-value of an experiment will show to what degree the intake of this experiment resembles the first or third process of Fig. 69. F may be considered to be a quantity which indicates the degree of steady cracking in a process.

Values of F measured from the experimental films are listed in Table VI. It may be seen that F has the capacity of varying over a broad range. (N.B. In defining F, no use is made of: mean value of (h_{max}/l_{max}). In the definition used longer cracks have more influence on F than short ones).

10.3.5. *Starting and running-out processes*

In the case of soil tillage we are primarily interested in the processes occurring when tool speed is constant and that are not affected by starting or running-out phenomena. This is comparable to fluid mechanics where pipe flow studies have been concentrated on the equilibrium situation that will arise some time after opening the valves. The simplest equilibrium situation involves pressures, flow rates, etc. that do not change with time. Fluid mechanics uses the expression 'steady state' for this. A flow in a given co-ordinate system is said to be steady if in any point belonging to the flow and fixed in the co-ordinate system, the velocity vector does not vary with time. The steady state concept has also been made applicable to turbulent flows by using mean velocity vectors instead of actual vectors. In this case the selected time interval over which velocities are to be averaged is large so as to achieve mean vectors that indeed remain constant with time (SHAMES, 1962). This also seems to be applicable to soil tillage processes. However, because soil break-up is less incidental than turbulent flow the following definition is chosen: a tillage process is called a steadily fluctuating process if, at any of its points fixed relative to the tool, the flow properties are repeated periodically, apart from incidental effects.

Returning to the experiments, the question arises whether steadily fluctuating processes occurred in the experiments, and, if so, in which parts of the experiments. Consider all soil that is successively in the intake zone. At the start of the test run the soil being taken in is only influenced by the tool share, which causes a specific process. As the tool progresses the blade is filled with soil, and this soil influences the intake shape. This influence is dependent on the way in which this soil was taken in (unsteadily fluctuating). If that dependence is negligible, then the intake process will attain its steadily fluctuating shape as soon as the blade is completely filled (that is when the amount of soil entering

the blade equals the amount leaving the blade). As soon as there is an output of soil being taken in in a steadily fluctuating way, the entire tillage process can be considered to be steady. Hence, it can be generally stated that the starting period will be shorter as:

- the intake zone is smaller,
- the external influences on the intake are smaller,
- the tool is shorter, so filled faster,
- the thickness of the soil mass on the tool does not much exceed the depth of cut (which means that less soil is needed to achieve complete filling),
- the filling efficiency is higher (filling efficiency is low if there is an output before complete filling occurs).

The starting process exists over a distance that is never shorter than about one tool length and may comprise many tool lengths.

Significance of the thickness of the soil mass on the tool. This is demonstrated in Fig. 70. This figure represents a soil flow that is only bent and a soil flow that is composed of pieces that are separated by parallel failure planes with an inclination of 45°. For output to occur the blade had to travel a distance 0.9 times the blade length in the former case, and 1.25 times the blade length in the latter case.

Filling efficiency. Filling efficiency seems to have a great influence on the length of the starting period. In E3 the amount of soil on the blade continued to increase during the entire experiment, even after the start of soil output. This phenomenon also appeared in other soils having high porosities.

External influences on the intake. The intake is affected by factors such as the following, which change during the starting period:

- the main flow,
- the subsoil,
- the load to which the soil in question was subjected prior to the time under consideration.

This is shown from the failure films of the first parts of the experiments. Fig. 71 gives these for series 1, 2 and 3. In this figure W3, L3, E1, E2 and E3 clearly show that crack formation is directed in a less upward direction as the tool progresses and later becomes steadily fluctuating. In the steadily fluctua-

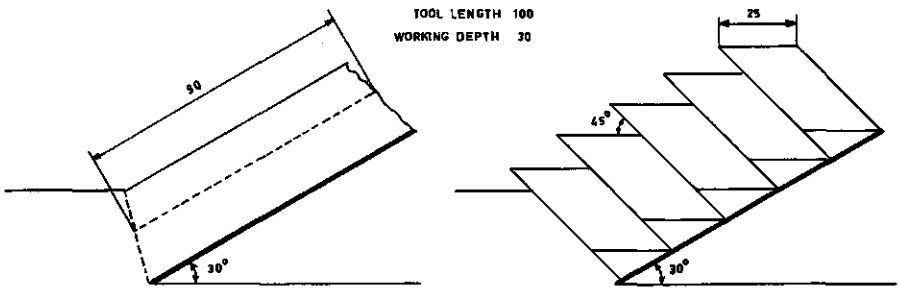

FIG. 70. Refers to starting processes.

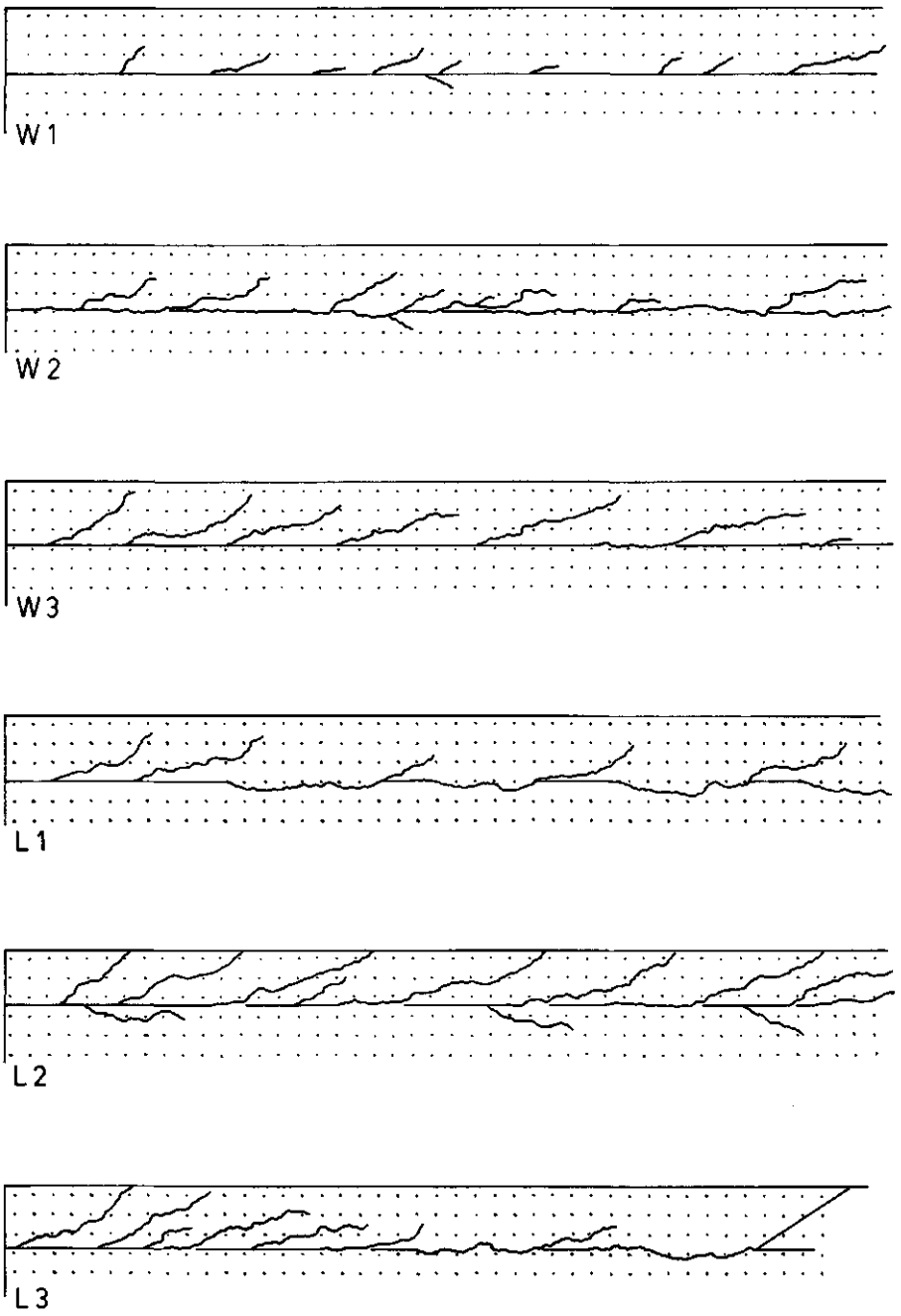

FIG. 71 (part 1). Failure films from the tool starting processes.

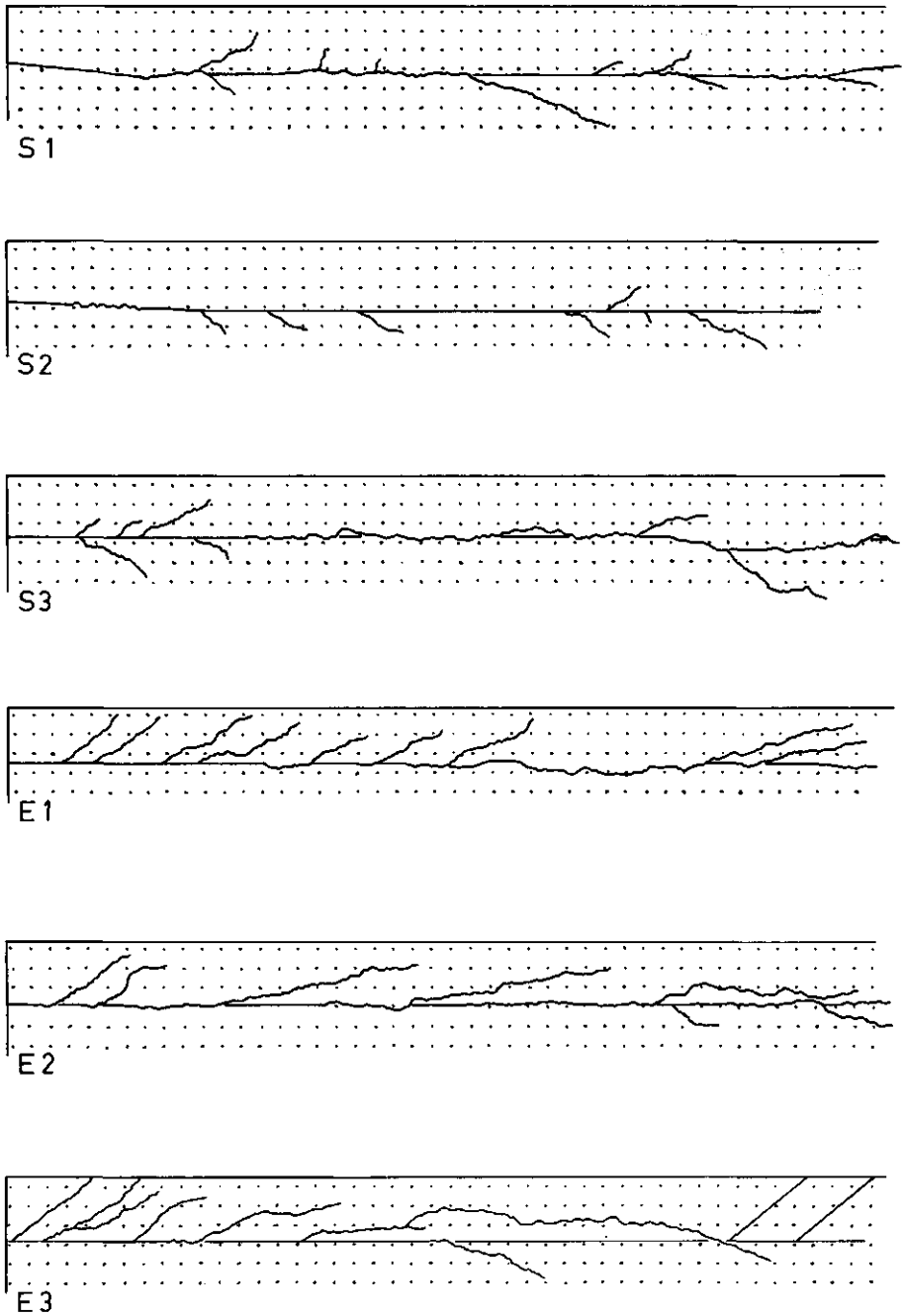

FIG. 71 (part 2). Failure films from the tool starting processes.

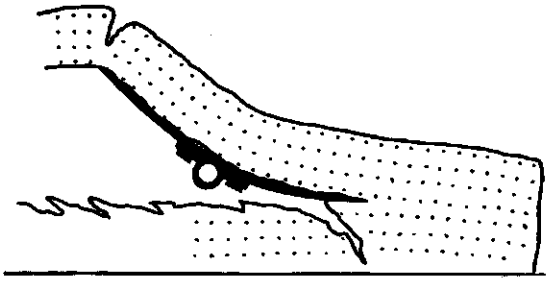

FIG. 72. Running-out effect.

ting state the intakes of L3 and E3 are of the shear-plane failure type. The figure shows this clearly. It also indicates that prior to the failure planes starting to occur there is open crack formation. In the period with open crack formation cracking direction is less upward as the tool travel length increases. Fig. 71 also shows that there is comparatively large penetration of firm soil in the starting period. Naturally, the share will start at nominal working depth. However, the share may push the soil forwards and upwards, making the working depth increase with increasing travelling distance, until the steadily fluctuating state occurs. This is clearly shown in S1 and S2.

Running-out process. When the tool is approaching the end of the soil mass then, at a certain moment, the intake process in its steadily fluctuating state will no longer fit in that part of the mass which is in front the of tool. The intake process then starts to differ. In the experiments the ends of the soil mass were not confined, allowing the soil to be taken in in such a way as to be entirely separated from the soil mass when the tool was running out. Fig. 72 shows this for S2.

10.3.6. *Speed effects*

In 10.3.1. to 10.3.5. intake phenomena concerning observations made at 32 cm/sec tool speed were discussed. For a preliminary examination of speed effects a few tests at tool velocities of 16 and 32 cm/sec were carried out, using a blade that was rather similar to that presented in 10.2.2. For a Lexkesveer soil with a moisture content of 19.5% and a porosity of 40%, tests at 3 cm depth exhibited intake with open crack formation and involved the speed effects

TABLE VII. Tool speed effects.

	Tool speed	
	16 cm/sec	32 cm/sec
(horizontally measured) maximum crack front velocity (cm/sec)	64	99
maximum horizontal crack front velocity/travelling speed	4	3
(horizontally measured) maximum distance between the share and the crack front (cm)	3.9	2.4
maximum piece thickness (cm)	3.7	3.3
piece length (cm), measured at half the working depth	10.5	6.2

shown in Table VII. As can be seen tool velocity is to be regarded as an important factor.

10.3.7. *Products of the intake*

The intake delivers a soil beam and a furrow bottom. The tool caused a plane of separation between them. This plane of separation does not usually pass along the soil particles that were originally at nominal working depth. Reasons for this are: the soil being pushed upwards at intake, and cracks extending below the share depth whereas all the soil on the top of the crack is taken in by the blade. It is also not true that the depth of the furrow bottom always equals share depth: with the soil being pushed upwards and forwards in the intake zone, part of the furrow bottom behind the share can be taken along. This is always accompanied by tongue opening in the furrow bottom. Also, tongues can adhere to the tool and are consequently moved forwards, and therefore also upwards.

The bottom of the furrow may be composed of cutting planes, failure planes and cracks under tongues. At the bottom of the furrow slices and holes may be present. The cutting planes are not usually completely smooth, but often have very small cracks that are similar to the larger ones under the tongues. These small cracks are inclined forwards and downwards from the cutting direction: so they may serve as an aid when the cutting direction is to be determined from an existing cutting plane. The upper part of the soil under the furrow bottom has usually been moved forwards to some extent.

The bottom of a soil beam that has just been taken in may exhibit phenomena that very much resemble those being described for the furrow bottom (cutting planes, failure planes, cracks above tongues, slices). The soil beam may be torn, broken or deformed, and may have a thickness equal to or larger than nominal working depth.

10.4. Some contributions to the predictability of intake processes

Section 10.3 showed that intake with open crack formation occurred most frequently. Now a treatise will follow in which the blade in question (at the tested speed and working depth) is considered to cause open crack formation in the 'normal' case, and shear-plane failure or steady cutting in some special cases. At first different evidence is presented to show that open cracks are brittle failures. Subsequently a (very simple) model based on brittle failure is discussed in order to explain several phenomena that have been observed. Circumstances are indicated in which steady cutting or shear-plane failure will occur.

10.4.1. *Evidence for the occurrence of tensile stresses in the intake*

Some indications are given below from which it can be deduced that tensile stresses can occur in the soil in the intake zone.

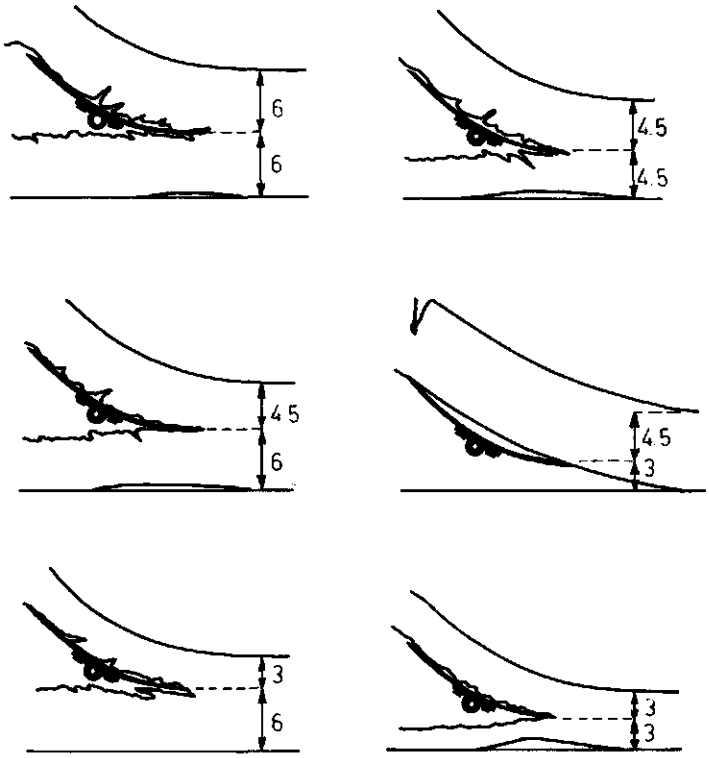

FIG. 73. Lifting as affected by tool depth and soil block thickness. Numbers in cm (Schinnen, porosity 45%, water content 26%).

The tendency of the blade to lift the sub-soil. In preliminary tests using the curved blade, the blade lifted the soil mass below the blade when the soil depth in the bin was low. Fig. 73 shows this effect for several working and soil depths. In the experiments described in section 10.2.2. the working depth was 3 cm and the soil depth was 12 cm, so that no lifting of subsoil occurred. From Fig. 73 it can be concluded that this particular blade at the working depth used exerts a tool reaction force that is in an upward direction. Such an upward reaction force must induce tensile stresses in the soil in the intake zone.

Theoretical considerations. Within the scope of this investigation a mathematical analysis has been made of Söhne's prediction method (SÖHNE, 1956) for the draught force of an inclined plane blade. This analysis is presented as an appendix. This showed that tensile stresses should be expected to occur in the intake in the case of small cutting angles and cohesive soil.

10.4.2. *The type of failure when tensile stresses are present*

Well-known failures in mechanics (HETÉNYI. 1950) are ductile failures and brittle failures, being defined as:

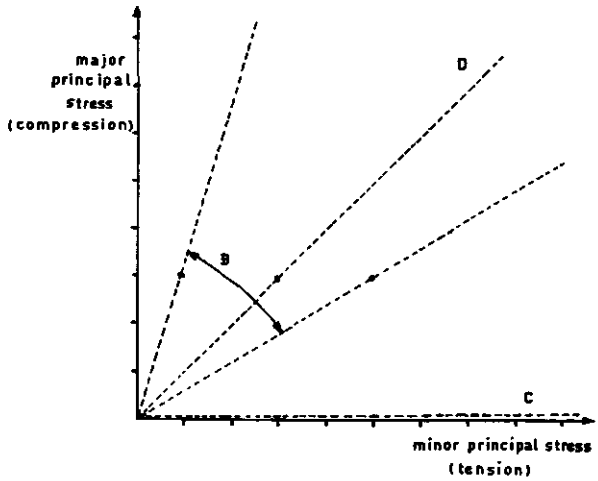

FIG. 74. Stress states in methods of failure strength determination involving tensile stresses.

- in the case of ductile failures the failure plane is inclined to the principal stress directions, and the point of failure is preceded by a significant amount of deformation,
- brittle failures are confined to those cases where tensile stresses are present and are characterized by a failure plane perpendicular to the largest tensile stress, and by very little deformation prior to failure.

Brittle failure is the subject of the rather new science of crack mechanics and the reader is referred to: GRIFFITH (1920), KERKHOF (1962), LEE and INGLES (1968). Ductile failure for soil is synonymous with shear failure which is well-known (TERZAGHI, 1954). In soil, brittle failure also occurs; this will be demonstrated using Fig. 74, in which the stress states that can occur in strength tests involving tensile stresses are presented. The area B in the figure was covered by traxial tests published in (BISHOP and GARGA, 1969). These tests performed on saturated 'blue London' clay all exhibited the brittle type of failure. Line D represents pure shear ($\sigma_1 = -\sigma_3$), which will occur in an annular shear device at zero normal load. Such tests have been carried out in the Soil Tillage Laboratory. In these tests, a self-hardening resin was used to fasten the (smooth) shear ring to the top of the soil sample, and the bottom of the soil container to the bottom of the sample. The soil inside and outside the ring area was removed. Fig. 75 shows the result of such a test, performed on Lexkesveer soil with 40% porosity and 20% moisture content. The diagonal direction of the cracks indicates brittle failure. Tensile tests performed on unconfined cylinders can be represented by line C. For a number of soil conditions under which the blade experiments were made, such tensile tests were conducted. They all exhibited brittle failure.

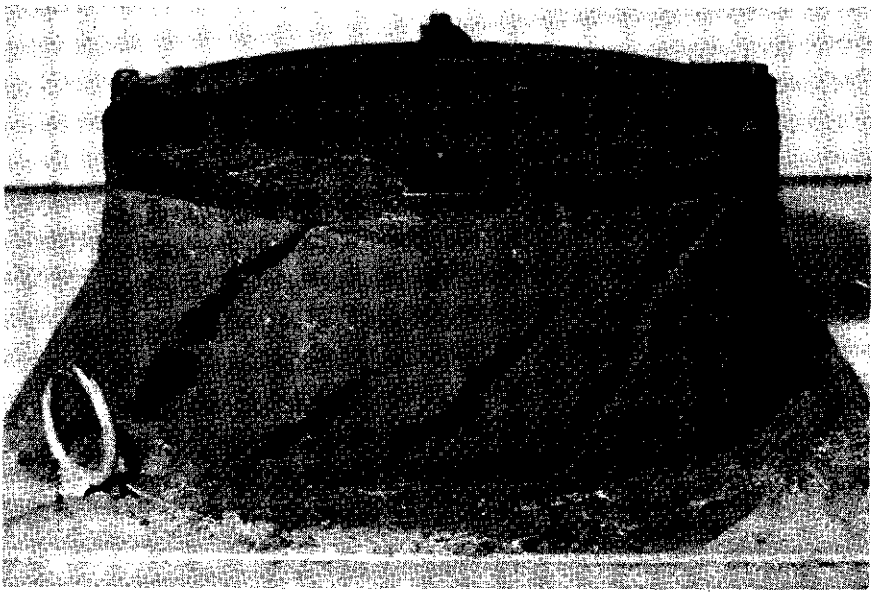

FIG. 75. Tensile cracks due to pure shear.

10.4.3. *The type of failure in the case of intake with open crack formation*

In order to examine what type of failure occurs in intake with open crack formation, stress analyses were carried out. Some results are presented in Fig. 76. The situations in this figure occurred just before a crack started to develop ahead of the share, and were taken from Lexkesveer series 1. The potential cracks are drawn as broken lines. The arrows indicate the direction of the largest principal strain in the region of such a crack. These directions were calculated from the strains of the quadrangles formed by the circles, using a method described on pp. 410–413 of (HETÉNYI, 1950). The strain itself was calculated using the method presented in section 10.2.6 under the title: 'Determination of small linear strains'. Assuming that principal stress directions and principal strain directions coincide, it can be conluded from Fig. 76 that the largest principal stress is almost always perpendicular to the potential crack direction, and that therefore the cracking is brittle failure. Using the same procedure the angle between the direction of the largest tensile stress and the crack direction for intake cracks in L2 and for tongue formation in S2 were determined. These analyses also indicated brittle failure.

The movement of a crack side relative to the direction of crack extension also gives information as to the type of failure. Fig. 77 (taken from S2) presents the flow paths of points painted on the soil above a crack for a short time interval, assuming the soil below the crack to be at rest. The broken line indicates the direction in which the crack is being extended during that time interval. The flow paths show that in the case of crack formation the soil moves away from the crack in a direction perpendicular to it. This means that the newly develop-

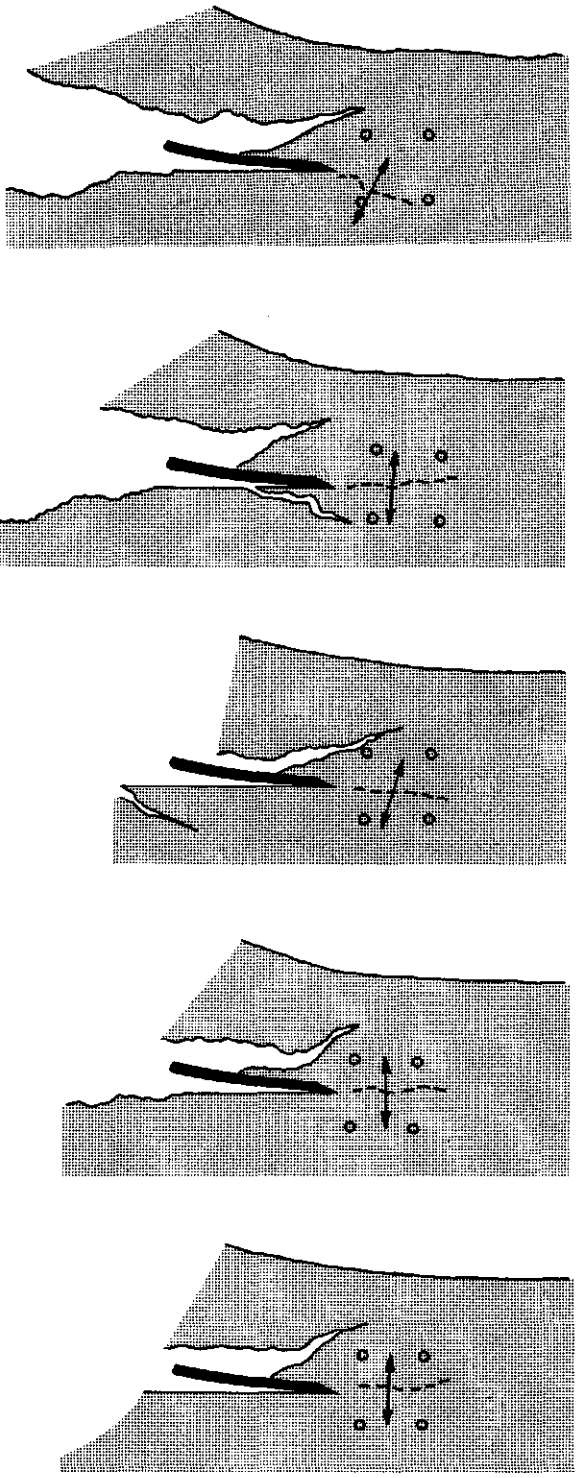

FIG. 76. Direction of maximum tensile stress just prior to crack development.

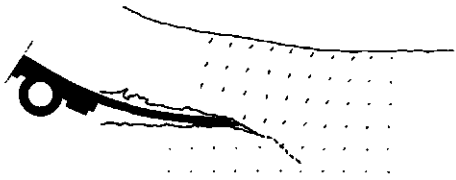

FIG. 77. Soil movements during crack development.

ed crack surface elements will still fit into each other, which is sometimes considered to be a further criterion for brittle failure. Such movement patterns were determined for cracks in other experiments, all leading to the same conclusion.

10.4.4. *A model describing open crack formation*

Assume a situation similar to the one presented in Fig. 54a. The blade edge has just started to penetrate the still firm soil. Initially, this penetrating process is comparable to the process that will occur when a penetrometer is forced into the soil: the soil in front of the blade edge is pushed away and the soil above and below the edge is loaded in pure shear to the extent that small cracks running in an inclined direction develop upwards and downwards from the horizontal. These cracks were mentioned in section 10.3.7. where cutting planes were discussed, and may be compared with the cracks that can be observed in the hole made by a penetrometer. A soil volume element in front of the edge is subjected to a horizontal compressive stress and a (smaller) vertical compressive stress.

As the share progresses, the upward force exerted by the blade onto the soil above the blade edge will be more significant and the vertical stress on the soil element mentioned will decrease: at a given moment this stress will even become negative; tensile stress therefore. As soon as this tensile stress attains tensile strength, brittle failure causes a crack, into which the share edge can usually penetrate like a wedge, by which means the cracking will continue.

This continued cracking (Fig. 78a) looks like the splitting process that occurs in the splitting test, outlined in Fig. 78b and described in (BENBOW and ROESLER, 1957). This test involves the splitting of a beam along its centre line. After making a starting point for the crack and applying the load Q, the force P is allowed to grow so that crack length s also grows. The splitting ability is determined by measuring crack width δ as a function of s. Load Q and the guiding B serve to prevent the crack from turning off upwards or downwards. Now, compare Fig. 78a with Fig. 78b. P is comparable to the force exerted by the blade on the soil being taken in. Crack width δ is related to blade edge thickness and blade cutting angle. Load Q is comparable to the load on the intake due to the main flow. If there was complete resemblance between the blade and the splitting test, the crack in Fig. 78a would maintain its horizontal travelling direction during its further development. However, the resemblance is rather limited:

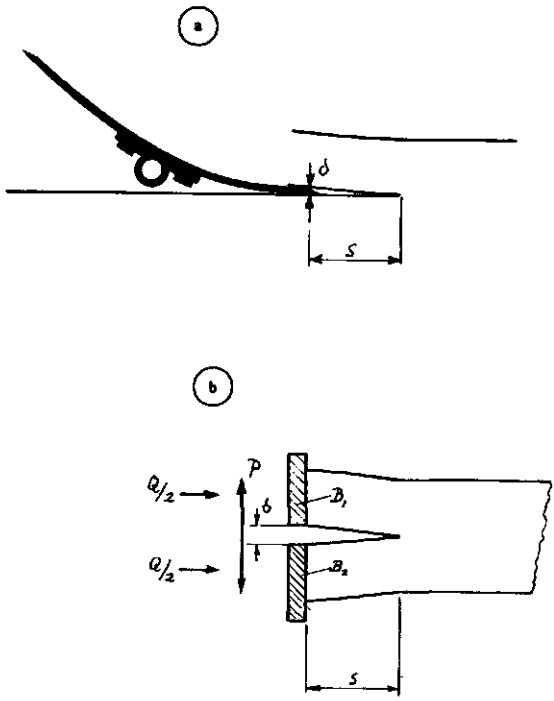

FIG. 78. Blade splitting effect (a) and Benbow and Roesler's splitting test (b).

- soil beam thickness is not equal to subsoil thickness,
- the main flow is indeed comparable to Q, but the pressure induced by the main flow cannot be controlled and does not act on the subsoil,
- the blade exerts a load that is more complicated than P,
- the guiding blocks mechanism is absent in the case of the blade.

Predominantly horizontal cracking was in fact only observed in a few experiments (S1, S3, E2). Many experiments showed a lot of cracking in either upward or downward directions.

10.4.4.1. Factors promoting upward crack progress

Some causes of upward crack progress are:

1. When crack length increases there is also an increase in the bending moment exerted by the blade onto the soil beam over the developing crack. This bending moment can cause additional tensile stresses (see Fig. 79), and make the direction of cracking turn off upwards. This phenomenon probably occurred in L5 and E1.
2. The position of the place of application of the force exerted by the blade on the intake, which can be estimated visually from the contact between the blade and the soil beam, may suddenly change causing the bending moment to increase and the crack to turn off upwards. The occurrence of such a shift in the

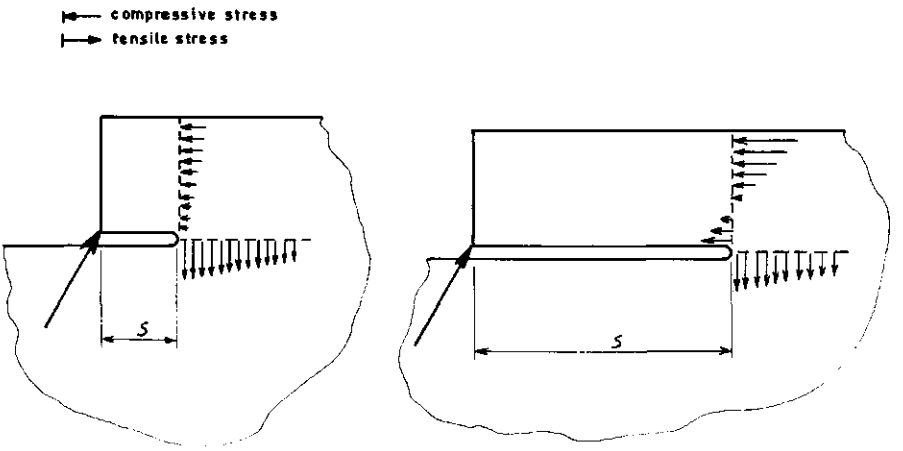

FIG. 79. A high bending moment may cause additional tensile stresses at larger s-values (s = crack length).

place of application is dependent on blade shape and variation in thickness of the soil that has been taken in (this thickness is also determined by small variations in the crack direction). It is illustrated in Fig. 56 (L1). Similar to the crack graphs and share graph, some 'place of application' graphs are presented in this crack propagation film. The 'place of application' graphs are the shaded areas. For given points in time they show the place of application as related to the blade edge. It can be clearly seen that there is a frequent sudden backward shift of the place of application away from the blade edge.

10.4.4.2. Factors promoting downward crack progress

Some causes of downward crack progress are:

1. Loading by the main flow. Fig. 71 comprises initial parts of crack films of several experiments. Of these, W3, L3, E1, E2, and E3 exhibit the phenomenon of cracks running in a less upward direction as the blade progresses. This may be explained as follows. The main flow exerts a compressive force on the intake and can thus decrease the tensile stresses caused by the bending moment from the blade edge. The crack direction therefore remains horizontal for a longer time. At the start of a test run the blade is not filled, and so this effect is absent: the cracks turn off very quickly. As the blade is filled more and more, the main flow effect increases and cracking will be more horizontal. The magnitude of the effect depends on the ratio between the pressure that the main flow can exert and the soil strength properties. L1 does not show the effect, and according to the above:

- the pressure that the main flow exerts would be too low to be effective,
- an additional load on the main flow would probably cause an effect.

The latter has been confirmed by tests on small soil blocks in which a main flow pressure was simulated by a loaded strip (Fig. 80). The strip was loaded

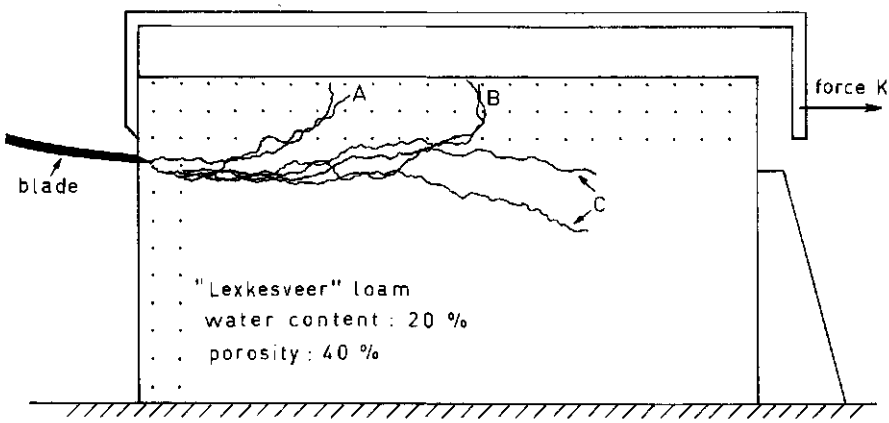

A : cracking when K = 0 (2 tests)
B : " " K = 0.33 kg/cm (load per unit of width) (2 tests)
C : " " K = 0.66 " " " " " " " "

FIG. 80. Blade action as affected by an additional load.

using weights that were connected to the strip by means of cords over a pulley. After applying the strip load the curved blade was moved into the soil until a first crack had been completed. Several test were performed at different strip loads. In the outline of the experimental set-up, given in Fig. 80, the experimental results for the different tests are also indicated.

2. Decrease of the stresses in the subsoil. Such a decrease took place, for instance, in the curved blade experiments when the blade approached the end of an (unconfined) soil mass. The experiments showed that in these cases crack extension is in a more downward direction. See Fig. 72.

10.4.4.3. Steady cutting as a special case

If the splitting test from Fig. 78b is performed on a purely elastic beam, then

$$T = \frac{3 \cdot E \cdot \delta^2 \cdot b^3}{64 \cdot s^4}$$

T = the specific fracture energy,
E = Young's modulus,
δ = the width of the crack at the end opened by the force,
b = the width of the beam,
s = the length of the crack.

So, s is a monotone decreasing function of T/E when δ and b are constant.

The value of s may become so small that the crack cannot be observed anymore. Consequently, this will occur at a particular (critical) value of T/E.

The above may be modified to the curved blade experiments as follows. In this case δ and b can be considered to be constant (δ is almost blade thickness when s is small), and a crack length s that cannot be observed may be considered to indicate intake by steady cutting. In order to estimate a T/E value for soil, we state:

$$T = \sigma_t \cdot \Delta l_t / 2$$
$$E = \sigma_{max} / \varepsilon_f$$

where:

δ_t = the soil tensile strength,
Δl_t = the displacement before the soil fails in tension,
σ_{max} = the unconfined compressive strength,
ε_f = the failure strain (fractional change in length before failure) in the unconfined compression test.

Hence

$$(T/E)_{soil} \approx \frac{\sigma_t \cdot \Delta l_t \cdot \varepsilon_f}{2 \cdot \sigma_{max}}$$

Assuming as a first approximation that
- σ_t is a constant fraction of σ_{max} (GRIFFITH, 1920; FARRELL et al., 1967),
- Δl_t is a constant fraction of ε_{max},

it follows that a critical T/E value involves a critical ε_f value. The above implies that in the blade experiments intake by steady cutting must have occurred when ε_f exceeded a particular value. It should be noted that such a critical ε_f value is specific for a blade shape, working depth, travelling speed combination.

The above theory is verified by carrying out unconfined compression tests for the soil conditions under which the blade experiments were performed (these soil conditions are given in Table II). Sample preparation was the same as that of the soil blocks in the blade experiments. Pore spaces as well as water contents in the blade tests differed no more than 0.5% from those of the corresponding unconfined compression tests. For W4 and S4, porosities in the unconfined compression tests exceeded those in the blade tests by 0.7% and 1.0% respectively. The unconfined compression tests were performed on 7.5 cm diameter samples with heights of 15 cm at the rate of $5.5 \times 10^{-3} \text{sec}^{-1}$. The results are given in Table VIII. In Fig. 81 the types of intake (Table V) are related to the unconfined compression tests (Table VIII). This shows that $\varepsilon_f = 0.185$ is a dividing-line between 'steady cutting' and the other types of intake. (Cross A in the figure was determined after the section 10.2.2 experiments in order to obtain further evidence. It applies to a heavy Almkerk clay of which ε_f was known to be 0.3).

TABLE VIII. Unconfined compression tests. σ_{max} = failure stress (bar). ε_f = failure strain (fractional change in length at failure).

Series	Wageningen		Lexkesveer		Schinnen		Ede	
	σ_{max}	ε_f	σ_{max}	ε_f	σ_{max}	ε_f	σ_{max}	ε_f
1	0.516	0.194	0.434	0.046	0.370	0.178	0.149	0.030
2	0.308	0.071	0.250	0.038	0.142	0.227	0.078	0.031
3	–	–	0.083	0.022	0.161	0.105	0.034	0.031
4	0.696	0.033	0.604	0.026	0.584	0.043	0.190	0.025
5	–	–	0.726	0.012	–	–	–	–

10.4.4.4. Shear-plane failure as a special case

If soil shear strength is low, soil in the intake may fail in shear due to the compressive force exerted by the main flow. This causes shear-planes in the intake zone. This is illustrated in E3 and L3 of Fig. 71: as the main flow becomes larger, the direction of cracking is more horizontal, and, at a given moment, crack formation makes way for shear-plane failure. This type of intake can only occur if shear strength is low. This is confirmed by the unconfined compression tests (see the small squares in Fig. 81).

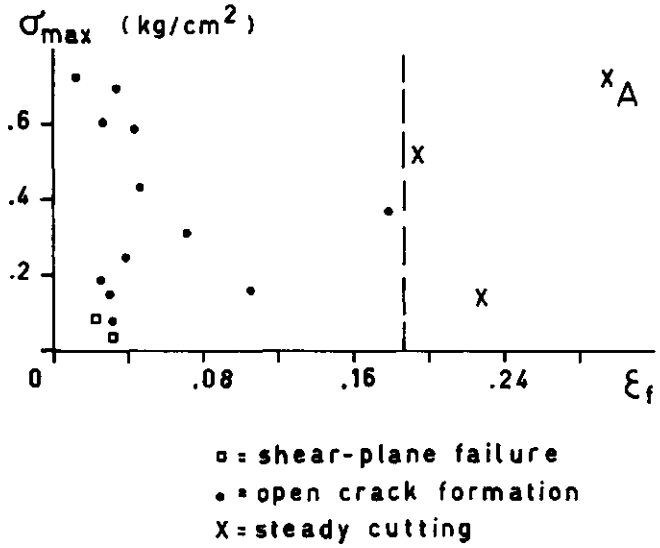

FIG. 81. Types of intake as related to unconfined compression tests.

10.5. The main flow

In section 4.2, which deals with curved blades, the following blades were distinguished:

- blades with a curvature that increases towards the end,
- blades with a curvature that decreases towards the end,
- blades having a constant curvature.

The investigated blade is a mixture of the first two cases, because:

- a small initial part of the blade has a curvature that increases towards the end, whereas the curvature after that initial part decreases towards the end (see Fig. 46),
- the cutting edge has a larger cutting angle than that which would be present if the blade was completely thin.

These facts must have affected the main flow.

The amount of fracture in the soil beam that the intake delivers to the main flow can be seen in the failure films and crack propagation films which are presented in Figs. 55 to 67. In a crack propagation film the share graph can be considered as being a boundary between the crack formation that occurred in the intake, and the crack formation during the main flow. Crack propagation below the share graph is an intake process; crack propagation above the share graph belongs to the main flow. The condition of the soil beam that the main flow delivers to the output can be seen in the indicator films presented in section 10.6. From a comparison of the soil that the main flow receives with the soil that the main flow delivers, it appears that this blade at the used working depth and forward speed induces very little tillage effect in the main flow: no large changes take place in the soil beam during the main flow. Comparisons can be made for W1, W3, L1, L3, S1, S3, S5, E1, E2.

10.5.1. *Classification of the main flow processes*

The main flows occurring in the experiments were classified as follows:

I. the main flow receives a soil beam that has been torn very slightly,
II. the main flow receives a soil beam that has been torn strongly,
III. the main flow receives soil pieces that move parallel to each other.

Table IX shows how the experiments fit into this system.

In addition to the presentation of main flows in section 4.2, a description of some observations follows below.

Table IX. Main flow processes.

Series	Wageningen	Lexkesveer	Schinnen	Ede
1	I	II	I	II
2	II	II	I	II
3	II	III	I	III
4	II	II	II	II
5	II	II	II	II

10.5.2. *Some main flow phenomena*

Parallel moving pieces. In experiments L3 and E3 the main flow received soil pieces from the intake that moved parallel to each other along their contact planes. When the pieces remained unbroken, this relative movement was maintained during the full period that these pieces were in the main flow. This is because they had to follow blade curvature. On some occasions a failure plane developed in the main flow, with one of its ends being near the blade leading edge, and the other being at (E3) or above (L3) the blade trailing edge. There, the soil under that failure plane formed an almost immobilized layer moving very slowly backwards along the blade, while the soil over the plane formed a 'new' main flow, in which any relative movement between pieces no longer existed. This new main flow was permanent in E3, and occurred incidentally in L3. A great deal of soil pulverization took place. Soil parts from the end of the main flow rolled in a forward direction over the original top surface of the main flow, by which means the amount of soil on the blade increased with increasing distance of tool travel.

Slightly torn soil beams. In 'intakes by steady cutting' and in 'intakes with open crack formation' that do not involve much upward crack development the soil beam delivered to the main flow by the intake is only slightly torn. This was the case in W1, S1, S2, S3. The soil beam was almost never entirely unbroken: small tongues were often present at the bottom. It was observed in W1 that the tips of such tongues tended to adhere to the blade surface and therefore lagged behind the rest of the soil beam to some extent. In that case, the tongue had to rotate somewhat, pushing the soil beam slightly upwards like a prop.

Strongly torn soil beams. In the case of the intake being of the type with open crack formation, the main flow can receive a soil beam that has been torn from the lower side to such an extent that the beam is composed in fact of a 'chain' of pieces, see Fig. 82 (L2). The soil beam part over the tip of such a tear is called a 'hinge', and the part under such a tear a 'beam tongue'.

During soil piece movement over the blade beam tongues may break off

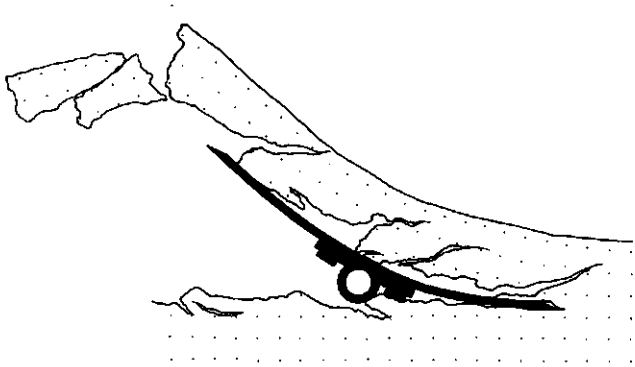

FIG. 82. Instantaneous picture from the L2 process.

and pulverize further (W3, W4, L1, L4, S4, E1, E2, E4). In L5 the entire lower side of the soil beam was pulverized.

Occassionally the hinges were torn further. The crack propagation films in section 10.3.2. show this for L1, L2, W3, E1, E2. Further tearing will mean that the crack graph above the share graph includes non-vertical parts. Also, small tensile cracks sometimes developed at the bottom of the soil beam. These are the small almost vertical cracks in the lower halves of the failure films. (See for this the failure films of S3, E1 and E2, which are presented in section 10.3.2). The phenomena of hinges being torn further and tensile cracks developing may have been due to the fact that the first part of the blade surface has a deviating curvature.

Hinges were sometimes loaded so heavily as to strongly deform or pulverize, although they still acted as hinges. On the soil surface, this strong deformation or pulverization appeared as a band (E2, L5, S5).

A hinge was sometimes disturbed to such an extent that contact between hinge halves was lost, and the piece behind slipped over the piece in front. By this mechanism a main flow of pieces moving parallel to each other can develop. This has been seen in W5 and E5. In these cases the amount of soil on the blade continued to increase during the experiment, due to soil rolling back.

Influence of blade curvature. The investigated blade had a curvature that mainly decreased towards the end. Besides this blade (blade 1) another blade (blade 2), which differed from the first blade in blade curvature only, was also investigated. Fig. 83 shows both blades, blade 1 being drawn fully, and the curvature of blade 2 being indicated by the broken line. So, both blades have the same bevel edge, cutting angle of the blade surface, lift angle at the blade rear end, length, height, width, and blade hollow depth (18 mm). Curvature of blade 2 mainly increases towards the end. It was stated in section 4.2 that

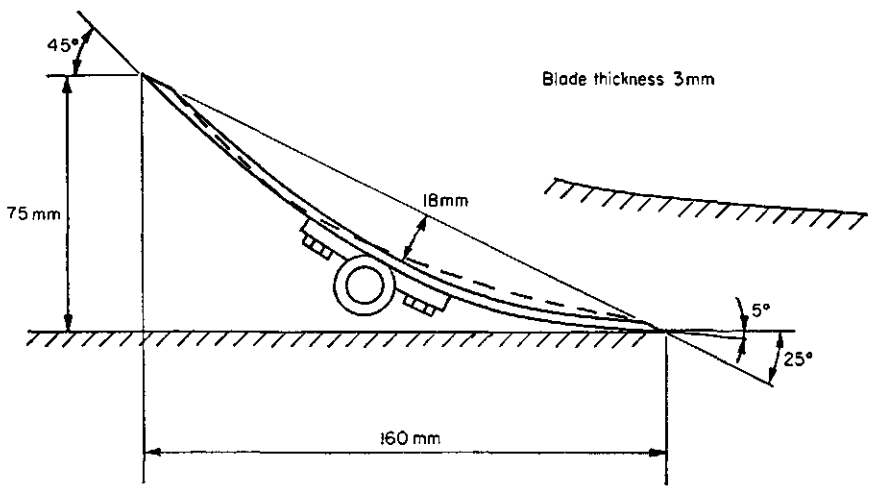

FIG. 83. Blades that differ in curvature only (KOOLEN, 1972).

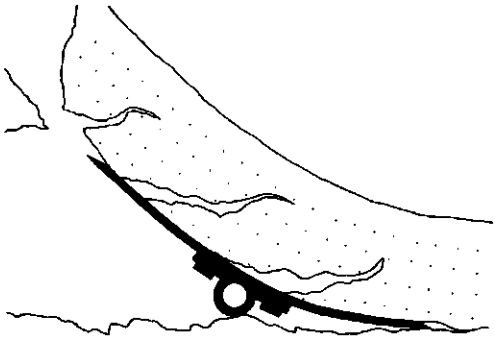

FIG. 84. Crack formation at a lower working depth in Lexkesveer soil (40% porosity, 20% moisture content).

blade curvature can have an influence on the process especially in the case of an only slightly torn soil beam entering the main flow. Such soil beams occurred in W1, S1, S2 and S3. In these cases, the void between beam and blade 1 was very small, whereas experiments with blade 2 in soil conditions similar to W1, S1, S2 and S3 showed a much larger void between blade and beam. This is understandable in view of the increasing curvature of blade 2.

In soil conditions similar to S3 the blade 2 process involved much rotating of the beam tongues, thus pushing the soil beam upwards. In S3 itself such rotating and pushing up did not occur. Obviously, the effect of adhering beam tongues can be strengthened by a curvature that increases towards the end.

An example of clear crack formation in the main flow. Using the curved blade 1 some testst were run at a greater working depth (4.5 cm). The soil conditions were similar to that in L1. Intake cracks developed further in the main flow to a distinct S-shape (see Fig. 84), which was not originally the case in L1. The S-shape can be explained by the crack tip travelling in an ever-changing stress-field during its formation. The phenomenon occurred very regularly.

10.6. SYSTEMATICS OF THE OUTPUT PROCESSES

The output process contains the changes in the soil-strip after it leaves the blade. If the soil-strip is extended further behind the end of the blade, the cross section over the end is stressed more and more. At a certain length this extending part starts to break or to shear. When the failure surface is completed, the separated piece of soil falls down freely. This free fall ends in a collision in the furrow where the piece joins previously formed pieces. At the same time the main flow produces the next piece and the process is repeated.

An example of such an output process is shown in Fig. 85a. This figure represents for L1 a number of instantaneous pictures from the movement of a piece in the output process. The breaking, falling and coming to rest are shown as

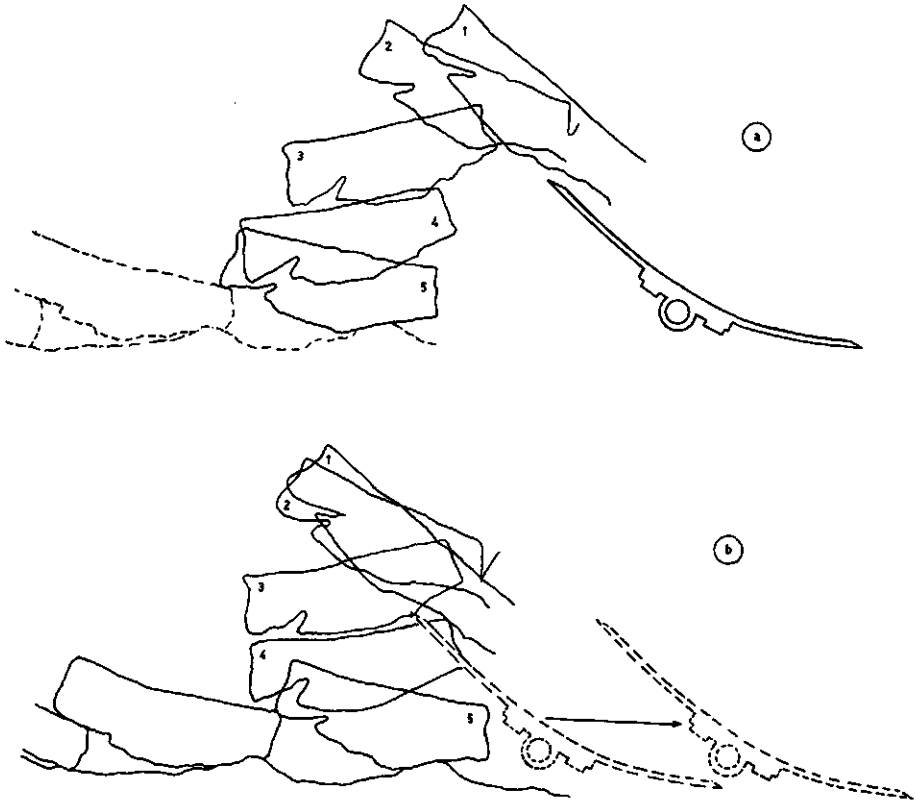

FIG. 85. The movement of a soil piece relative to the tool (a) and relative to the resting soil (b). Pictures from Lexkesveer series 1.

movements relative to the tool. The time between two successive instantaneous pictures was $^{1}/_{15}$ sec. Fig. 85b shows the movement again for the same piece, but it is now relative to the non-moving soil.

10.6.1. *Some indicator films*

Indicator films for the situation at the end of the blade were made from the cine films of a number of experiments. The fracture surfaces that developed when a soil piece was separated from the strip at the back of the blade are indicated in the indicator films by broken lines. These indicator films will be discussed below.

Wageningen series 1 (Fig. 86). This indicator film shows that in this experiment very long pieces are formed in the output.

Wageningen series 3 (Fig. 87), Lexkesveer series 1 (Fig. 88), Lexkesveer series 2 (Fig. 89). Here, the pieces being put out are shorter. Output cracks often occur at places where cracks have already developed during the intake. In these cases the separation of the piece is usually accompanied by the breaking

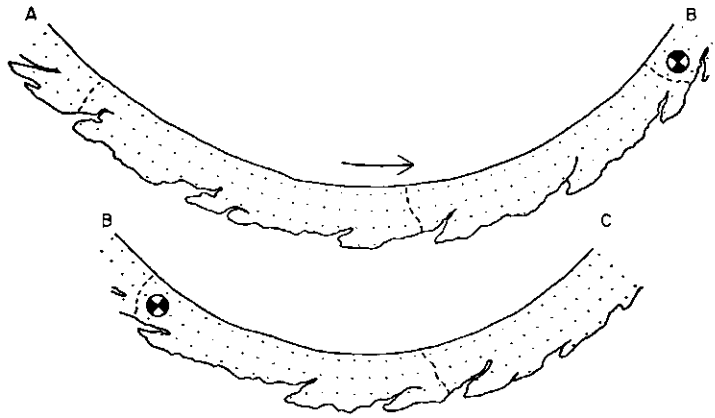

FIG. 86. Wageningen series 1 (KOOLEN, 1972).

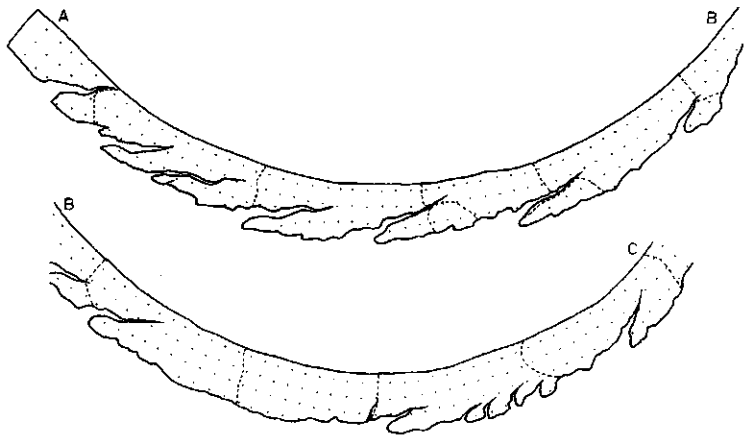

FIG. 87. Wageningen series 3.

of the beam tongue that belongs to the intake crack. Sometimes there is an output crack between two intake cracks.

Schinnen series 1 (Fig. 90) and Schinnen series 3 (Fig. 91). No relationships between intake and output cracks are visible in these indicator films. The pieces being put out are longer in S1 than in S3. The output cracks are often curved.

Schinnen series 5 (Fig. 92). The output cracks definitely prefer places where an intake crack is present. The soil has already been cracked in the intake so intensively that the output cracks need to be only very small. In the lower part of the strip there was a lot of loose soil (which has not been drawn).

Ede series 1 (Fig. 93) and Ede series 2 (Fig. 94). The output cracks again prefer places with intake cracks. Beam tongues break. Loose material is present on some locations in the lower part of the soil beam (shaded).

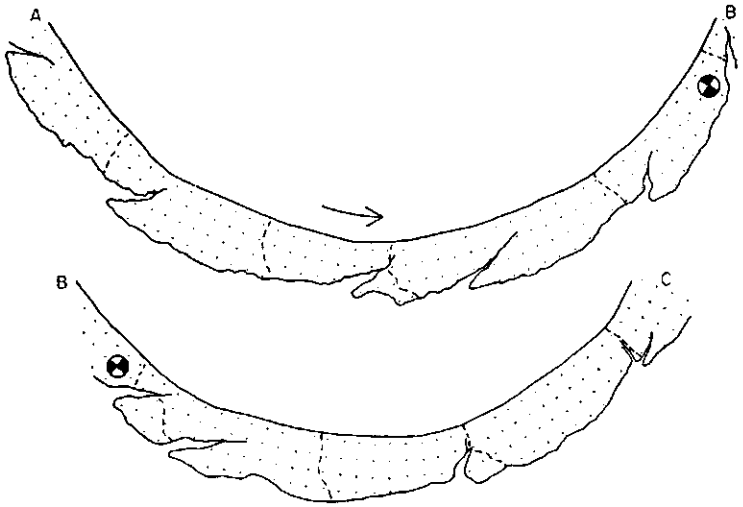

FIG. 88. Lexkesveer series 1 (KOOLEN, 1972).

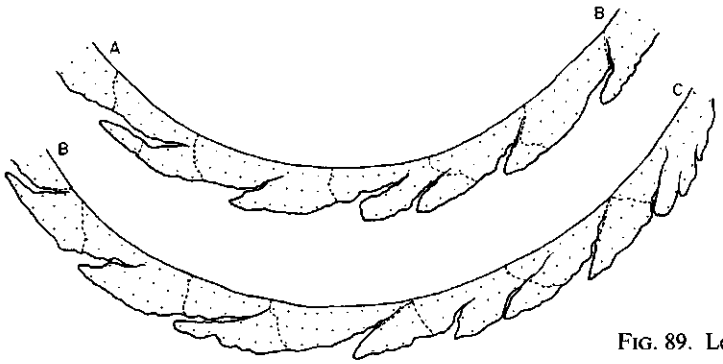

FIG. 89. Lexkesveer series 2.

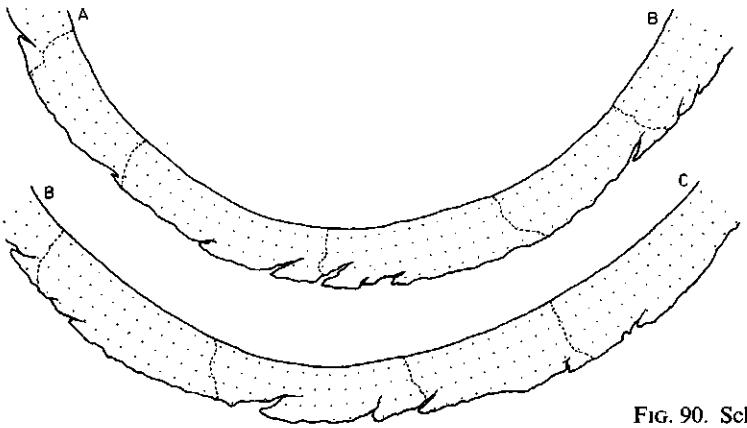

FIG. 90. Schinnen series 1.

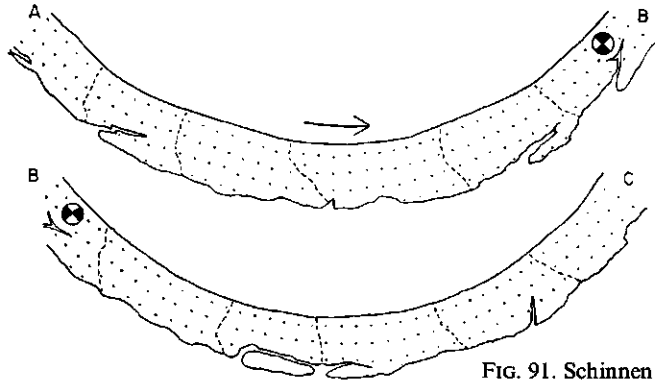

FIG. 91. Schinnen series 3 (KOOLEN, 1972).

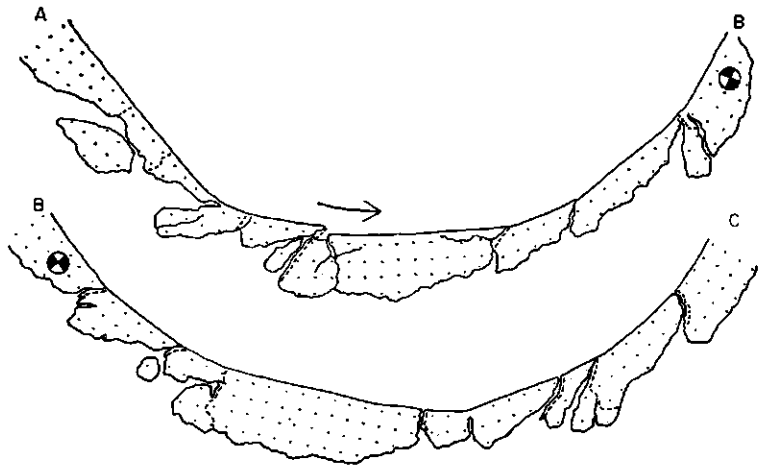

FIG. 92. Schinnen series 5 (KOOLEN, 1972).

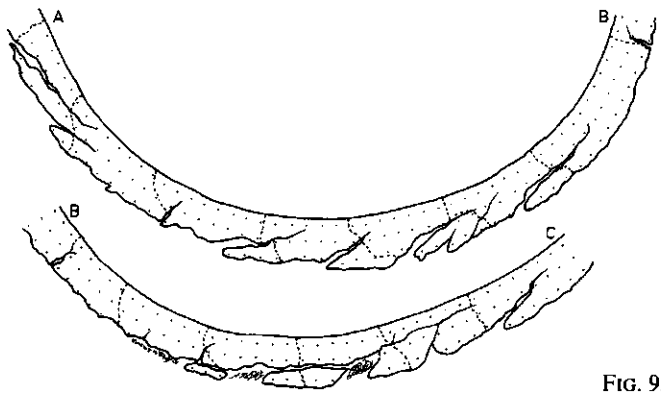

FIG. 93. Ede series1.

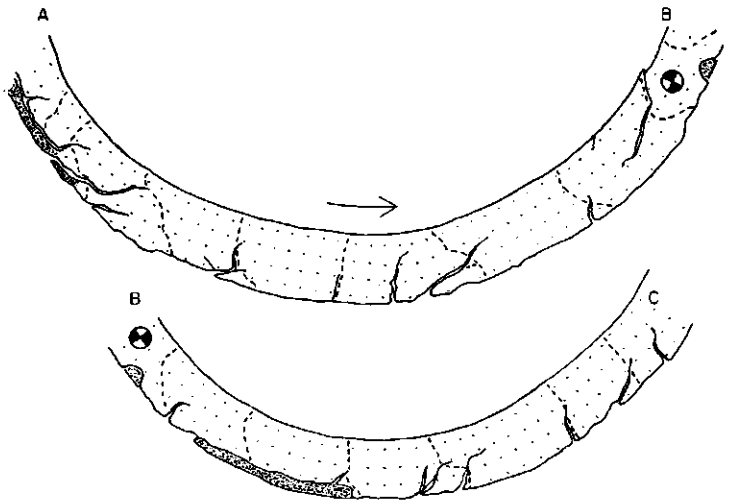

FIG. 94. Ede series 2 (KOOLEN, 1972).

10.6.2. *Output phenomena and classifications*

For the outputs that ocurred in the experiments a classification system comprising the following categories was established.

A. The main flow delivers to the output a rather rigid, cohering soil beam that has been torn slightly. The output cracks are not related to the intake cracks.
B. The main flow delivers to the output a rather rigid cohering soil beam that has been torn further than in the case of the previous category. There is a relationship between the output cracks and the intake cracks.
C. The main flow only delivers chunks and crumbs.
D. The main flow delivers a cohering soil beam requiring strong deformation before failure will occur.

Table X gives the classification of the experiments according to this system.

The experiments in which the main flow only delivered chunks and crumbs (W5, L3, E3, E5), showed pieces moving parallel to each other in the main flow. As these pieces were travelling in the main flow, they were pulverized to such an extent that, at the end of the main flow, only a mass of chunks and crumbs was left, without any regularity.

When an output crack develops over the tip of an intake crack, thus in a hinge, one of the two following phenomena will occur:

- when the hinge is breaking the beam tongue breaks or is separated simultaneously (W2, W3, W4, L1, L2, L4, S4, E1, E2, E4),
- the hinge breaks as the piece is turning over around the beam tongue or the blade end.

This turning over means that the rear part of the piece is moving downwards, and the front part upwards. Such output cracks do not occur above the blade end but develop at a place that lies more in front of it. They have been observed in S5 and in L5.

TABLE X. Output processes.

Series	Wageningen	Lexkesveer	Schinnen	Ede
1	A	B	A	B
2	B	B	D	B
3	B	C	A	C
4	B	B	B	B
5	C	B	B	C

In the outputs classified as B rather loose soil was sometimes present in the bottom part of the soil delivered by the main flow (see section 10.5). This loose soil fell to the furrow bottom just behind the tool. The separated soil pieces landed on top of that loose soil.

As the pieces landed some further crack formation sometimes occurred (W4, L1, L2, E1, L5, E2, E4).

The following configurations in the soil that came to rest after being put out were observed:

- the roofing-tile configuration as shown in Fig. 85b (W1, W2, W3, W4, L1, L2, L4, L5, S4, S5, E1, E2, E4),
- a configuration where the soil pieces lie horizontally one behind the other, with their original upper side also directed upwards. Both halves of each output crack again face each other (S1, S2, S3),
- an irregular mass of chunks and crumbs (W5, L3, E3, E5).

Sometimes a piece remained vertical after the fall, that means, maintained a position in which the side being part of the original soil surface, was vertical and backwards directed (L4, L5). Sometimes such a piece fell backwards from the vertical position (E4), directing the original part of the soil surface downwards.

10.7. SOME CONTRIBUTIONS TO THE PREDICTABILITY OF OUPUT PROCESSES

In this section a model is outlined for the outputs that can occur in the case of a 2-dimensional blade. This model consists of mechanisms, treated merely qualitatively. The model has the capacity of explaining the output phenomena mentioned in section 10.6, and provides indications for the existence of output phenomena that have not yet been reported. It should be kept in mind here that many of the statements have not been verified by experiments. This is also not very urgent, in view of the current character of soil tillage in practice. Verification and quantification of the model will be especially necessary where tools are developed which are intended to work in specific soil conditions, and based on a full control of the soil movements during the tillage process. The possibility of designing such tools will be shown in this section.

Important aspects of the output are:

- the forces and the couples that it exerts on the main flow,

- its influence on the soil configuration left by the process,
- consumption of energy obtained from the main flow in the forms of potential energy, kinetic energy, and flow work (SHAMES, 1962).

The amount of flow work that is supplied per second equals the vector-product $\mathbf{K} \cdot \mathbf{V}$, where $\mathbf{K}$ is the (vectorial) force exerted by the main flow on the output, and $\mathbf{V}$ is the (vectorial) soil velocity at the main flow end. When the output is hindered the flow work may be significant and may increase tool draught.

The form of the output can differ widely, and this is most striking at low forward velocities and small linear dimensions. At higher speeds and larger linear dimensions the inertia forces prevail in the process, and the output varies less with varying circumstances. On the basis of the soil received we may distinguish the following types of output behaviour:

- the main flow delivers to the output a rigid, cohering flow without any cracks,
- the main flow delivers a rigid soil beam that has only been cracked in a thin lower part,
- the delivered soil beam exhibits cracks that have penetrated far into the beam from the bottom,
- the main flow delivers short pieces, being separated by parallel failure planes,
- the main flow only delivers chunks and crumbs,
- the delivered soil beam is able to deform strongly before a crack develops.

These types will be dealt with subsequently. The first type will be discussed in detail, while for the other types only the phenomena in which they differ from the first type will be given. It will be shown that the mutual differences are smaller as the speed and the linear dimensions increase.

10.7.1. *Output behaviour when a rigid, cohering flow without any cracks is received*

The output process of a soil piece may be separated into a number of stages:

- the start of breaking as a soil beam extends far enough behind the blade,
- the breaking period,
- the free fall of the piece,
- joining the earlier pieces (landing).

The following theories apply to homogeneous, rigid, cohering, undisturbed soil beams having constant rectangular cross-sections.

The start of breaking

In the case of:

- *a low delivery rate,*
- *a soil beam being delivered horizontally, and*
- *a piece length being large relative to piece thickness*, the piece length may be calculated from the stress-strain relationships in tension and compression of the soil. This calculation follows the bending theory for beams which is based on the assumptions of:

- strain in the direction of the longer axis being proportional to the distance from the neutral surface,
- the fibres being able to elongate or shorten independent of each other.

Regarding the first assumption, MAURER and WITHEY (1940) noted that 'cross-sections of a beam become curved, in general, during bending. But if the beam has a portion at every section of which the shearing force V is zero, then original cross-sections of such portion do not become curved, and the assumption holds. If a beam has a portion at all cross-sections of which the shearing forces of V are equal (but $\neq 0$), then the curved forms, which original cross-sections assume, are all alike, and the assumption holds. If the beam has a portion which sustains a distributed load, so that V changes from section to section in such portion, then the curved forms which original cross-sections assume, are unlike, and *strictly* the first assumption does not hold: but the error is slight and negligible unless the beam is relatively short, say, less than ten times its height'. Regarding the assumption of fibres elongating or shortening independently, MAURER and WITHEY (1940) state that 'it is strictly speaking not correct, for adjacent fibres *do* press upon and exert shear stresses upon each other'. Where external forces act on the beam, the fibres also load each other.

The following formulae from simple beam theory apply at the moment of failure (Fig. 95a):

$$M = \frac{1}{2} \cdot g \cdot \rho \cdot b \cdot d \cdot l^2$$

$$\sigma_t = \frac{M}{C \cdot b \cdot d^2},$$

where:

g = acceleration of gravity,
l = length of extending beam part,
ρ = soil bulk density,

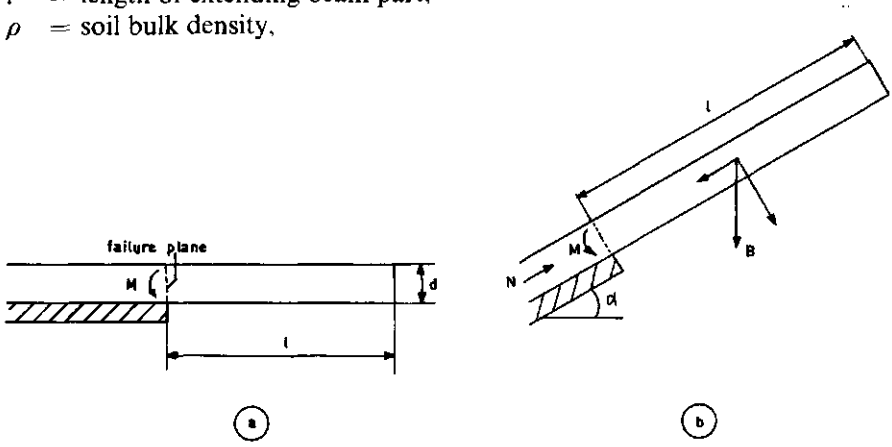

FIG. 95. Breaking of a slowly moving, relatively long soil piece that is delivered horizontally (a) or in an inclined direction (b).

σ_t = soil tensile strength,
M = bending moment that the weight of the extending beam part exerts on the cross section over the blade end,
b = beam width,
d = beam thickness,
C = a dimensionless parameter, depending on the shape of the stress-strain relationship in uni-axial loading of the soil.

If that stress-strain relationship is linear, $C = {}^1/_6 \approx 0.166$. If it is the relationship that applies to an ideal-plastic material, $C = 0.25$. FARRELL et al. (1967) measured a C-value of 0.22–0.24 on a loam soil having a non-linear stress-strain relationship, the value being independent of the soil moisture content. In the case of a non-linear stress-strain relationship C probably also depends on
- beam length,
- beam thickness,
- beam width.

MAURER and WITHEY (1940) report tests on highly loaded cast iron and wood, showing these dependences.

The following is a numerical example of a soil piece length calculation using the above equations. M can be eliminated from these equations by substituting the first equation into the second, which results in:

$$\frac{1}{2} \cdot g \cdot \rho \cdot b \cdot d \cdot l^2 = \sigma_t \cdot C \cdot b \cdot d^2,$$

or

$$l^2 = \frac{2 \cdot \sigma_t \cdot C \cdot d}{g \cdot \rho}.$$

Let beam thickness d be 3 cm, soil bulk density ρ be 2000 kg/m^3, C be 0.22, soil tensile strength be 0.2 bar, and acceleration of gravity be 10 m/sec^2, then the last formula calculates a piece length l equal to 11 cm.

In the case of:
- *a low delivery rate,*
- *a soil beam being delivered in an inclined direction, and*
- *a piece length being large relative to piece thickness,*

the vector of the weight B of the extending part is no longer parallel to the beam cross-section at the blade end (see Fig. 95b). This cross-section is therefore not only loaded by a couple M, but also by a normal force N. Equilibrium of forces requires.

$$N = B \cdot \sin \alpha$$
$$M = \frac{1}{2} \cdot B \cdot l \cdot \cos \alpha,$$

where α is angle of beam inclination. Provided the stress-strain relationship is

linear, the tensile stress in the highest fibres of the cross-section may be calculated using the principle of superposition: tensile stress in the highest fibres equals the highest stress due to M (being $6 \cdot M/b \cdot d^2$) minus the compressive stress due to N (being $N/b \cdot d$). This tensile stress is the highest tensile stress: if l becomes so large that this stress equals the soil tensile strength, failure will start.

This superposition cannot be applied to soils having a non-linear stress-strain relationship, but it can generally be stated that, provided the tensile strength is low in relation to the compressive strength, soil piece length increases with increasing inclination of the soil beam being delivered for the following two reasons:

- at equal lengths of the extending beam the bending moment on the heaviest loaded cross section decreases as the inclination increases,
- the tensile stresses due to the bending moment are decreased by a component of the extending beam weight. This decrease becomes larger as the inclination increases.

For similar reasons the compressive stress in the lowest fibres strongly increases with increasing inclination. It may therefore be possible at large inclinations for failure to occur because compressive strength is attained, thus by shearing.

In the case of:

- *a high rate of delivery*,

the above also applies, so long the beam that is delivered in the breaking period is *not* longer than the piece itself. After a piece of soil starts to break some time will elapse before failure is completed. In this breaking period the piece still exerts forces on foregoing soil pieces. When the rate of delivery is so high that the length of the soil delivered in the breaking period exceeds the length at which failure is initiated, then more pieces will break at the same time. As the rate of delivery increases, the states of movement of successive pieces at any one moment are more equal, and the output will more closely resemble a continuous flow.

The condition of:

- *long soil pieces in relation to piece thickness*,

will occur in model tests involving 1–5 cm thick soil beams if soil cohesion has an intermediate or high value. Piece lengths in soils having a low cohesion will be comparatively short at these beam thicknesses. As beam thickness is increased, the length to thickness ratio decreases, so that in full scale tests the condition of 'soil pieces being long relative to piece thickness' does not occur for any soil. This will be illustrated by the following numerical example, using again the formula $l^2 = (2 \cdot \sigma_t \cdot C \cdot d)/(\rho \cdot g)$, which applies to a horizontal, slow delivery (p. 123). Let ρ be 2000 kg/m^3, σ_t be 0.2 bar, C be 0.22, then $l^2 = 44\ d$. Table XI was calculated from this result.

The breaking period

As soon as the soil tensile strength has been attained in the highest fibres of

TABLE XI. Piece dimensions as affected by soil beam thickness.

Piece thickness d (cm)	piece length l (cm)	l/d
2	9.4	4.7
4	13.1	3.3
6	16.2	2.7
8	18.8	2.3
10	21.0	2.1
12	23.0	1.9

the heaviest loaded cross-section, crack formation starts. The crack propagates as the piece rotates around a point near the crack tip. This rotation makes the potential energy of the piece decrease. The energy released in this way has been partly used for the crack formation. The remaining part is transformed into kinetic energy. After a certain angular rotation, the crack is completed, and the piece begins to fall freely.

When the energy consumed in crack formation is indicated by E_s, and the angular rotation in the period of breaking by β, then the following energy balance applies to the period of breaking at low delivery rates:

$$M \cdot g \cdot \Delta h = E_s + \frac{1}{2} \cdot I_o \cdot \omega^2,$$

where:

M = piece mass,
g = acceleration of gravity,
Δh = decrease in height of the centre of gravity of the piece: Δh is a function of β,
I_o = moment of inertia relative to the centre of rotation,
ω = angular velocity at the time when the crack is just completed.

In the case of:

- *a low rate of delivery, and*
- *only a small angular rotation being needed to reach complete failure,*

the potential energy is still high after failure, and the angular speed of the piece is low. In accordance with brittle material behaviour, the breaking period will be short.

In the case of:

- *a low rate of delivery,*
- *a large angular rotation necessary for complete failure, and*
- *a high energy consumption in the crack formation,*

the piece rotates considerably in the breaking period, but the angular velocity is low. After crack completion the remaining potential energy as well as the angular velocity is low.

In the case of:

- *a low rate of delivery,*
- *a large angular rotation being needed, and*
- *a low energy consumption in cracking,*

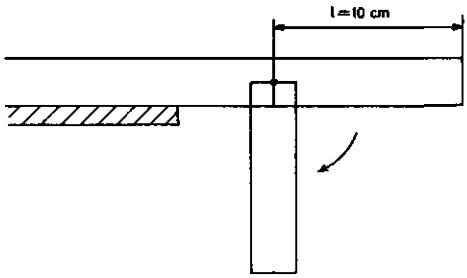

FIG. 96. Refers to the angular speed calculation.

much potential energy is transferred into kinetic energy. Angular velocity after crack completion is high. The time to reach complete failure and the angular speed may be calculated from pendulum mechanics, as shown in the following numerical example. When: the delivery is horizontal, the necessary angular rotation is $\pi/2$ radials, the piece length is 10 cm, and the centre of rotation is assumed to be the centre of the potential plane, then (see Fig. 96) $\Delta h = l/2 = 5$ cm, $E_s = 0$, $I_o = M \cdot l^2/3 = 100\ M/3$, and ω can be solved using the energy balance $M \cdot g \cdot \Delta h = E_s + {}^1/_2 \cdot I_o \cdot \omega^2$ given on page 125. This will result in $\omega = 17$ rad/sec. The length of the breaking period would follow from the (elementary mechanics) condition $M_o = I_o \cdot \dot{\omega}$, where M_o = moment of M relative to the centre of rotation, and $\dot{\omega}$ = angular acceleration. By expressing M_o and $\dot{\omega}$ in terms of the rotation angle θ the following differential equation is obtained:

$$\frac{d^2\theta}{dt^2} - \frac{3 \cdot g}{2l} \cdot \sin \theta = 0.$$

Solving this equation for the boundary conditions would give the length of the breaking period (for further details the reader is referred to MCLEAN and NELSON, 1962, page 234).

In the case of:

– *a higher rate of delivery*,

the previous considerations apply provided there is never more than one piece breaking at the same time, and the system of reference axes, in which lengths etc. are measured, is assumed to be fixed on the still unbroken part of the output ($x - y$ system in Fig. 97). Such a reference system is inert and moves without rotation relative to the tool. When speed is high, more pieces break at the same time. If the reference system is fixed on a succeeding piece that is breaking, the system is no longer inert, and the process will become much more complicated than defined above.

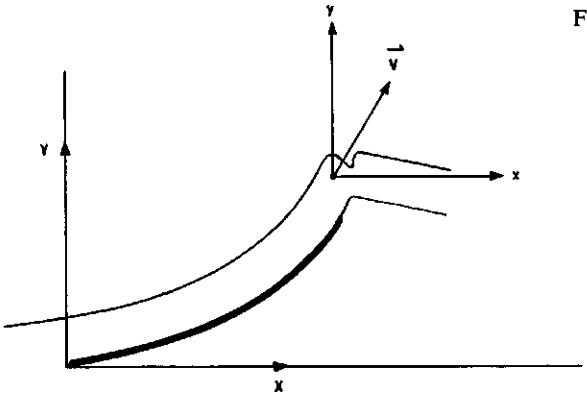

FIG. 97. Reference systems.

The free fall

In Fig. 97 the system of reference axes $X-Y$ is fixed on the tool. The inert $x-y$ system, which is fixed on the still unbroken part of the output, moves with respect to the $X-Y$ system, and the velocity of this movement will be indicated by **V**.

At the end of the breaking period the piece rotates around the centre of rotation at an angular velocity ω. This means that the centre of gravity of the piece has a velocity $l \cdot \omega/2$ in the $x-y$ system. Just after failure the piece is completely free and its state of movement in the $x-y$ system is defined by:

- an angular velocity ω around the centre of gravity,
- a linear velocity $l \cdot \omega/2$ of the centre of gravity.

Then, its state of movement relative to the $X-Y$ system just after failure is:

1. an angular velocity ω,
2. a linear velocity $\mathbf{V}_p$ of the centre of gravity, being equal to $\mathbf{V} + l \cdot \omega/2$.

Other pertinent factors that determine the free fall are:

3. the initial position of the piece (defined by the angular rotation at the time of failure),
4. the height of fall.

During the free fall the vertical velocity increases, but the horizontal velocity remains constant. Depending on the height of fall and the initial velocity $\mathbf{V}_p$, the fall takes a certain time t. During this time t, the angular rotation is $\omega \cdot t$. This angular rotation, added to the initial position, gives the position of the piece at the end of the free fall. At the end of the free fall the state of the piece is defined by:

- its position (angular rotation),
- its angular velocity,
- the velocity of its centre of gravity relative to the tool.

The pieces are said to be more *separated*, when the failure surfaces between two successive pieces maintain their original relative position less during the free fall. Separation takes place when the pieces break one by one, so when the rate of delivery is low. Separation also takes place during the free fall; a lot of separation will occur when:

– the angular rotation during the free fall is large,
– the falling time is long, in the case of more pieces falling at the same time (the acceleration of gravity makes the distance between successive pieces ever increase during the fall, so that the distance between pieces is larger as the falling time is longer).

The pieces are said to be *fully separated* if the pieces land one by one.

At high rates of delivery, so many pieces can be breaking at the same time, that they inhibit the pieces from falling freely during the output.

The following numerical example is given. For a height of fall h of 10 cm the falling time t can be calculated from $h = g \cdot t^2/2$ as 0.14 sec. If the angular velocity of the piece is 10 rad/sec, then the angular rotation in the free fall is $\omega \cdot t = 1.4$ rad $\approx 90°$. If the piece were released from a vertical position at an angular velocity of 10 rad/sec, the centre of gravity of the 10 cm long piece would have a horizontal velocity of $\omega \cdot l/2 = 50$ cm/sec, due to the breaking process.

Joining the foregoing pieces

When the end of the free fall is reached, the piece has a certain velocity relative to the still unbroken output. Adding that velocity to the unbroken output velocity relative to the tool, the piece velocity relative to the tool will be obtained. This velocity added to the furrow velocity (which equals travelling speed) will give the piece velocity at the end of the free fall relative to the furrow, which velocity is said to be the *velocity of collision*. The horizontal component of the collision velocity generally increases when:
– travelling speed is increased,
– the beam delivered to the output is steeper,
– angular velocity of the piece increases.

The vertical component of the collision velocity generally increases when:
– travelling speed is increased,
– the beam delivered to the output is steeper,
– angular velocity of the piece decreases.

A large horizontal component may cause the pieces to roll when they touch the ground: *rolling effect*. A large vertical component may cause a great deal of pulverization or compaction.

To complete the picture, the concept of *piece elongation* will be introduced, which will be defined as m/l, where l is the original length of a given soil beam that is broken into pieces, the largest dimensions of which add up to the length m. The piece elongation is larger than 1, if the pieces break along surfaces that are not perpendicular to the beam-axis. It is smaller than 1 if the failure planes are almost perpendicular, and the beam has been compacted in previous process parts. Also, the piece elongation is smaller than 1 if the piece ends have crumbled off.

The free fall ends when the piece touches the furrow or pieces which have already landed. The piece at that moment has:

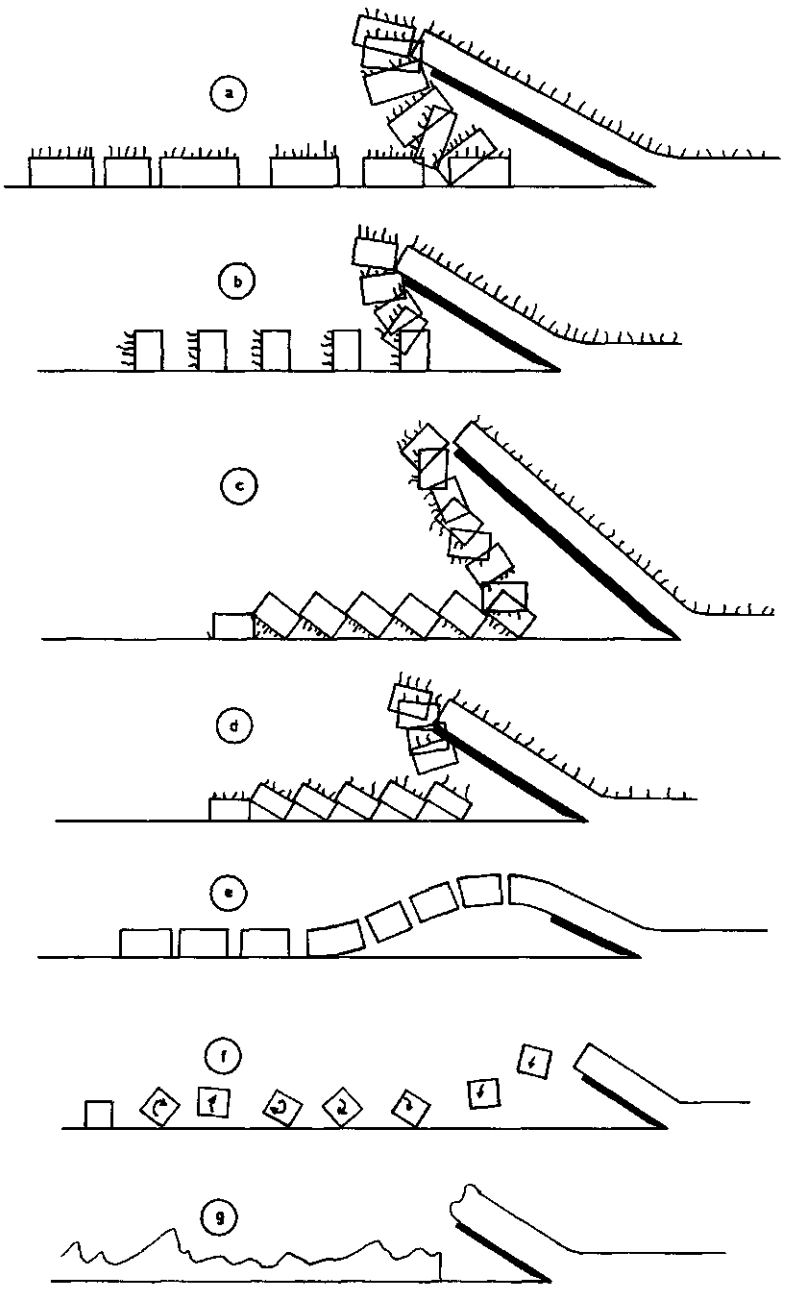

FIG. 98. Some configurations that may be achieved in the output.

- a certain position and a certain shape,
- a certain velocity of collision,
- a certain piece elongation,
- a certain degree of separation.

How these factors determine the way of joining the foregoing pieces, will also depend on the configuration of the pieces that have already been put out. As separation increases, it is more likely that an output will exhibit its own, characteristic way of joining foregoing pieces. The chance that pieces recover their original relative positions is less if the piece elongation is larger. In the case of a low degree of separation, the pieces that have come to rest, will have largely maintained their relative positions. The relative positions are fully maintained where there is no separation, which occurs in outputs that do not include a free fall.

Some ways of joining foregoing pieces are presented in Fig. 98.

- Unchanged configuration in the case of a high degree of separation (Fig. 98a). This can occur with a piece elongation smaller than 1 and a low rate of delivery.
- Half inversion in the case of a high degree of separation (Fig. 98b). It can occur with a certain amount of angular rotation and a low rate of delivery: at higher speeds the horizontal component of the collision velocity causes turning to the right.
- Inversion in the case of a high degree of separation (Fig. 98c); roofing-tile configuration. It can be present at a certain (large) angular rotation and a low rate of delivery.
- Roofing-tile configuration in the case of a high degree of separation (Fig. 98d). This can occur when the angular rotation is small, the delivery rate low, and the piece elongation not smaller than 1.
- Unchanged configuration in the case of non-separated pieces (Fig. 98e). This will occur when the rate of delivery is high and the inclination of the delivered beam is small, or when the output does not include a free fall.
- Output showing a rolling-effect (Fig. 98f), which is promoted by a large horizontal component of the collision velocity.
- Pulverizing output (Fig. 98g), which is promoted by high collision velocities and low soil cohesion values.

Landing of the soil may involve further crumbling. Pertinent to this are the internal soil strength of a piece on the one hand, and the impact load on the other. The impact load will depend on the mass of the soil piece, its velocity, its shape, the elasticity of the piece and the material with which it collides, as well as where on the piece surface the collision takes place.

10.7.2. *Output behaviour when a rigid soil beam is received that has been cracked only in a thin lower part*

A beam which is extended behind the blade is subjected to bending, so that normal stresses act on each cross-section. Above the neutral layer these stresses are tensile stresses, and below compressive stresses. Provided the compressive

stresses are not affected by cracks in the compressive zone, a beam that has been disturbed *below the neutral layer* will behave like an undisturbed beam. Generally, cracks in soil are so irregular, that they hardly influence compressive stresses. The next hypothesis seems therefore be justified: 'outputs receiving rigid soil beams that have only been cracked below the neutral layer (case 10.7.2.) behave like outputs receiving rigid undisturbed soil beams (case 10.7.1.)'.

The determination of whether or not a distortion extends across the neutral layer, is only possible if the position of this layer in undisturbed beams is known.

The position of the neutral layer in undisturbed beams

In the case of
- *a horizontal delivery*,
- *an output not yet broken, and*
- *the extending length being large in relation to the beam thickness*,

the position of the neutral layer at the start of failure is fully determined by the stress-strain relationships in tension and unconfined compression. Because this case involves:
- pure bending (the sum of the tensile and compressive forces is zero for each cross-section),
- rectangular cross-sections having 2 sides perpendicular to the plane of bending,
- a soil tensile strength being much smaller than the soil compressive strength,

the following mechanics method applies (MAURER and WITHEY, 1940). Fig. 99 indicates the stress-strain relationships in tension and unconfined compression. Tensile strength is indicated by AB, and compressive strength by DC. After measuring the area OAB a vertical line FE is selected so as to satisfy area OAB being equal to area OFE. The following then holds:

$$\frac{\text{compressive zone thickness}}{\text{tensile zone thickness}} = \frac{FO}{OA}$$

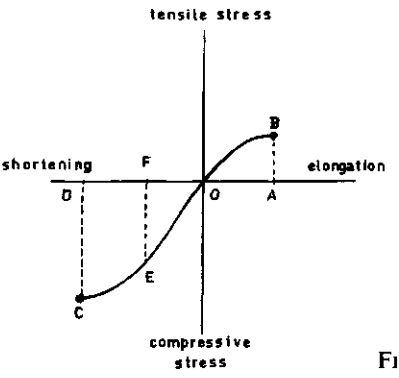

FIG. 99. Stress-strain diagram.

When the stress-strain relationship in tension and the stress-strain relationship in compression have been plotted in one and the same graph using absolute stress and strain values, 4 cases may easily be distinguished:

- If these relationships are equal, the neutral layer lies in the middle of the beam.
- If the tension curve is above the compression curve, the compressive zone is thicker than the tensile zone: the position of the neutral layer is above the middle of the beam.
- If the tension curve is below the compression curve, the tensile zone is thicker than the compressive zone: the position of the neutral layer is below the middle of the beam.
- If the curves cross each other, area measurements according to the previous mechanics method are necessary before a statement can be made.

In bending tests on small soil beams performed by FARRELL et al. (1967) the compressive zone was thinner than the tensile zone. VOMOCIL and CHANCELLOR (1969) published calculations based on stress-strain measurements, showing a large compressive zone, and a smaller tensile zone. FARRELL et al. found a better agreement between their stress-strain measurements and bending tests than VOMOCIL and CHANCELLOR.

When the stress-strain relationships are not equal, the neutral layer shifts as the bending moment (being proportional to length of extending beam) is changed.

In the case of:

- *an inclined delivery,*
- *an output not yet broken, and*
- *the extending length being large in relation to thickness,*

the cross-sections are loaded not only be a couple, but also by a component of the beam weight. Where the soil stress-strain relationships in tension and compression are linear and equal, superposition allows the position of the neutral layer to be determined: 'the neutral layer shifts upwards as the inclination of the received soil beam increases'. For non-linear stress-strain relationships an exact calculation is no longer possible but the above qualitative statement probably remains applicable.

A differenc with the previous type of output (10.7.1)

Both the output cracks and the distortions in the compressive zone occur periodically, each at their own frequency. A certain percentage of output cracks will therefore coincide with distortions and consume less energy than the normal output cracks. Thus, these deviating cracks will exhibit deviating crack progression, making this type of output more irregular than the previous type (10.7.1.).

10.7.3. *Output behaviour when a severely distorted rigid soil beam is received*

This type of output occurs when in previous process parts cracks developed from the lower side of the beam far into the tensile zone, thus crossing the

compressive zone. The still unbroken beam part over such a crack is very weak in relation to the other beam cross-sections, and is therefore called a 'hinge'. When such a soil beam is extended behind the blade so far as to induce failure it becomes obvious that the failure strongly prefers to occur in a hinge. This type of output is characterized by a low energy consumption and much interaction between the soil piece lengths and the previous process parts.

Depending on the ratio of hinge strength to strength of the undisturbed beam parts, one of the following three cases will occur.

- Where the hinges are weak and the undisturbed beam parts are strong, failure occurs in each hinge, and the undisturbed beam parts remain unbroken.
- When significant strength has been left in the hinges, the weight of one undisturbed beam part may not be sufficient to cause hinge failure. A number of hinges remain unbroken, and the output piece length is a multiple of the length of the undisturbed beam parts.
- When the internal soil beam strength is low (in sand, for instance), output cracks will also occur *between* hinges: hinge cracks and cracks according to type 10.7.1. succeed each other. The process progresses very irregularly.

Cracks of the previous process parts have often developed from the lower side of the beam forwards and upwards in an inclined direction. This allows, for a low rate of delivery, the occurrence of the following specific form of output failure, which form will be indicated as 'tilting effect'. Its mechanism is outlined in Fig. 100. Three forces are pertinent in the equilibrium of forces on the beam part behind the hinge:

- the piece weight B,
- the tensile force T in the hinge,
- the reaction force R that the beam tongue tip exerts on the soil piece.

As soon as these forces no longer balance each other (due to the tensile strength being attained in the hinge), the soil piece is separated and tilts around the beam tongue tip. The tilting piece may load the tongue tip so as to break it. This gives rise to a separate output of tongues.

Generally, this type of output is characterized by a large piece elongation. A roofing-tile configuration will therefore occur when the output involves a high degree of separation.

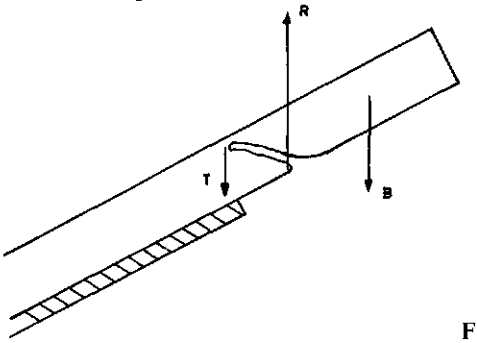

FIG. 100. Tilting effect.

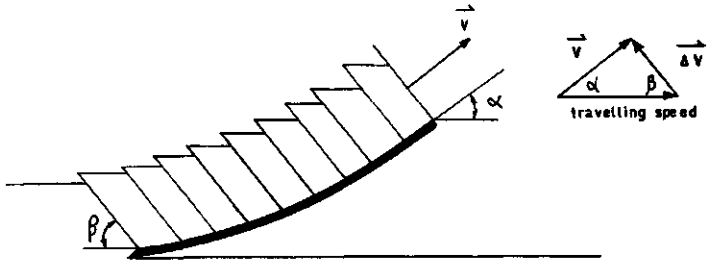

FIG. 101. Some pertinent quantities.

10.7.4. *Output behaviour when short pieces, being separated by parallel failure planes, are received*

The start of falling

The following quantities are pertinent in this type of output (Fig. 101):
- ratio of the soil flow thickness on the blade to the working depth,
- angle of soil failure in the intake β,
- soil velocity at the blade end **V**,
- horizontal soil piece thickness,
- angle of soil to soil friction ϕ,
- angle at which the soil is delivered to the output α.

In the case of:
- *a low rate of delivery, and*
- $\phi < \beta$

the pieces slip off one by one because, as shown in Fig. 102, the friction force on the piece (W) due to the weight component N of the piece is smaller than the weight component K of the piece. This is true because the condition $W < K$ means that

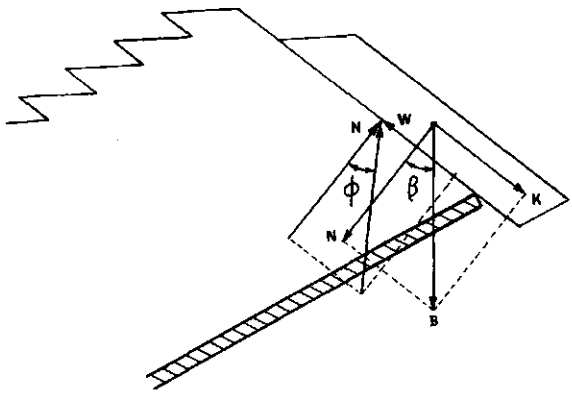

FIG. 102. Forces on a piece that slips off.

$$W = N \cdot \tan \phi = B \cdot \cos \beta \cdot \tan \phi < K = B \cdot \sin \beta,$$

or:

$$\cos \beta \cdot \tan \phi < \sin \beta,$$

or:

$$\phi < \beta,$$

being the second condition of the case under consideration. As soon as more than half the piece has slipped off, tilting around the blade end occurs, and the piece starts to fall freely with an initial velocity composed of a linear velocity and an angular velocity.

In the case of:

- *a low rate of delivery, and*
- $\phi > \beta$,

the weight of the extending piece can no longer cause sliding along the following piece: the friction force always balances the weight component that is parallel to the interface of the pieces. Here, output cracks occur similar to those in the output where a rigid, undisturbed soil beam is received (10.7.1.). This is illustrated in Fig. 103. In this case the output pieces have a small length to thickness ratio because:

- this case is usually restricted to processes having intakes with shear-plane failure. This type of intake only occurs where soil cohesion is low,
- the thickness of the soil flow on the blade is greater than the working depth.

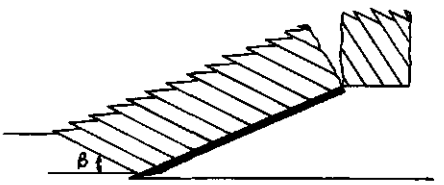

FIG. 103. Pieces being inhibited from slipping.

In the case of:

- *a high rate of delivery, and*
- $\phi < \beta$,

more pieces are put out at the same time. Successive pieces slide along each other, and the longer the piece is involved in the output, the more it tilts around the rear edge of its succeeding piece (Fig. 104a). When the piece strength is low

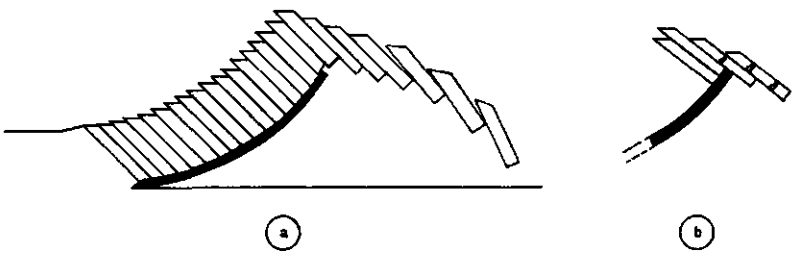

FIG. 104. Slipping accompanied by tilting (a) or fracturing (b).

such rear edges may crumble due to tilting of preceding pieces. Neighbouring pieces may load a piece so as to induce tensile cracks that are almost perpendicular to its shear-planes (Fig. 104b).

Joining the foregoing pieces

The piece elongation is very large, allowing a roofing-tile configuration to occur in many cases where there is a high degree of separation. Some ways of joining foregoing pieces that may occur in this type of output, are:

- Inversion in the case of a high degree of separation. It will occur at a low rate of delivery and a small height of fall (Fig. 105a).
- Roofing-tile configuration in the case of a high degree of separation. It will occur at a greater height of fall, a pronounced tilting effect, and a low rate of delivery (Fig. 105b).
- An unchanged configuration, occurring at high rates of delivery (Fig. 105c).
- Pulverization (Fig. 105d). Pulverization due to collision with the furrow, or with the soil that has already been put out, will occur at low cohesion values.

Generally, parallel shear-planes are only present in low cohesion soils, so that joining of the foregoing pieces in this type of output will often be accompanied by strong pulverization.

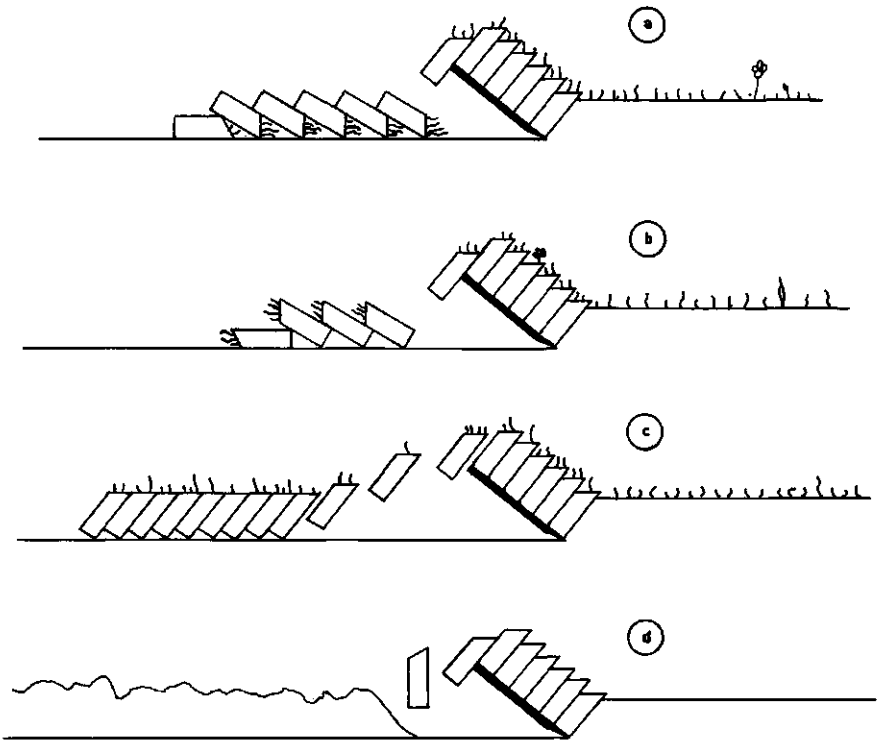

FIG. 105. Some configurations that may be achieved when the main flow delivers parallel moving pieces.

10.7.5. *Output behaviour when only chunks and crumbs are received*

When the soil has been strongly pulverized in previous process parts, the output only receives chunks and crumbs. In the case of a mass of loose material travelling over the blade end *at a low speed*, rolling occurs at an inclination equal to the material angle of repose (Fig. 106). So the chunks and crumbs obtain an angular velocity.

This rotation process hardly occurs *at high speeds* of delivery: many chunks and crumbs are put out at the same time. The state of movement of a particle is almost equal to those of the neighbouring particles, and as soon as the particles have reached the highest point of the flow they start to fall freely, excluding any mutual influence.

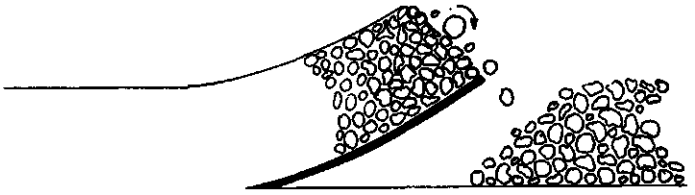

FIG. 106. Output of chunks and crumbs at low travelling speeds.

10.7.6. *Output behaviour when the soil beam is able to deform strongly before a crack develops*

When a deformable, cohesive soil is loaded, a deformation process is induced in the soil, which will end in a state of rest (equilibrium) or in failure.

When support L is removed from the experimental set up of Fig. 107, the extending beam part must sag before the cross-section DD′ has been fully loaded. Sagging will take a certain time: so, the soil deforms for a while before failure occurs. If the soil beam is extended behind the blade at a very low speed, there is plenty of time for the soil to deform. Assume that in this case the piece breaks at a length l. When the speed is high, soil deformation is opposed by inertia forces, and piece length will then become longer than l: piece length increases with increasing rate of delivery.

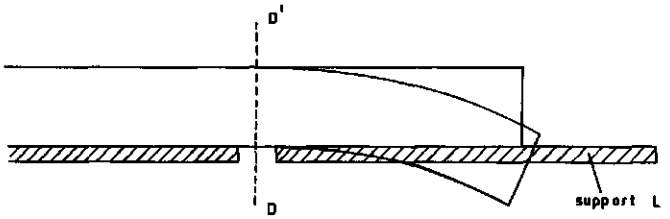

FIG. 107. The beam capacity of sagging in the case of deformable soil.

10.7.7. *A comparison between the output model and the blade experiments*

Some of the blade experiments in section 10.2.2. had outputs that received

TABLE XII. Piece lengths and soil strengths for output type A.

	Mean piece length (cm)	σ_{max} (bar)	tensile strength (bar)
W1	19	0.52	0.18
S1	12	0.37	0.06
S3	7.5	0.16	0.04

cohesive, rigid soil beams showing hardly any cracks (W1, S1, S3). From a comparison between the output-piece lengths of these three experiments (which can be deduced from the section 10.6.1. indicator films) and the soil strengths it will be seen that the soil piece length increases with soil strength; Table XII indicates this. S2 showed much deformation (sagging) of the soil beam prior to the development of output cracks. This is probably connected with a large tensile strength to unconfined compressive strength ratio together with comparatively low values of both strengths, and a large failure strain in unconfined compression. In that case the gravity force is a relatively large load encountering a situation where large deformations are possible. Large tensile strength to unconfined compressive strength ratios occur in the case of plastic soils. (typical values for 'normal' soils and plastic soils are 0.125 and 0.4, respectively). In most experiments the delivered soil beam was cohering, rigid and severely disturbed. There, the output cracks showed a preference to occur in places having input cracks, a probable reason for this being the presence of distortions across the beam neutral layer. A second reason is the fact that the previous process parts have already often weakened the beam tongues to the extent that the effective beam thickness near the beam tongues has been decreased.

The rotation of a piece that is breaking can clearly be seen in Fig. 85. The maximum piece angular velocity occurred at position 3, and equalled ± 12 rad/sec as could be measured from the film. It can be concluded from the small angular rotation between positions 3 and 4 that the piece in position 4 already touches the previous piece. This is not obvious in the drawing, due to piece shape variation across the width.

L5 and S5 show significant tilting around beam tongues or the blade end. The conditions in the soil beams delivered by the main flow in these tests were favourable for this: the pieces were long, rigid and strong, whereas the hinges were extremely weak.

It was remarkable that L1 and L2 did, and L4 did not involve further pulverization when the pieces landed. It may be explained by L4 having a larger compressive strength and smaller (less heavy) pieces in the output.

After landing the soil pieces in S1, S2 and S3 showed a configuration in which the sides of the pieces that formed the original soil surface were again directed upwards and horizontal, the output crack surfaces that belong to each other facing each other. This agreed with the observation that the soil beam was shortened in the direction of its axis during the tillage operation in these experiments. This shortening was $\pm 5\%$ in S1. Where the roofing-tile configuration occurred, the piece elongation was usually large.

11. CONCLUSION

In section 10. a systematic treatise of the phenomena that can be induced by a curved blade having a small cutting angle and a small working depth-blade height ratio was presented, together with some prediction methods for the process aspects. For the prediction of the type of intake a method was proposed which was based on observed relationships between the types of intake and soil characteristics. These relationships are presented in a graph. The field of application of this graph comprises the blade in question that operates in an arbitrary soil at a speed of 32 cm/sec and at a working depth of 3 cm. A (qualitative) approximate method based on the knowledge of the mechanism of open crack formation has been presented for the intake type with open cracks. Finally a method has been given that is able to predict some output aspects. This method is based on knowledge of the mechanisms involved and may be considered as exact.

A number of questions on the curved blade have been left unanswered. This especially concerns the question of what would be the effect of enlarging the blade (and thus also enlarging working depth), and/or increasing the forward speed. The effect of a greater soil heterogeneity on the processes also remained unexplored. In practice, tillage will be performed in rather heterogeneous soils. The effect of a tool shape variation in the direction of the third space dimension as, for instance, the effect of a blade curve in planes perpendicular to the direction of travel was also not investigated. Prediction of aspects within a process type, such as the degree of soil pulverization in the case of intake with open cracks was also hardly touched upon.

This report presents to the reader a systematic treatise of the processes that can occur in the case of tines and plough-bodies, as well as a systematic treatise of prediction methods for aspects of soil loosening processes, and techniques that may facilitate observations on soil loosening processes.

The systematic treatise of the processes that may be induced by tines and plough-bodies consists of the presentation of process types or mechanisms that a tool or a tool part is able to induce at a certain working depth, for a number of tools and working depths. Which process type or mechanism will actually be induced by a particular tool or tool part at a particular working depth will depend on soil type, soil conditions and tool speed. If information on process types or mechanisms that can be induced by a tool or a tool part at a certain working depth is required, then there is a good chance that the relevant information can be obtained from this report. If this is not the case, the report may still provide features of those process types or mechanisms, because of the similarities between the various tools. If that is also not possible, the presented systematics with its classifications and terminology may support further research into those process types.

When further research is intended, the report, in addition, provides information on experimental techniques and methods to elaborate experimental data, including references to literature on such techniques and methods.

If aspects of a soil loosening process are to be predicted, then there is again a good chance that a suitable prediction method can be found in this report. If this is not the case, and a new prediction method needs to be developed, this report may help in defining the problem, and in selecting a suitable field of application and soil and tool characteristics which can be used for the particular prediction problem.

SUMMARY

The soil movements and the inter-particle forces in the vicinity of an operating tool of a tillage implement may be called a soil tillage process. Examples are the tillage processes of tines, plough-bodies etc. (soil loosening processes) and the influence on the soil of land rollers, wheels etc. (load bearing processes). The report is limited to soil loosening processes. Modern farming requests that the energy consumption and the results (in terms of soil pulverization, soil configuration after tillage etc.) of soil loosening processes can be predicted. This necessitates not only prediction methods, but also a systematics of soil loosening processes.

The report presents a systematics of soil loosing processes, which starts with the distinction between tines and plough-bodies. The latter group includes rotatiller blades, harvester lifting blades etc. The plough-bodies are considered to be composed of 3 parts; firstly, the part that loosens still firm soil; then, the part that induces a further tillage; and, finally, the part where the soil is leaving the sphere of direct influence of the tool. For a number of basic shapes of tines and plough-body parts, the process types that may be induced by these basic shapes are presented. Which process type will occur in a given situation, will depend on the soil type, soil porosity, soil moisture content, soil structure, and tool speed. The proposed basic shapes are not intended to keep a permanent place in the systematics; as the requirements of agricultural practice change and research advances, other shapes may become basic. In the current situation, the 2-dimensional curved blade with a small cutting angle and a small working depth-blade height ratio is an important basic tool. An investigation into this blade is reported in detail.

The report also presents a systematic treatise of the methods that are available for the prediction of process aspects (such as the amount of energy consumption and the degree of soil pulverization), together with a discussion on the advantages and disadvantages of these methods, as well as directives for use in the development of new prediction methods. New contributions to the predictability of aspects of 2-dimensional blades are published in the report.

When it is necessary to extend the systematics or to develop new prediction methods, experiments must be performed. A survey of aids to analysis is, therefore, included.

SAMENVATTING

De beweging en de belasting van de gronddeeltjes in de nabijheid van een in actie zijnd element van een grondbewerkingswerktuig kan men een grondbewerkingsproces noemen. Voorbeelden zijn de bewerkingsprocessen van tanden, ploeglichamen etc. (losmakende processen) en de beïnvloeding van de grond door landrollen, wielen etc. (afsteunende processen). Het rapport beperkt zich tot de losmakende processen. In de moderne landbouw is het gewenst de energiebehoefte en het resultaat (uitgedrukt in verkruimeling, wijze van weglegging van de grond etc.) van losmakende processen te kunnen voorspellen. Dit maakt naast voorspellingsmethodes ook een systematiek van losmakende processen noodzakelijk.

Het rapport geeft een systematiek van losmakende processen welke begint met het onderscheiden van tanden en ploeglichamen. Onder deze laatste worden ook freesbladen, rooischaren etc. verstaan. De ploeglichamen worden opgebouwd gedacht uit delen: allereerst het deel welke de nog vaste grond losmaakt, vervolgens het deel dat de grond een verdere bewerking geeft, en tenslotte het deel waar de grond buiten de direkte invloedssdeer van het werktuig begint te komen. Voor een aantal basisvormen van tanden en ploeglichaamdelen zijn aan de orde gesteld de procestypen die bij deze basisvormen op kunnen treden. Welk procestype in een bepaalde situatie op zal treden hangt af van de grondsoort, het porienvolume, het bodemvochtgehalte, de bodemstructuur en de rijsnelheid. Het is niet de bedoeling dat de gegeven basisvormen een vaste plaats in de systematiek innemen: naarmate de praktijk andere eisen stelt en het onderzoek voortschrijdt kunnen andere vormen basis worden. In de huidige situatie is een belangrijke basisvorm het 2-dimensionale gekromde blad met een kleine snijhoek en een kleine werkdiepte-bladhoogte verhouding. Een onderzoek van dit blad wordt in het rapport gedetailleerd verslagen.

Het rapport geeft ook een systematische behandeling van de methodes die beschikbaar zijn voor het voorspellen van proces-aspecten (zoals energieverbruik en mate van grondverkruimeling), met inbegrip van de voor- en nadelen van deze methodes, alsmede richtlijnen om te komen tot nieuwe voorspellingsmethodes. Enkele nieuwe bijdragen aan de voorspelbaarheid van aspecten van 2-dimensionale bladen zijn in het rapport gepubliceerd.

Wil men de systematiek uitbreiden of nieuwe voorspellingsmethodes ontwikkelen, dan zijn experimenten noodzakelijk. Daarom is een overzicht van analysemiddelen toegevoegd.

APPENDIX

MATHEMATICS OF TILLAGE PROCESS MECHANISMS FOR 2-DIMENSIONAL BLADES WITH SMALL CUTTING ANGLES

In this appendix mathematical descriptions of the process mechanisms that can be caused by 2-dimentional blades with small cutting angles are analysed and compared with each other.
Some of the points made are:
- indicating conditions for which Söhne's model is incompatible. In these cases tensile failures are to be expected,
- how to calculate the angle of forward failure surface in Söhne's model according to the minimal energy criterion,
- a demonstration of the increase of ε in Gorjatchkin's formula by the fact that part of the blade reaction forces is usually balanced by a slade or a supporting wheel, and by the fact that the direction of pull is usually inclined.

For process mechanisms in the case of blades with large cutting angles (that is, not smaller than $45°-{}^1/_2\ \phi$ where ϕ is the angle of internal soil friction), reference is made to classical soil mechanics theories (HETTIARATCHI et al., 1966).

1. *The momentum equation*

Fig. A1 shows a soil flow on a curved blade, where it is assumed that:
- the travelling speed of the tool, V_t, is constant and linear (a list of symbols is added at the end of the appendix),
- the soil flow on the blade is continuous and steady,
- the bulk density of the soil, ρ, is constant ($\rho = \gamma/g$, where γ bulk volume weight and g = acceleration of gravity),
- soil beam thickness is constant.

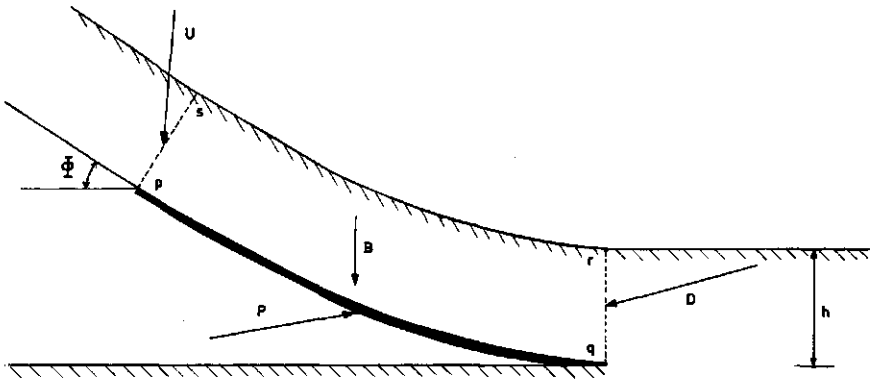

FIG. A1. Refers to the momentum equation.

The forces that act on the soil mass p, q, r, s are indicated: P is the total reaction force that the blade exerts on the soil, D is the reaction force that the still firm soil exerts on the plane q, r.

U is the reaction force on plane p, s, exerted by the soil that has left the blade,
B is weight of the soil mass in p, q, r, s,
h is working depth,
Φ is angle of the blade trailing edge.

Application of the momentum equation (SHAMES, 1962) results in:

$$P_x = D_x + U_x + \rho \cdot b \cdot h \cdot V_t^2 \cdot (1 - \cos \Phi) \quad (1)$$

$$P_{ij} = D_{ij} + U_{ij} + B + \rho \cdot b \cdot h \cdot V_t^2 \cdot \sin \Phi. \quad (2)$$

where b is the width of the process and indices x and ij indicate components in in the horizontal and the vertical directions, respectively.
Provided V_t and U are negligibly small,

$$P_x = D_x \quad (1\text{-a})$$

$$P_{ij} = D_{ij} + B$$

However, on some occasions the force U is not negligibly small; for instance, where the soil leaving the blade is hindered by soil that has already left the blade.

2. *Gorjatchkin's formula*

In 1898 W. Gorjatchkin published the following formula for the draught force of plough-bodies (SÖHNE, 1959).

$$\frac{P_x}{b \cdot h} = z + \varepsilon \cdot V_t^2 \quad (3)$$

where z is draft at zero speed and ε is a constant that is specific for a certain blade shape and soil conditions. SÖHNE (1960) and BERNACKI (1963) concluded from experiments that ε is a function of ϕ and formulated

$$\frac{P_x}{b \cdot h} = z + \varepsilon' \cdot (1 - \cos \Phi) \cdot V_t^2, \quad (3\text{-a})$$

where ε' is a constant that is specific for a shape of the initial blade part and soil conditions.

3. *Söhne's model for a plane blade*

3.1. Geometrical aspects

This model (SÖHNE, 1956) is shown in Fig. A2. Plane q, r is a potential failure surface along which the cohesive force and the frictional force are fully developed.
B is weight of the soil in p, q, r, s, t,

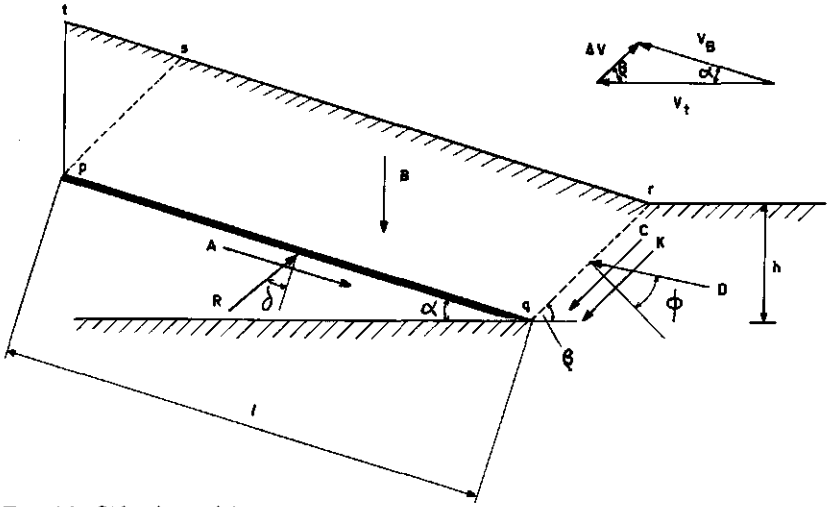

FIG. A2. Söhne's model.

C is cohesive force,
K is force due to the soil acceleration,
R is the force that the blade exerts on the soil, being a normal force plus an associated frictional force,
D is the force that the still firm soil exerts on q, r, being a normal force plus an associated frictional force,
A is adhesion force,
l is blade length,
α is cutting angle,
β is angle of forward failure surface,
δ is soil to metal friction angle.

The soil beam thickness to working depth ratio is indicated as S. S and the forward displacement and the velocity of the soil depend on the geometry of the model. See Fig. A3. S is defined as j/h, so that

$$S = \frac{\sin(\alpha + \beta)}{\beta} \tag{4}$$

From the velocity diagram it follows that

$$\Delta V = V_t \cdot \frac{\sin \alpha}{\sin(\alpha + \beta)} \tag{5}$$

Let V_v be the horizontal component of the velocity of the soil leaving the blade relative to the furrow bottom, then

$$V_v = V_t - \Delta V \cdot \cos \alpha \tag{6}$$

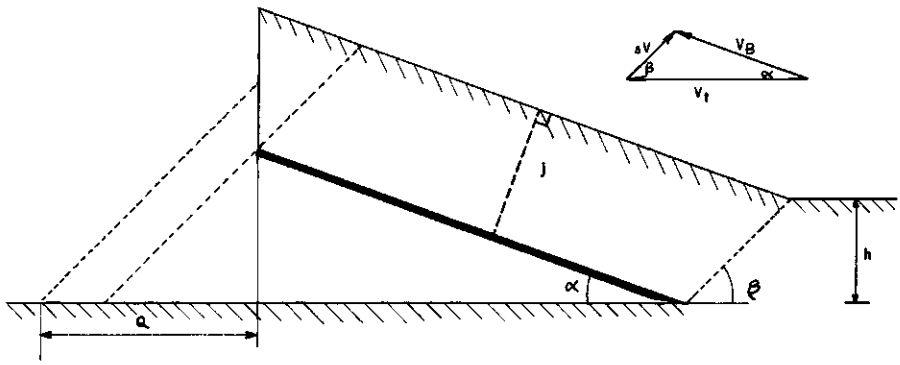

FIG. A3. Kinematical aspects of Söhne's model.

In the figure, the minimal horizontal displacement is indicated as Q. The horizontal displacement increases as V_t (and thus V_v) is increased. The acceleration force can be calculated from ΔV: a soil particle is accelerated during a time interval Δt. The mean acceleration is therefore $\Delta V/\Delta t$.

The mass that is being accelerated at one moment, is $\rho \cdot b \cdot h \cdot V_t \cdot \Delta t$. The acceleration force can now be calculated, using (5):

$$K = (\rho \cdot b \cdot h \cdot V_t \cdot \Delta t) \cdot \frac{\Delta V}{\Delta t} = \frac{\sin \alpha}{\sin (\alpha + \beta)} \cdot \rho \cdot b \cdot h \cdot V_t^2 \tag{7}$$

If can further be derived that

$$C = \frac{h \cdot c}{\sin \beta}, \tag{8}$$

$$A = l \cdot a, \tag{9}$$

where c is cohesion and a is adhesion, and that

$$B = \rho \cdot g \cdot l \cdot h \cdot \frac{\sin (\alpha + \beta)}{\sin \beta} + 0.5 \cdot \rho \cdot g \cdot h^2 \cdot \frac{\sin (\alpha + \beta) \cdot \cos \beta}{\sin^2 \beta \cdot \cos \alpha} \tag{10}$$

The last term in formula (10) accounts for the soil in s, t, p, and the last but one for the soil in p, q, r, s.

3.2. The equilibrium of forces

SÖHNE's model involves three unknowns, namely R, D and β. The requirement of equilibrium in the horizontal and vertical directions provides two simultaneous equations, which means that D may be calculated in terms of β. Also, R may be calculated in terms of β. From R calculated in this way it is possible to express P_x in terms of β, because

$$P_x = R_x + A_x \tag{11}$$

The result is:

$$\frac{P_x}{b} = N_c \cdot h \cdot c + N_a \cdot l \cdot a + N_{\rho 1} \cdot g \cdot l \cdot h \cdot \rho + N_{\rho 2} \cdot g \cdot h^2 \cdot \rho + \\ + N_v \cdot \rho \cdot h \cdot V_t^2 \tag{12}$$

$$\frac{D}{b} = M_c \cdot h \cdot c + M_a \cdot l \cdot a + M_{\rho 1} \cdot g \cdot l \cdot h \cdot \rho + M_{\rho 2} \cdot g \cdot h^2 \cdot \rho + \\ M_v \cdot \rho \cdot h \cdot V_t^2, \tag{13}$$

where:

$$N_c = \frac{\sin(\alpha + \delta) \cdot \cos \phi}{\sin \beta \cdot \sin(\alpha + \delta + \phi + \beta)} \text{ (influence of cohesion)} \tag{14-a}$$

$$N_a = \cos \alpha \; - \frac{\sin(\alpha + \delta) \cdot \cos(\alpha + \phi + \beta)}{\sin(\alpha + \delta + \phi + \beta)} \\ \text{(influence of adhesion)} \tag{14-b}$$

$$N_{\rho 1} = \frac{\sin(\alpha + \delta) \cdot \sin(\phi + \beta) \cdot \sin(\alpha + \beta)}{\sin \beta \cdot \sin(\alpha + \delta + \phi + \beta)} \\ \text{(influence of weight of soil in p, q, r, s)} \tag{14-c}$$

$$N_{\rho 2} = 0.5 \cdot \frac{\sin(\alpha + \delta) \cdot \sin(\phi + \beta) \cdot \sin(\alpha + \beta) \cdot \cos \beta}{\sin^2 \beta \cdot \cos \alpha \cdot \sin(\alpha + \delta + \phi + \beta)} \\ \text{(influence of weight of soil in s, t, p)} \tag{14-d}$$

$$N_v = \frac{\sin(\alpha + \delta) \cdot \sin \alpha \cdot \cos \phi}{\sin(\alpha + \beta) \cdot \sin(\alpha + \delta + \phi + \beta)} \\ \text{(influence of velocity)} \tag{14-e}$$

$$M_c = \; - \frac{\cos(\alpha + \delta + \beta)}{\sin \beta \cdot \sin(\alpha + \delta + \phi + \beta)} \tag{15-a}$$

$$M_a = \frac{\cos \delta}{\sin(\alpha + \delta + \phi + \beta)} \tag{15-b}$$

$$M_{\rho 1} = \frac{\sin(\alpha + \delta) \cdot \sin(\alpha + \beta)}{\sin \beta \cdot \sin(\alpha + \delta + \phi + \beta)} \tag{15-c}$$

$$M_{\rho 2} = 0.5 \cdot \frac{\sin(\alpha + \delta) \cdot \sin(\alpha + \beta) \cdot \cos \beta}{\sin(\alpha + \delta + \phi + \beta) \cdot \sin^2 \beta \cdot \cos \alpha} \tag{15-d}$$

$$M_v = \frac{\cos(\alpha + \delta + \beta) \cdot \sin \alpha}{\sin(\alpha + \delta + \phi + \beta) \cdot \sin(\alpha + \beta)} \tag{15-e}$$

For fixed values of α, δ and ϕ all N and M factors are functions of β only. The form of the equations (12) and (13) is similar to that of the 'fundamental earth moving equation' developed by REECE (1965).

3.3. The minimal energy criterion

Using (12), P_x can be calculated for a series of β-values, and that β-value, for which P_x is at a minimum, may be assumed to occur. This is justified by the following assumptions.

- That β will occur, for which the energy consumption, and therefore the force P_x is at a minimum.
- The energy consumption is mainly determined by the forces indicated in Fig. A2. These forces are thus assumed to be present during the whole duration of the tillage process. This is doubtful especially for C and D (C may decrease sharply after failure).

3.4. The case where the influence of the cohesion is predominant

Generally, P_x in (12) is mainly determined by the cohesion and/or the weight of p, q, r, s. Therefore, the most significant N factors are N_c and $N_{\rho 1}$.
Where a situation is considered in which the influence of the cohesion is predominant, the following applies:

$$\frac{P_x}{b} = N_c \cdot h \cdot c = \frac{\sin(\alpha + \delta)\cdot\cos\phi}{\sin\beta\cdot\sin(\alpha + \delta + \phi + \beta)} \cdot h \cdot c \tag{16}$$

$$\frac{D_x}{b} = M_c \cdot h \cdot c = -\frac{\cos(\alpha + \delta + \beta)}{\sin\beta\cdot\sin(\alpha + \delta + \phi + \beta)} \cdot h \cdot c \tag{17}$$

Equation (16) is equal to Merchant's cutting model for machining metals (ARMAREGO and BROWN, 1969), and, according to that model, P_x is at a minimum for

$$\beta = 0.5\cdot(180^\circ - \phi - \delta - \alpha) \tag{18}$$

Substituting β in (17) by (18), D can be calculated.

$$\frac{D}{b} = -\frac{\cos(90^\circ + 0.5\cdot\delta + 0.5\cdot\alpha - 0.5\cdot\phi)}{2\cdot\cos(0.5\cdot\alpha + 0.5\cdot\delta + 0.5\cdot\phi)} \cdot h \cdot c \tag{19}$$

The model can only be compatible if D is not negative. The denominator on the right hand side of (19) is positive for normal values of α, δ, and ϕ, so that D is positive if the nominator on the right hand side is negative.
Hence, D is positive if

$$\alpha > \phi - \delta \tag{20}$$

Where (20) is not satisfied, the model is not compatible. Possibly, tensile stresses are then present in the soil.

Even if D calculated from (19) is positive, there may be tensile stresses in the soil. This appears from (17), which shows that for a β-value smaller than β at which P_x is minimal, D is negative if $\cos(\alpha + \delta + \beta) > 0$, thus if $\alpha + \delta + \beta < 90^\circ$ In that case tensile stresses are present in the soil below the forward failure plane calculated using the minimal energy criterion. These tensile stresses may

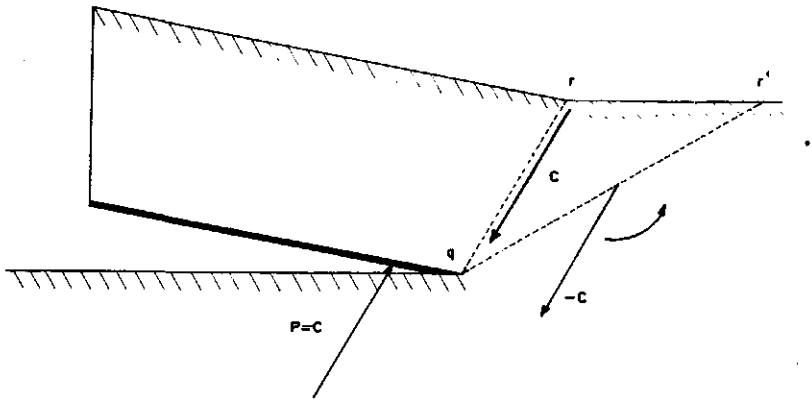

FIG. A4. Stress state of an arbitrary plane q, r'.

cause tensile failure, which deviates from the failure type assumed by Söhne's model. The existence of such negative D values is demonstrated for $\delta = 20°$ and $\alpha = 10°$ in Fig. A4. In this case P_x is at a minimum for $\beta = 60°$, so the predicted failure plane is q, r.

D on q, r is found to be zero, and P equals C. The force resultant on the arbitrary plane q, r' is calculated from the equilibrium of forces on q, r, r' as $-C$. This resultant is a tensile force and is parallel to q, r, which implies a negative D on q, r'.

3.5. The case where the influence of the weight is predominant

Where the influence of the weight of the soil predominates, $N_{\rho 1}$ and $N_{\rho 2}$ are the most significant N factors. If, in addition, the blade length is large compared with the working depth, the influence of $N_{\rho 2}$ can be neglected, and, from (12) and (13),

$$\frac{P_x}{b} = \frac{\sin(\alpha + \delta)\cdot\sin(\phi + \beta)\cdot\sin(\alpha + \beta)}{\sin\beta\cdot\sin(\alpha + \delta + \phi + \beta)}\cdot\rho\cdot g\cdot l\cdot h \tag{21}$$

$$\frac{D_x}{b} = \frac{\sin(\alpha + \delta)\cdot\sin(\alpha + \beta)}{\sin\beta\cdot\sin(\alpha + \delta + \phi + \beta)}\cdot\rho\cdot g\cdot l\cdot h \tag{22}$$

From (21) it can be derived that P_x is minimal if

$$|\lambda - 2\cdot\beta| = \arccos\left\{-\frac{2\cdot\sin\delta\cdot\cos\lambda}{A_2}\right\}, \tag{23}$$

where:

$$\lambda = \arctan(A_1/A_2)$$
$$A_1 = -4\cdot\cos(\phi + \alpha + \delta)\cdot\sin\phi\cdot\sin\alpha$$
$$A_2 = 2\cdot\cos(\phi + \alpha + \delta)\cdot\sin(\phi + \alpha) - 2\cdot\sin(\phi + \alpha + \delta)\cdot\cos(\phi - \alpha)$$

Table AI is calculated from (23) for $\delta = 20°$ and $\phi = 30°$

TABLE A I. Angle of forward failure surface (β) as a function of cutting angle (α) for 2-dimensional plane blades when the influence of soil weight is predominant ($\delta = 20°$, $\phi = 30°$).

α	5°	10°	20°	30°	40°	50°
β	20° 45′	28° 25′	34° 41′	35° 55′	34° 50′	32° 30′

3.6 Values for the angle of foward failure surface

In Fig. A5, equation (18) and Table AI are presented by solid lines for $\delta = 20°$ and $\phi = 30°$. If both N_c and $N_{\rho 1}$ are significant, other influences being negligible, β lies between those lines.

It can be derived from N_a that at significant values of the adhesion the value of β decreases. Significant influences of soil weight in s, t, p make β increase. When the travelling speed is increased β in Fig. A5 shifts in the direction of the broken line.

If may be noted from Fig. A2 that the entire process geometry changes with a change in β. For geometrical changes with speed in the case of tines the reader is referred to (TERPSTRA, 1977).

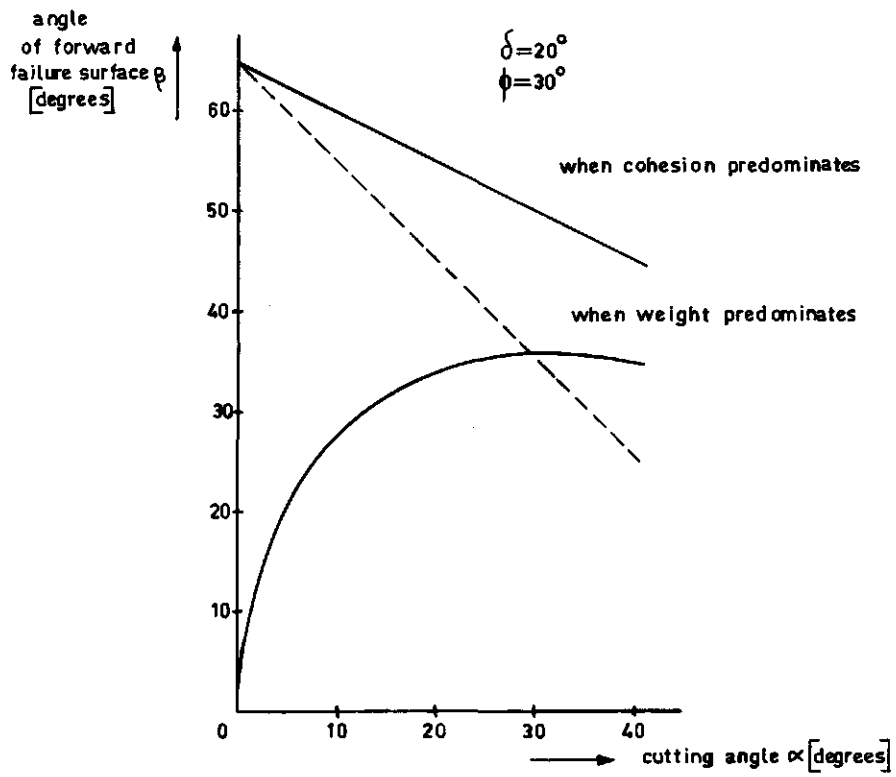

FIG. A5. Angle of forward failure surface as a function of cutting angle for 2-dimensional plane blades.

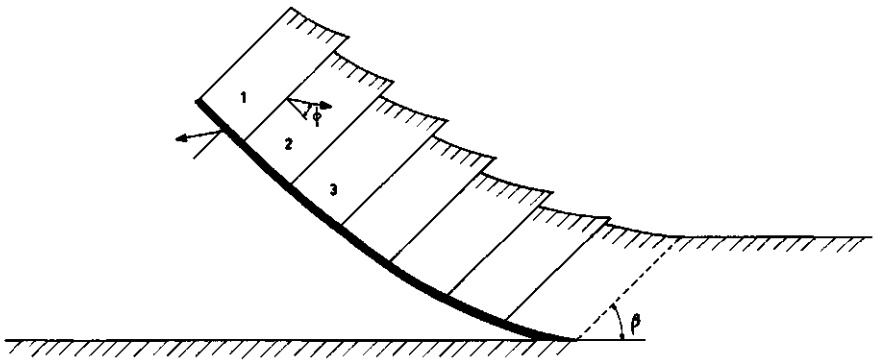

FIG. A6. Söhne's model for a curved blade.

4. *Söhne's model applied to curved blades*

The geometry of Söhne's model for a curved blade (SÖHNE, 1956) is outlined in Fig. A6. A number of pieces move parallel to each other as they progress on the blade. Each piece exerts a reaction force on the blade, and a reaction force on the next piece. For piece labelled 1 both these reaction forces can be calculated using Söhne's plane blade model. After the reaction force exerted by piece 1 on piece 2 has been calculated in this way, Söhne's plane blade model can again be applied to calculate the reaction force that piece 2 exerts on piece 3. Treating all pieces in this way, the total blade draught force can be calculated for any β. (It can be shown that the distance between successive failure planes, i.e. the number of pieces, only has a slight influence on the result).

The mould-board studies in (CARLSON, 1961) and (O'CALLAGHAN and MCCOY 1965) use mathematical models which for 2-dimensional curved blades are identical to Söhne's model with $\beta = 90°$ and $\phi = 0°$.

5. *Speed effects for a plane blade as reflected in the various models*

Here, $\alpha = \Phi$. When force U is neglected, the momentum equation (1) becomes:

$$\frac{P_x}{b \cdot h} = \frac{D_x}{b \cdot h} + (1 - \cos \alpha) \cdot \rho \cdot V_t^2 \tag{24}$$

Equations (3) and (3-a) were:

$$\frac{P_x}{b \cdot h} = z + \varepsilon \cdot V_t^2 \tag{25}$$

$$\frac{P_x}{b \cdot h} = z + \varepsilon' \cdot (1 - \cos \alpha) \cdot V_t^2 \tag{26}$$

Equation (12) may be written as:

$$\frac{P_x}{b \cdot h} = Z + N_v \cdot \rho \cdot V_t^2, \tag{27}$$

where both Z and N_v are functions of β.

Equations (26) and (27) are not identical because N_v is not proportional to $(1-\cos\alpha)$. Neither are (25) and (27) identical, for, according to Fig. A5, β, and therefore N_v, will change with speed. The equations (24) and (26) would only be identical where $\rho = \varepsilon'$.

For $\alpha = 20°$, $\delta = 20°$, $\rho = 1800\ \text{kg/m}^3$, the following numerical examples are presented. These values involve $(1-\cos\alpha)\cdot\rho = 108\ \text{kg/m}^3$, so that momentum equation (24) becomes:

$$\frac{P_x}{b\cdot h} = \frac{D_x}{b\cdot h} + 108\cdot V_t^2\ (\text{N/m}^2) \tag{28}$$

If it is also assumed that $\beta = 45°$ and $\phi = 30°$, $N_v\cdot\rho = 418\ \text{kg/m}^3$, so that (27) derived from Söhne's model, becomes:

$$\frac{P_x}{b\cdot h} = Z + 418\cdot V_t^2\ (\text{N/m}^2) \tag{29}$$

From a comparison between (28) and (29) it is shown that D_x increases with increasing speed. Equation (13) already showed this.

6. *Slades, supporting wheels and inclined directions of pull*

The vertical component of the reaction force that the soil exerts on the blade is often balanced via a sledge or a supporting wheel. In addition, the direction of pull is often not equal to the travelling direction. These circumstances occur in Fig. A7, where the direction of pull is parallel to the blade surface. Here, the horizontal draught force component is not P_x but P_x'. If A_x is assumed to be zero, (11) gives $P_x = R_x$, and P_x' can be calculated in terms of P_x using the triangle of forces:

$$P_x' = 1.65\cdot P_x \qquad (\text{N/m}^2) \tag{30}$$

Equations (29) and (30) combine to:

$$\frac{P_x'}{b\cdot h} = 1.65\cdot Z + 691\cdot V_t^2\ (\text{N/m}^2) \tag{31}$$

From a comparison between (29) and (31) it is shown that the slade and the inclination of the direction of pull make ε in Gorjatchkin's formula increase by as much as 65%.

7. *Symbols used in the appendix*

A adhesion force
B weight of a soil mass
C cohesive force
D the reaction force of the still firm soil, being a normal force plus an associated frictional force

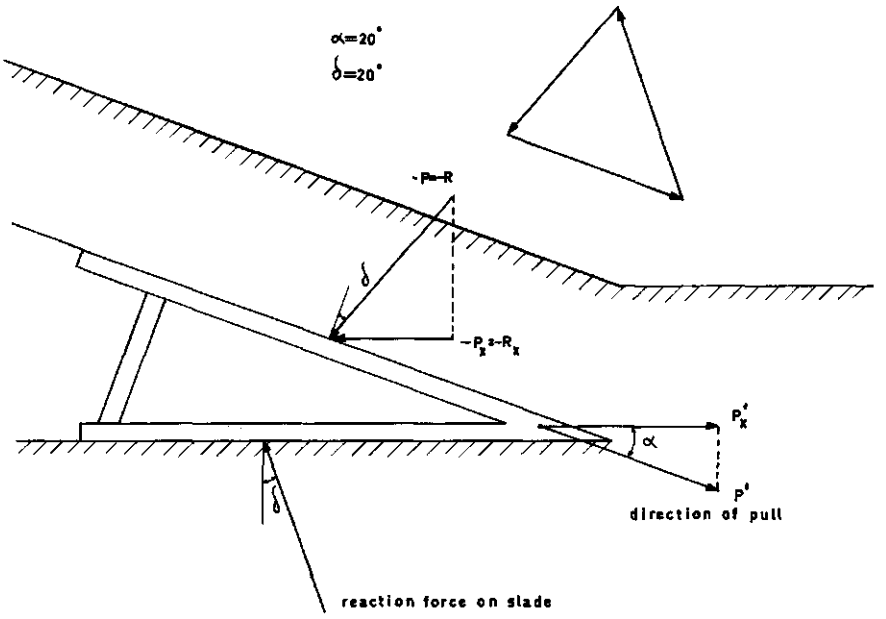

FIG. A7. Influence of slade and direction of pull on tool draught.

K force due to the soil acceleration
N, M dimensionless functions of α, δ, ϕ, β
P, P' tool draught
Q horizontal displacement of the soil
R the force that the blade exerts on the soil, being a normal force plus an associated frictional force
S j/h
U reaction force, exerted by the soil that has left the blade
V_t travelling speed
ΔV change in soil velocity at the intake
Δt time interval
V_B soil velocity on the blade
V_v horizontal component of the velocity of the soil leaving the blade relative to the furrow bottom
Z a constant
a adhesion
b width of the process
c cohesion
g acceleration of gravity
h working depth
j soil beam thickness on the blade
l blade length

x, y reference axes
z draught at zero speed
Φ angle of the blade trailing edge
α cutting angle
β angle of forward failure surface
γ bulk volume weight of the soil
δ soil-metal friction angle
$\varepsilon, \varepsilon'$ constants
ρ bulk density of the soil
ϕ angle of internal soil friction

REFERENCES

ARMAREGO, E. J. and R. H. BROWN: The machining of metals. Englewood Cliffs, 1969, 38–45.

BAILEY, A. C.: Compaction and shear in compacted soils. Transactions of the ASAE **14** (1971), 201–205.

BAILEY, A. C.: Shear and plastic flow in unsaturated clay. Transactions of the ASAE **16** (1973), 218–221, 226.

BAILEY, A. C. and G. E. VANDENBERG: Yielding by compaction and shear in unsaturated soil. Transactions of the ASAE **11** (1968), 307–311, 317.

BAKHTIN, P. U., K YU. KIRTBAYA, I. N. NIKOLAEVA, V. I. VOLOTSKAYA: Resistance of soils in the USSR to deformation and ploughing. Transactions of the 9th Intern. Congress on Soil Science (1968) 1, 781–792.

BEKKER, M. G.: Theory of land locomotion. Ann Arbor, 1956.

BENBOW, J. J. and F. C. ROESLER: Experiments on controlled fractures. Proc. Phys. Soc. B, **70** (1957), 201–211.

BERNACKI, H.: Ergebnisse der Untersuchung an Schnellpflugkörpern. Deutsche Agrartech. **13** (1963), 493–494.

BISHOP, A. W. and V. K. GARGA: Drained tension tests on London clay. Géotechnique **19** (1969), 309–313.

BISHOP, A. W. and D. J. HENKEL: The measurement of soil properties in the triaxial test. London, third edition, 1964.

BOELS, D. and G. P. WIND: Enkele cultuurtechnische aspecten van de oogstproblemen van 1974. Landbouwk. tijdschrift/pt **87** (1975), 96–100.

BUISHAND, T.: Teelt van stamslabonen. Teeltbeschrijving nr. 7 Consulentschap in algemene dienst voor de groenteteelt in de vollegrond in Nederland te Alkmaar, Alkmaar, 1973.

BUTTERFIELD, R. and K. Z. ANDRAWES: A consistent analysis of a soil cutting problem. Proc. 4th ISTVS conf. Vol. 2, Stockholm, 1972, 3–20.

CARLSON, E. C.: Plows and computers. Agric. Engin. **42** (1961), 292–295, 307.

CHANCELLOR, W. J. and R. H. SCHMIDT: Soil deformation beneath surface loads. Transactions of the ASAE **5** (1962), 240–246, 249.

CHASE, L. W.: A study of subsurface tiller blades. Agric. Engin. **23** (1942), 43–45, 50.

CHEN, WAI-FAH: Limit analysis and soil plasticity. Developments in Geotechnical Engineering 7, Amsterdam, 1975.

COOK, P. E. R. and A. R. REECE: Theory of bulldozer action in friable soil. 2nd International Conference of ISTVS, Quebec, 1966.

DALLEINE, E. and J. F. BILLOT: Evolution des matériels classiques de travail du sol. Procédé's nouveaux de travail du soil. Tome 1. Bulletin Technique d'Information, No. 302–303, sept–oct 1975, 521–537.

DEXTER, A. R. and D. W. TANNER: The response of unsaturated soils to isotropic stress. J. Soil Sci. **24** (1973), 491–502.

DEXTER, A. R. and D. W. TANNER: Time dependence of compressibility for remoulded and undisturbed soils. J. Soil Sci. **25** (1974), 153–164.

DONER, R. D. and M. L. NICHOLS: The dynamic properties of soil. V. Dynamics of soil on plow moldboard surfaces relating to scouring. Agric. Engin. **15** (1934), 9–13.

DREES, G.: Untersuchungen über das Kraftespiel an Flachbagger-Schnittwerkzeugen im Mittelsand und schwach bindigem, sandigem Schluff unter besonderer Berücksichtigung der Planierschilde und ebenen Schürfkübelschneiden. Dissertation, T. H. Aachen, 1956.

DUNLAP, W. H. and J. A. WEBER: Compaction of an unsaturated soil under a general state of stress. Transactions of the ASAE **14** (1971), 601–607.

ELIJAH, D. L. and J. A. WEBER: Soil failure and pressure patterns for flat cutting blades. ASAE paper no. 68–655, St Joseph, 1968.

FARRELL, D. A., E. L. GREACEN, W. E. LARSON: The effect of water content on axial strain in a loam under tension and compression. Soil Sci. Soc. of Amer. Proc. **31** (1967), 445–450.
FLORESCU, C. I. and A. CANARACHE: Draft requirement and soil physical properties as related to planning of mechanised agriculture. 6th Intern. Conf. on Soil Tillage, Wageningen 1973.
FORD, H.: Advanced mechanics of materials. London, 1963.
FREITAG, D. R., R. L. SCHAFER, R. D . WISMER: Stimilitude studies of soil machine systems. Transactions of the ASAE **13** (1970), 201–213.
GILL, W. R. and G. E. VANDENBERG: Soil dynamics in tillage and traction. Agriculture Handbook no. 316, Washington, 1967.
GILL, W. R.: Influence of compaction hardening of soil on penetration resistance. Transactions of the ASAE **11** (1968), 741–745.
GILL, W. R.: Soil deformation by simple tools. Transactions of the ASAE **12** (1969), 234–239.
GRIFFITH, A. A.: The phenomenon of rupture and flow in solids. Phil. Trans. R. Soc. A **221** (1920), 163–198.
GUPTA, C. P. and A. C. PANDYA: Behaviour of soil under dynamic loading. Its application to tillage implements. Transactions of the ASAE **10** (1967), 352–358, 363.
HAWKINS, J. C.: The design of potato harvesters. J. agric. Engng Res. **2** (1957), 14–24.
HÉNIN, S., R. GRAS, G. MONNIER: Le profil cultural. Paris, 1969.
HETÉNYI, M.: Handbook of experimental stress analysis. New York, 1950.
HETTIARATCHI, D. R. P., B. B. WITNEY, A. R. REECE: The calculation of passive pressure in 2-dimensional soil failure. J. agric. Engng Res. **11** (1966), 89–107.
HETTIARATCHI, D. R. P. and A. R. REECE: Symmetrical 3-dimensional soil failure. Journal of Terramechanics **4** (1967) 3, 45–67.
JOHNSON, L. E. and W. F. BUCHELE: Energy in clod-size reduction of vibratory tillage. Transactions of the ASAE **12** (1969), 371–374.
JOHNSON, L. E., G. MURPHY, W. G. LOVELY, R. L. SCHAFER: Indentifying soil dynamic parameters for soil-machine systems. Transactions of the ASAE **15** (1972), 9–13.
KAROL, R. H.: Soils and soil engineering. Englewood Cliffs, 1960.
KAWAMURA, N.: Study of the plow shape (3). Study on soil cutting and pulversation (1). J. Soc. Agric. Mach. Japan **14** (1952) 3, 4.
KERKHOF, F.: Vorgänge beim Bruch. in: Struktur und physikalisches Verhalten der Kunststoffe, edited by K. A. Wolf. Berlin 1962, 440–484.
KIM, J. I. and L. M. STALEY: Soil deformation measurement by the Moiré technique. Transactions of the ASAE **16** (1973), 232–235.
KOENIGS, F. F. R.: The mechanical stability of clay soils as influenced by the moisture conditions and some other factors. V.L.O. 67.7 Wageningen, 1961.
KOOLEN, A. J.: Mechanical behaviour of soil by treatment with a curved blade having a small angle of approach. J. agric. Engng Res. **17** (1972), 355–367.
KOOLEN, A. J.: Failure patterns in different soils produced by a curved blade with a small angle of approach. NIAE Subject day on mechanical behaviour of agricultural soils. Silsoe 1973, paper 4.
KOOLEN, A. J.: A method for soil compactibility determination. J. agric. Engng Res. **19** (1974), 271–278.
KOOLEN, A. J.: Mechanical properties of precompacted soil as affected by the moisture content at precompaction. The 7th Conference of the International Soil Tillage Research Organisation, Sweden, 1976, paper 20.
KRAUSE, R.: Der Verdrängungsvorgang um Untergrundwerkzeuge in trockenem Sand. Landbauforschung Völkenrode, Sonderheft 20, 1973.
KUIPERS, H.: Bodemfysische metingen op het grondbewerkingsproefveld ZZH 691 op de proefboerderij Mariënhof te Westmaas 1954–1957. I.B. Groningen, C 8161, 1959.
KURTAY, T. and A. R. REECE: Plasticity theory and critical state soil mechanics. Journal of Terramechanics **7** (1970) 3 and 4, 23–56.
LEE, I. K. and O. G. INGLES: Strength and deformation of soils and rocks. in: 'Soil mechanics,

selected topics', edited by I.K. Lee. London, 1968, 195–294.
MAURER, E. R. and M. O. WITHEY: Strength of materials. New York, 1940.
MCLEAN, W. G. and E. W. NELSON: Engineering mechanics, statics and dynamics. Second edition. New York, 1962.
MURPHY, G.: Similitude in engineering. New York, 1950.
NICHOLS, M. L. and T. H. KUMMER: The dynamic properties of soil IV. A method of analysis of plow moldboard design based upon dynamic properties of soil. Agric. Engin. **13** (1932), 279–285.
NICHOLS, M. L. and C. A. REAVES: Soil reaction: to subsoiling equipment. Agric. Engin. **39** (1958), 340–343.
NICHOLS, M. L. and I. F. REED: Soil dynamics. VI. Physical reactions of soils to moldboard surfaces. Agric. Engin. **15** (1934), 187–190.
NICHOLS, M. L., I. F. REED, C. A. REAVES: Soil reaction: to plow share design. Agric. Engin. **39** (1958), 336–339.
N.N.: ASAE Yearbook 1975, St Joseph, 1975.
N.N.: ASTM Special technical publication no. 381, Philadelphia, 1964.
N.N.: Soiltest, Inc. General catalog, volume 2 a, Evanston, 1971.
NOVIKOV, J. F.: Bodendichte und Bodenspanning beim Pflügen. Landtechn. Forschung **17** (1967) 5, 146–148.
O'CALLAGHAN, J. R. and K. M. FARRELLY: Cleavage of soil by tined implements. J. agric. Engng Res. **9** (1964), 259–269.
O'CALLAGHAN, J. R. and J. G. MCCOY: The handling of soil by mouldboard ploughs. J. agric. Engn Res. **10** (1965), 23–35.
O'CALLAGHAN, J. R. and P. J. MCCULLEN: Cleavage of soil by inclined wedge-shaped tines. J. agric. Engng Res. **10** (1965), 248–254.
OLSON, D. J. and J. A. WEBER: Effect of speed on soil failure patterns in front of model tillage tools. Transactions of the Society of Automotive Engineers **74** (1966) 4, 298–310.
OMETTO, D. A.: Influence of humidity on the coefficient of resistance in soils when being plowed. Working Conf. of the 3rd Section of CIGR, Wageningen, 1970, 136–137.
OSMAN, M. S.: The mechanics of soil cutting blades. J. agric. Engng Res. **9** (1964), 313–328.
PANWAR, J. S., G. N. CLARK, J. A. WEBER: Similitude prediction of model tool forces in artificial soils. Transactions of the ASAE **16** (1973), 824–829, 830.
PAYNE, P. C. J.: The relationship between the mechanical properties of soil and the performance of simple cultivation implements. J. agric. Engng Res. **1** (1956), 23–50.
PAYNE, P. C. J. and D. W. TANNER: The relationship between rake angle and the performance of simple cultivation implements. J. agric. Engng Res. **4** (1959), 312–325.
POESSE, G. J. and C. VAN OUWERKERK: Ristervorm en ploegsnelheid I.L.R. Wageningen, publikatie no. 103, 1967.
REECE, A. R.: The fundamental equation of earth-moving mechanics. Symp. on Earth-moving Mach., Auto. Div. Instn mech. Engrs, 1965.
ROWE, R. J. and K. K. BARNES: Influence of speed on elements of draft of a tillage tool. Transactions of the ASAE **4** (1961), 55–57.
SCOTT, R. F.: Principles of soil mechanics. Reading, 1963.
SELIG, E. T. and R. D. NELSON: Observations of soil cutting with blades. Journal of Terramechanics **1** (1964) 3, 32–53.
SHAMES, I. H.: Mechanics of fluids. New York, 1962.
SIEMENS, J. C., J. A. WEBER, T. H. THORNBURN: Mechanics of soil as influenced by model tillage tools. Transactions of the ASAE **8** (1965), 1–7.
SMITS, F. P.: Boundary value problems in soil mechanics as related to soil cutting. Soil Mechanics Laboratory, Delft, 1973.
SÖHNE, W.: Einige Grundlagen für eine Landtechnische Bodenmechanik. Grundlagen der Landtechnik, Heft 7 (1956), 11–27.
SÖHNE, W.: Untersuchungen über die Form von Pflugkörpern bei erhöhter Fahrgeschwindigkeit. Grundlagen der Landtechnik, Heft 11 (1959), 22–39.
SÖHNE, W.: Anpassung der Pflugkörperform an höhere Fährgeschwindigkeiten. Grundlagen

der Landtechnik, Heft 12 (1960), 51–62.
SÖHNE, W. and R. MÖLLER: Über den Entwurf von Streichblechformen unter besonderer Berücksichtigung von Streichblechen für höhere Geschwindigkeit. Grundlagen der Landtechnik, Heft 15 (1962), 15–27.
SPRINKLE, L. W., T. D. LANGSTON, J. A. WEBER, N. M. SHARON: A similitude study with static and dynamic parameters in an artificial soil. Transactions of the ASAE **13** (1970), 580–586.
SPRONG, M. C.: Trekkrachtmetingen aan vastetandscultivatoren. I.L.R. rapport 212, Wageningen, 1972.
STEFANELLI, G.: Soil resistance to cutting with a wire. Transactions 9th Intern. Congress of Soil Science Vol. 1, paper 75, 1968.
TANNER, D. W.: Further work on the relationship between rake angle and the performance of simple cultivation implements. J. agric. Engng Res. **5** (1960), 307–315.
TELISCHI' B., H. F. MCCOLLY, E. ERICKSON: Draft measurement for tillage tools. Agric. Engin. **37** (1956), 605–608.
TERPSTRA, R.: Draught forces of tines in beds of glass spheres. J. agric. Engng Res. **22** (1977), 135–143.
TERZAGHI, K.: Theoretical soil mechanics. New York, 1954.
TOWNER, G. D. and E. C. CHILDS: The mechanical strength of unsaturated porous granular material. J. of Soil Science **23** (1972), 481–498.
VOMOCIL, J. A. and W. J. CHANCELLOR: Energy requirements for breaking soil samples. Transactions of the ASAE **12** (1969), 375–388.
VORNKAHL, W.: Dynamik gezogener Bodenwerkzeuge im Modelversuch. Fortschritt Berichte VDI-Z Reihe **14**, nr 7, 1967.
WHITMORE, R. L.: Drag Forces in Bingham Plastics. Proceedings of the fifth internat. congress on Rheology held at Kyoto 1968, Vol 1, 353–360, Tokyo, 1969.
WILLATT, S. T. and A. H. WILLIS: A study of the trough formed by the passage of tines through soil. J. agric. Engng Res. **10** (1965), 1–4.
WILLATT, S. T. and A. H. WILLIS: Soil compaction in front of simple tillage tools. J. agric. Engng Res. **10** (1965), 109–113.
WIND, G. P.: Application of analog and numerical models to investigate the influence of drainage on workability in spring. Neth. J. agric. Sci. **24** (1976), 155–172.
WISMER, R. D. and H. J. LUTH: Performance of plane cutting blades in clay. Transactions of the ASAE **15** (1972), 211–216.
WISMER, R. D., D. R. FREITAG, R. L. SCHAFER: Application of similitude to soil-machine systems. Journal of Terramechanics **13** (1976) 3, 153–182.
WITNEY, B. D.: The determination of soil particle movement in two-dimensional failure. Journal of Terramechanics **5** (1968) 1, 39–52.
YONG, R. N.: Analytical predictive requirements for physical performance of mobility. Journal of Terramechanics **10** (1973) 4, 47–60.
ZOZ, F. M.: Factors affecting the width and speed for least cost tillage. the Agricultural Engineer **29** (1974) 3, 75–79.